Deliverable

2.2. Cross-sectorial drought impacts

This deliverable includes different analysis related to the cross-sectorial drought impacts in some of the basins involved in the project. This includes i) an evaluation of the connection between meteorological, hydrological and ecological droughts in the Aragón basin in the upper Pyrenees, ii) assessment of the influence of vegetation changes on the availability of water resources in the Aragón basin, iii) influence of the arterial and land drainage on hydrological droughts in the Boyne basin and iv) assessment of the cross-sectorial drought impacts in the Boyne basin using newspapers. All these analysis provide a wide picture of the complexity of interactions of droughts considering ecological, hydrological and socioeconomic systems.

Section i)

Cross-interactions of ecological and hydrological droughts in the central Spanish Pyrenees

1. Introduction

Drought is one of the most complex natural hazards given the challenges of quantification (Lloyd-Hughes, 2014), and the occurrence of different drought types: meteorological, agricultural, ecological and hydrological (Wilhite and Buchanan-Smith, 2005; Wilhite and Pulwarty, 2017). Drought severity strongly depends on the impacts that drought produces (Vicente-Serrano, 2016). Nevertheless, given the common lack of impact data, drought severity is usually quantified using drought indices based on different hydro-climatic variables (Mukherjee *et al.*, 2018). Drought metrics are typically constructed using one or a combination of variables, including precipitation, atmospheric evaporative demand (Tsakiris *et al.*, 2007; Vicente-Serrano *et al.*, 2010), streamflow (Shukla and Wood, 2008; Vicente-Serrano *et al.*, 2012) and other usually simulated by models such as evapotranspiration and soil moisture (Padrón *et al.*, 2020). These variables are commonly related to drought impacts (Bachmair *et al.*, 2016, 2018; O'Connor *et al.*, 2022; Quiring and Papakryiakou, 2003; Wang *et al.*, 2016) and used to assess drought hazard probability (Domínguez-Castro *et al.*, 2019) and to develop drought monitoring systems (Trnka *et al.*, 2020; Vicente-Serrano *et al.*, 2022).

A key challenge in assessing drought severity is the variety of its impacts since droughts affect different environmental systems and socioeconomic sectors, usually in a cascading way (Vicente-Serrano, 2021; Wilhite *et al.*, 2007). Thus, it is common to observe a spatio-temporal propagation of drought impacts through different systems and territories (Zhang *et al.*, 2022), which makes it very difficult to evaluate the severity of a particular event and develop drought thresholds and early warning approaches.

The effects of droughts on socioeconomic systems are widely recognized as being highly complex. Less recognized is the complexity of impacts for natural systems. Anomalies in climate conditions may cause a decrease in soil moisture and runoff (Barker *et al.*, 2016; Peña-Gallardo *et al.*, 2019; Tian *et al.*, 2018; Yuan *et al.*, 2020), with knock-on consequences for vegetation given water consumption by plants (Ukkola *et al.*, 2016; Zeng *et al.*, 2018). Thus, previous studies suggest that the partitioning of precipitation between vegetation consumption and runoff could affect the severity of hydrological droughts downstream (Orth and Destouni, 2018).

Moreover, different studies suggest that increases in vegetation coverage contributes to decreases in water yield at the basin scale (Filoso *et al.*, 2017; Hoek van Dijke *et al.*, 2022; Teuling *et al.*, 2019), particularly during dry years (Vicente-Serrano *et al.*, 2021a). The effects of these cross-interactions between vegetation effects and water resources availability are not well understood in regulated hydrological basins given dam management and the seasonality of water demands.

Although interactions between vegetation and hydrological systems have been recognized when determining streamflow trends, there is limited knowledge on how vegetation

characteristics and different hydrological cycle components (e.g., soil moisture, streamflow) respond to meteorological drought, and how droughts propagate to different components of environmental and hydrological systems. These issues are challenging to address as the focus is not on long-term changes (e.g. land cover changes) but on the temporal variability of different vegetation and hydrology metrics at time scales from months to years. For some of these metrics (e.g., soil moisture, leaf area, vegetation production), observations are not available for the long-term and models are required to generate data to analyse cross-drought interactions.

Meteorological droughts usually reduce vegetation activity and growth in natural ecosystems (Hsiao, 1973), but also the availability of water in the soil, rivers and reservoirs. Nevertheless, we hypothesize a differential effect of meteorological droughts on vegetation and hydrological systems. Moreover, although long-term vegetation changes may have an effect on streamflow, the impact of interannual vegetation variability on water resources is likely to be small.

In this study we model the water cycle and assessed ecological processes in a case study basin located in the Spanish central Pyrenees. The water resources generated in the basin are very important for maintaining irrigated agriculture downstream (López-Moreno *et al.*, 2004; Vicente-Serrano, 2021). In the last decades, land use has been drastically transformed in the basin as consequence of human depopulation and the abandonment of mountain agriculture and livestock. This has resulted in natural revegetation of the landscape with important morphodynamic and ecohydrological consequences (García-Ruiz *et al.*, 2015), causing a substantial decrease in water resources (Beguería *et al.*, 2003; López-Moreno *et al.*, 2011). In addition, there is some sensitivity of natural ecosystems such as forests to drought in the region (Camarero *et al.*, 2011; Peguero-Pina *et al.*, 2007).

The objective of this study is to analyse in detail how meteorological droughts differentially affect hydrological system components and ecological variables, and the possible interactions and links between ecological and hydrological drought conditions.

2. Study area

The upper Aragón basin is located in the Central Spanish Pyrenees (Fig. 1), with a total area of 2181 km^2. There are large topographic gradients in the basin, with elevations from 420 to 2883 m.a.s. l. The basin receives annual rainfall totals exceeding 1500 mm in the northernmost sector, declining to 800 mm in the inner depression. There is a summer dry season with higher precipitation totals recorded in spring and autumn. The mean annual air temperature is 10 °C, and snow cover is recorded from December to April (López-Moreno *et al.*, 2020; López-Moreno and García-Ruiz, 2004). The basin contains a large reservoir, the Yesa reservoir with a capacity of 446.8 hm3, located at the outlet. It provides water resources for irrigation to the Bardenas region (81,000 has), located 80 km to the South (López-Moreno *et al.*, 2004).

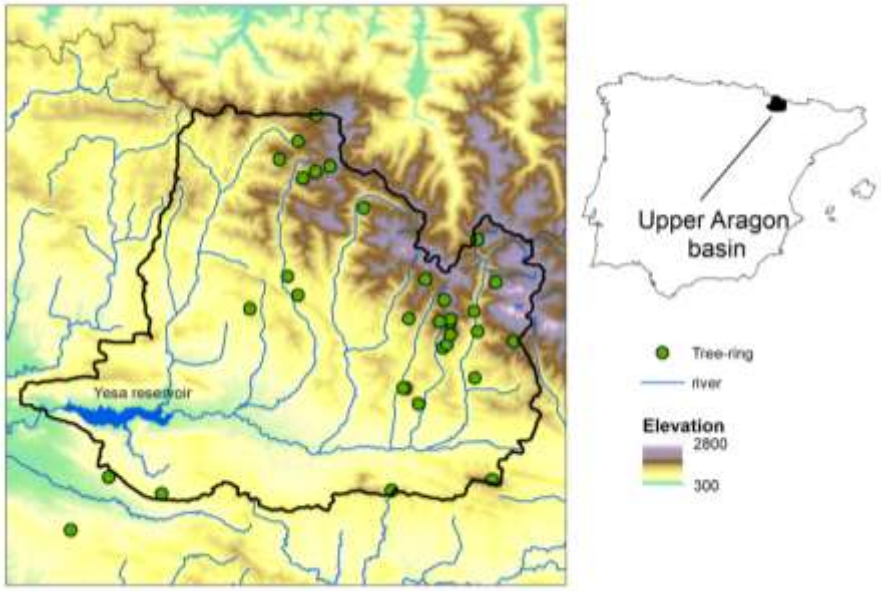

Figure 1: Location of the study area, topography and hydrological network, including the Yesa reservoir.

Vegetation cover in the upper basin is characterized by the dominance of conifers (e.g. *Pinus sylvestris* L., *Pinus uncinata* Ram., *Abies alba* Mill., *Pinus nigra* J.F. Arn.) and hardwood species (e.g. *Fagus sylvatica* L., *Quercus faginea* Lam.), while shrubs dominate the understory (e.g., Buxus sempervirens L.) and are distributed on steep slopes and poor soil areas (García-Ruiz *et al.*, 2015). Vegetation cover in the basin has been strongly impacted by human activities. Historically, cultivated areas were found below 1600 m a.s.l. in valley bottoms, perched flats, and steep, south-facing hillslopes, which were managed even under shifting agriculture systems (Garcia-Ruiz and Lasanta-Martinez, 1990). The basin has undergone a land cover transformation in the 20th century, due to rural depopulation (Garcia-Ruiz and Lasanta-Martinez, 1990), resulting in a gradual natural revegetation process (Lasanta-Martínez *et al.*, 2005; Sanjuán *et al.*, 2018). Since the 1960s, vegetation changes have been characterized by secondary succession, with coniferous forests being replaced by mixed and broadleaf forests and some croplands and grasslands being invaded by shrubs and conifers.

3. Data and methods

3.1. Data

Two different climate datasets were used in this study. First, we employ daily precipitation and temperature series from available meteorological stations in the basin (14 series of daily precipitation and daily maximum and minimum temperatures from 1970 to 2020). These series were used to run the hydro-ecological model described in section 3.2, which requires daily meteorological data. Second, we employ weekly gridded climate data a spatial resolution of 1.1 km, averaged over the whole basin (Vicente-Serrano *et al.*, 2017). The variables contained in the weekly climate data were precipitation, maximum and minimum temperature, relative humidity, solar radiation and wind speed. Atmospheric Evaporative Demand (AED) necessary to calculate some of the drought metrics was calculated using the FAO-56 Penman-Monteith equation (Pereira *et al.*, 2015).

Data on surface flows and storage levels for the Yesa reservoir were obtained from the Ebro Basin Management Agency (Confederación Hidrográfica del Ebro; http://www.chebro.es/), and includes monthly inflows into the reservoir and downstream releases (i.e. to the Aragón River and the Bardenas channel). Inflows are primarily influenced by climatic conditions since there is no other regulation upstream, while all other hydrological variables (Yesa storage, Bardenas channel and the Aragón flows downstream Yesa) largely depend on water management.

To validate vegetation variables simulated by the model we used tree-ring width data collected from six representative tree species listed above in the study area description. Data from 37 sites with forest growth were used in this work. Overall, the tree-ring width data were processed using dendrochronological methods (Fritts, 1976). Further details of this processing can be found in Vicente-Serrano *et al.* (2021b). We also used satellite derived Normalized Difference Vegetation Index (NDVI) from 1981 to 2020 at a biweekly scale obtained from the fusion of a NOAA-AVHRR NDVI dataset from 1981 to 2015 (Vicente-Serrano *et al.*, 2020) and the MODIS NDVI dataset (Huete *et al.*, 2002). NDVI data were used to evaluate the Leaf Area Index (LAI) output simulated by the eco-hydrological model.

Finally, we used land cover and topography information necessary for the modelling. We used a 25 m spatial resolution digital elevation model to describe the topographical features of the study area. Forest and land-cover types were obtained from the Spanish National Forest Map and the Third National Forest Inventory (period 2006–2016). Soil classes were taken from the European Soil Database (available at http://eusoils.jrc.ec.europa.eu).

3.2 Eco-hydrological modelling

We used the RHESSys hydro-ecological model (Tague and Band, 2004) to model the eco-hydrological processes in the basin from 1970 to 2020. RHESSys couples an ecosystem carbon cycling model with a spatially distributed hydrology model to simulate integrated water, carbon and nutrient cycling and transport over complex terrain at small to medium scales. More recent refinements of energy, moisture and carbon cycling model are described on RHESSys website (https://github.com/RHESSys/RHESSys). We used the model to obtain reliable estimates of variables like soil moisture, net primary production and leaf area, which are not available from observations for the whole period considered in this study. The RHESSys model has been previously used to simulate hydrological and plant processes in different vegetation and basin types including mountain areas (see review in Chen *et al.*, 2020).

Soil parameters in RHESSys typically require calibration since soil and geologic inputs do not account for complex controls on drainage rates such as hillslope scale preferential flow path distributions. The following four parameters were calibrated: (i) depletion of hydraulic conductivity with depth (m); (ii) hydraulic conductivity in saturated soils (K); (iii) infiltration through macropores (gw1); and (iv) lateral water fluxes from hillslopes to the main channel (gw2). Parameters were selected using a Monte-Carlo procedure based on 1600 simulations run. Parameters that produced monthly streamflow estimates that gave a Nash–Sutcliffe (NSE) efficiency coefficient > 0.7 where retained.

Figure 2 shows the monthly evolution of different key variables in the basin simulated by RHESSys for the period 1970-2018. Validation of model simulations was undertaken using

observed streamflow data, the average tree-ring width of the samples available in the basin (see 3.1) and the NDVI data from NOAA-AVHRR and MODIS satellites. Figure 3 shows the relationship between the average annual tree-ring growth and the cumulative NPP recorded at different time-scales (1-24 months), the evolution of the observed and simulated monthly streamflow and observed NDVI and simulated LAI in the basin. NPP shows a correlation of 0.53 with the 10-month NPP in September, which suggests a good agreement with the tree growth. In addition, agreement between simulated and observed streamflow is also high (r = 0.79), with the model performing well during periods of high and low flows. Temporal variability of the simulated LAI shows high agreement with the NDVI (r = 0.84), which suggests that the model simulated variables show a reasonable robustness and can be used for comparisons to observations.

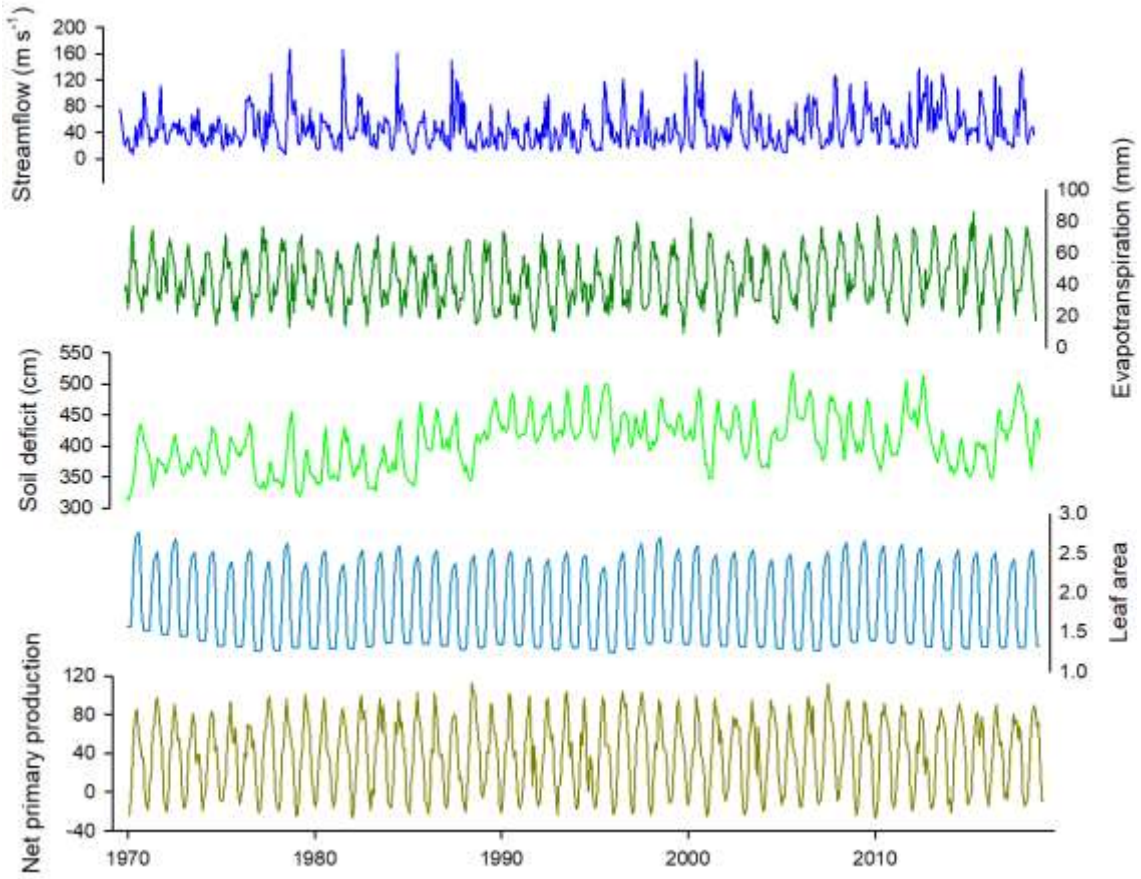

Figure 2. Observed (red) and modelled streamflow (blue) and modelled eco-hydrological variables in the Aragon

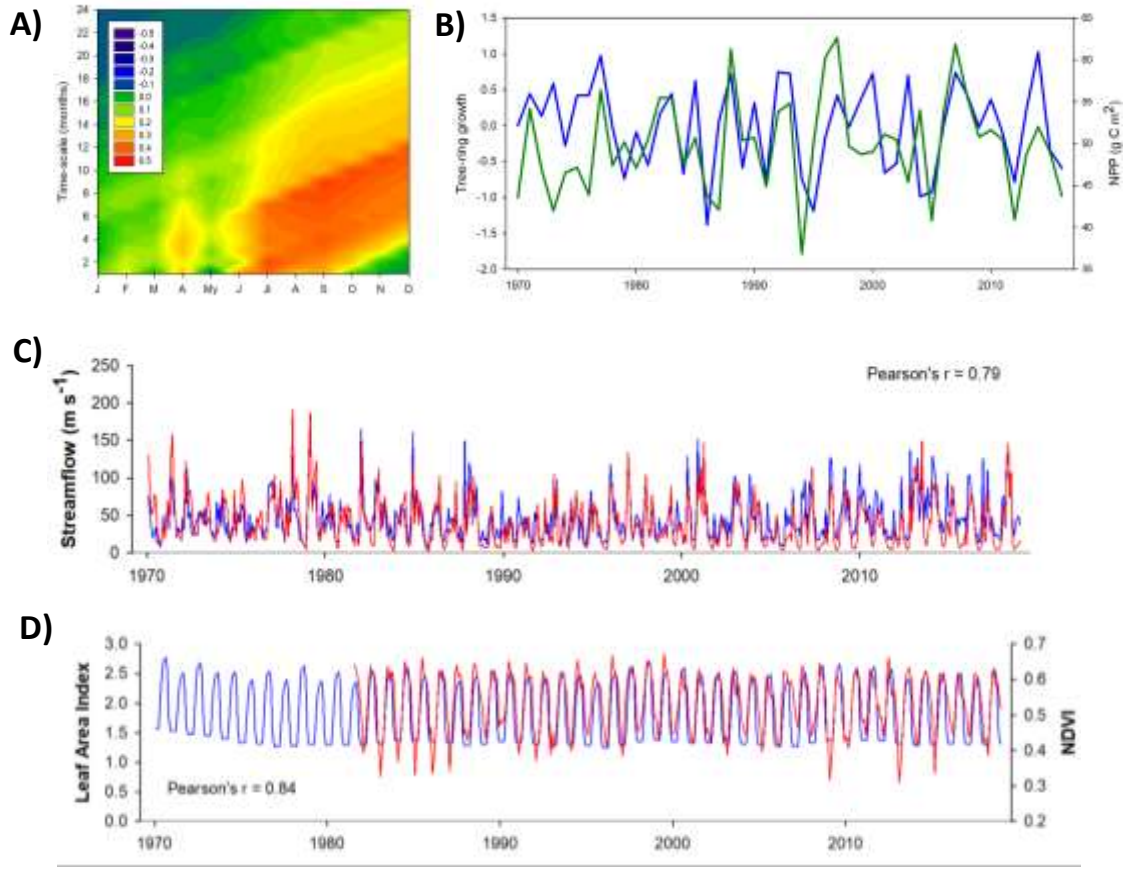

Figure 3. Validation statistics based on the comparison of simulated data of streamflow, NPP and LAI with observed streamflow, tree ring growth and NDVI.

3.3. Drought index calculations

To assess the influence of meteorological droughts on hydrological and ecological variables, we used the Standardized Precipitation Index (SPI) (McKee *et al.*, 1993) based on precipitation, the Standardized Precipitation Evapotranspiration Index (SPEI) (Vicente-Serrano *et al.*, 2010) based on the difference between Precipitation and AED, the Standardized Evapotranspiration Deficit Index (SEDI) (Kim and Rhee, 2016), based on the difference between actual evapotranspiration (Eta) and AED, the Standardized Precipitation minus Evapotranspiration (SPET) and the Evaporative Demand Drought Index (EDDI) (Hobbins *et al.*, 2016), which is based on the AED. The hydrological and ecological variables obtained from the hydro-ecological modelling (soil moisture, NPP and LAI) and from observations (streamflow, reservoir storages and outflows) were also standardized at time scales from 1 to 36 months. For this purpose, we used the probability distribution that showed the best fit with the monthly series of each variable and time scale, following the procedure used to calculate the Standardized Streamflow Index (SSI) (Vicente-Serrano *et al.*, 2012).

3.4. Analysis

We calculated the Pearson's correlation (r) between de-trended drought indices at time scales between 1 and 36 months. Correlations were calculated for each monthly series to determine the month and timescale that meteorological drought has greatest influence on other

variables. We also calculated partial correlations (Baba *et al.*, 2004) to determine the independent role of each metric on the others, thus allowing analysis of the propagation of drought effects across systems and the most important effects among different variables.

4. Results

4.1 Influence of meteorological drought on eco-hydrological variables

Figure 4 shows the correlations between the values of SPI obtained at time-scales from 1 to 36 months and soil moisture, LAI and NPP from RHESsys simulations aggregated over the basin and observed streamflow, reservoir storages and outflows. The results show strong correlations between SPI and soil moisture at time scales longer than five months for the majority of months. Correlations with LAI are weak and statistically non-significant but there are significant correlations between NPP and SPI in summer months. Correlations with streamflow are strong at short time scales (1-5 months), particularly during the winter season. Correlations of SPI with reservoir storages and outflows are also strong and statistically, with the strongest correlations recorded at time scales between five and ten months.

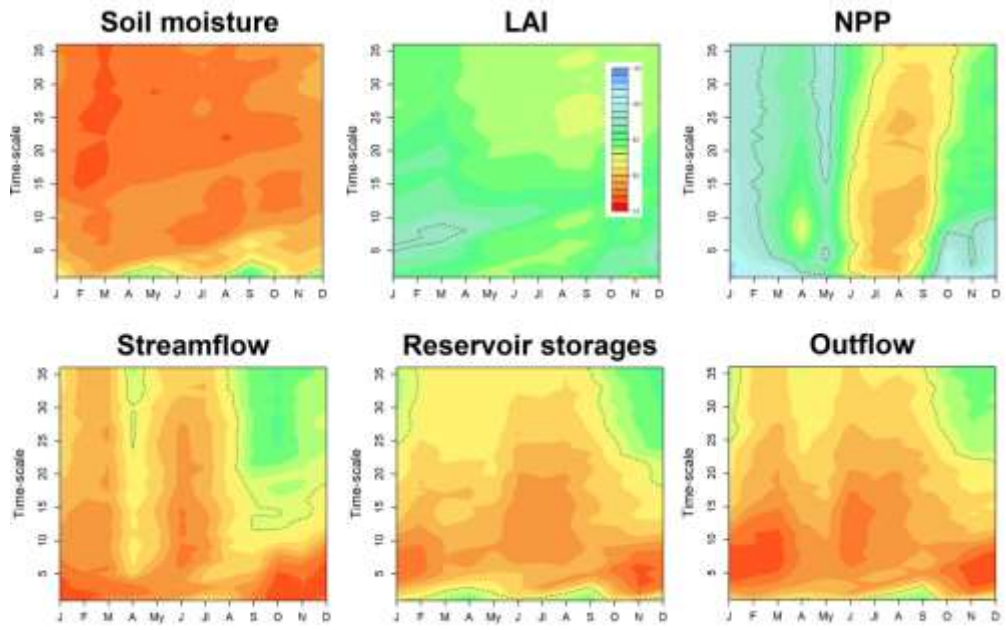

Figure 4. Monthly Pearson's r correlations between the basin Standardized Precipitation Index (SPI) and different hydrological and ecological variables. Dotted lines frame months and time-scales in which the correlations are statistically significant.

Correlations of each variable with SPEI and the standardized difference between Precipitation and Et are similar to those for SPI (Figures 5 and 6). Nevertheless, the correlations between SEDI and the different eco-hydrologic variables show interesting differences (Figure 7). The first is related to the soil moisture which shows strongest positive correlations with SEDI during the summer months at time scales between 4 and 12 months. LAI also shows positive correlations with SEDI, statistically significant from May to September for longer time scales (15-20 months). There are also statistically significant positive correlations between SEDI and NPP from June to September at time scales between 1 and 10 months. For hydrological variables (streamflow, reservoir storages and outflows) the

strongest correlations with SEDI are found during the summer months, showing differences with the other drought indices.

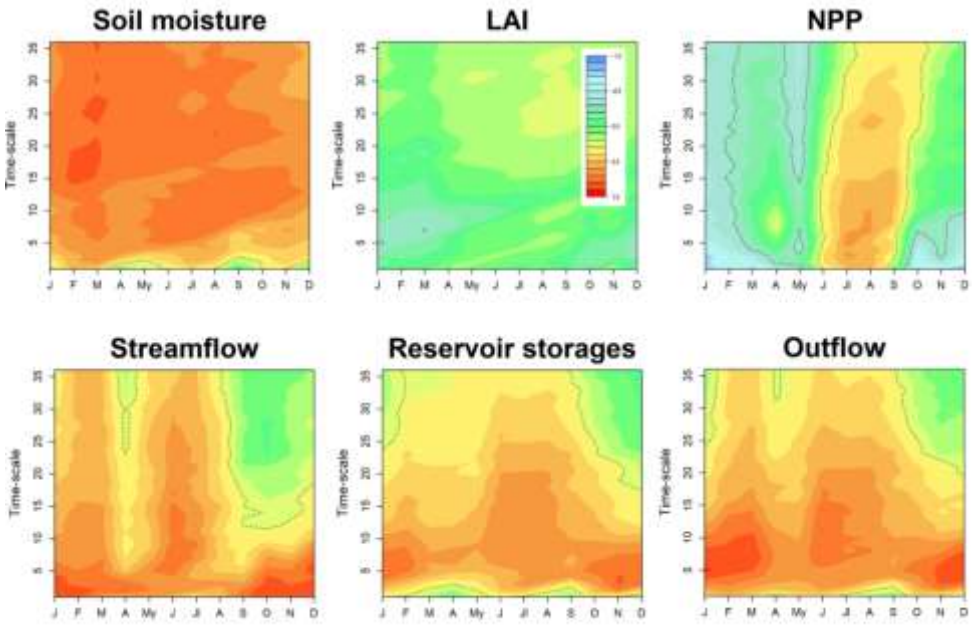

Figure 5. Monthly Pearson's r correlations between the basin Standardized Precipitation Evapotranspiration Index (SPEI) and different hydrological and ecological variables. Dotted lines frame months and time-scales in which the correlations are statistically significant.

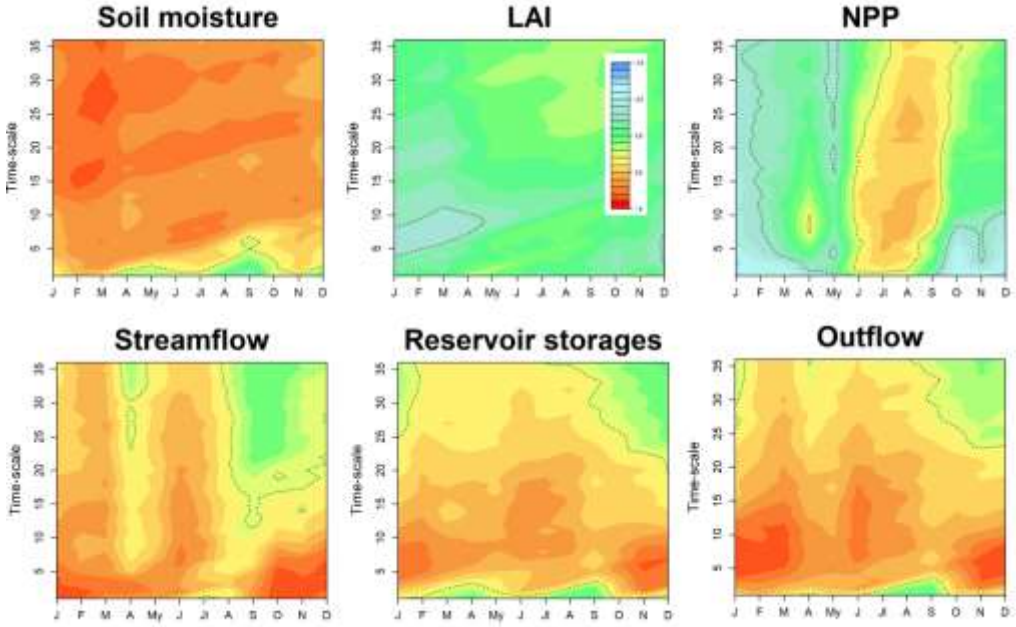

Figure 6. Monthly Pearson's r correlations between the basin Standardized difference between Precipitation and Evapotranspiration and the different hydrological and ecological variables. Dotted lines frame months and time-scales in which the correlations are statistically significant.

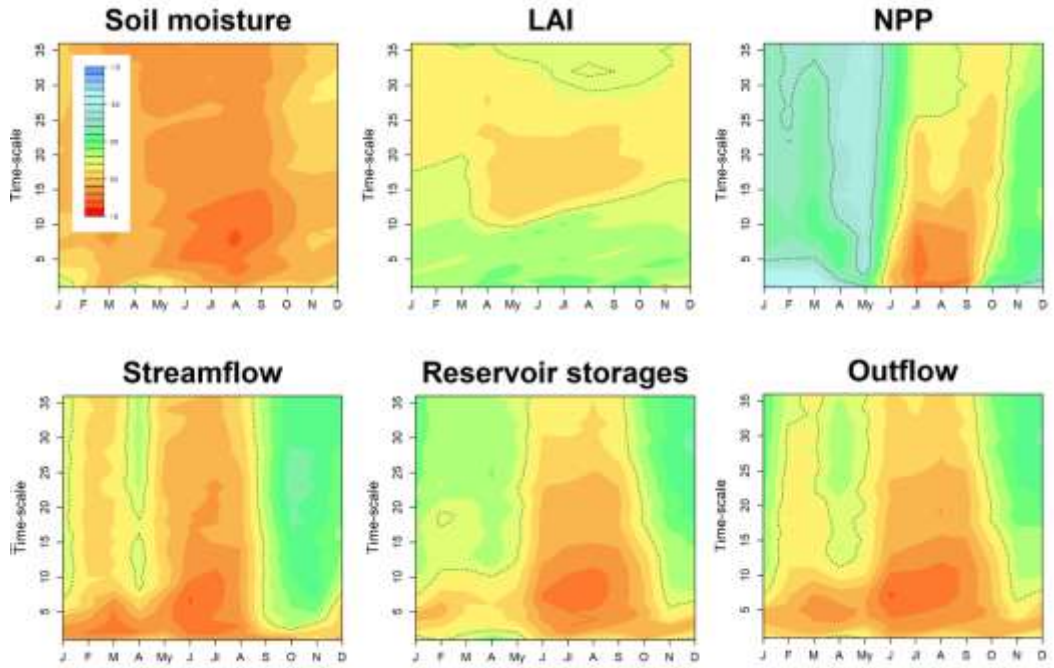

Figure 7. Monthly Pearson's r correlations between the basin Standardized Evapotranspiration Deficit Index (SEDI) and different hydrological and ecological variables. Dotted lines frame months and time-scales in which the correlations are statistically significant.

4.2 Relationship between different eco-hydrological variables recorded on different time-scales

Figure 8 shows the correlations between LAI anomalies recorded at time scales between 1 and 36 months and other eco-hydrological variables. The different plots show very weak correlations of LAI with other metrics, with the exception of NPP, where long time scales of LAI show a positive correlation with NPP. Standardized values of NPP show positive and significant correlations with soil moisture in summer months, especially at short time scales, and also with streamflow and reservoir storages and outflows, suggesting that higher values of carbon uptake in the basin are in agreement with higher water generation and availability (Figure 9). Correlations between soil moisture and different hydrological variables are also significant, especially for soil moisture anomalies at short time-scales, and particularly during the summer season (Figure 10). Correlations between streamflow and reservoir storages and outflows are in general strong in all months, but particularly during the winter season. Nevertheless, there are some particularities. While correlations between streamflow and reservoir storages are strong between June and August, weaker correlations aree found with outflows for the same months (Figure 11). Finally, the relationship between the standardized reservoir storages and the outflows is strong, especially at short time-scales and from July to December (Figure 12).

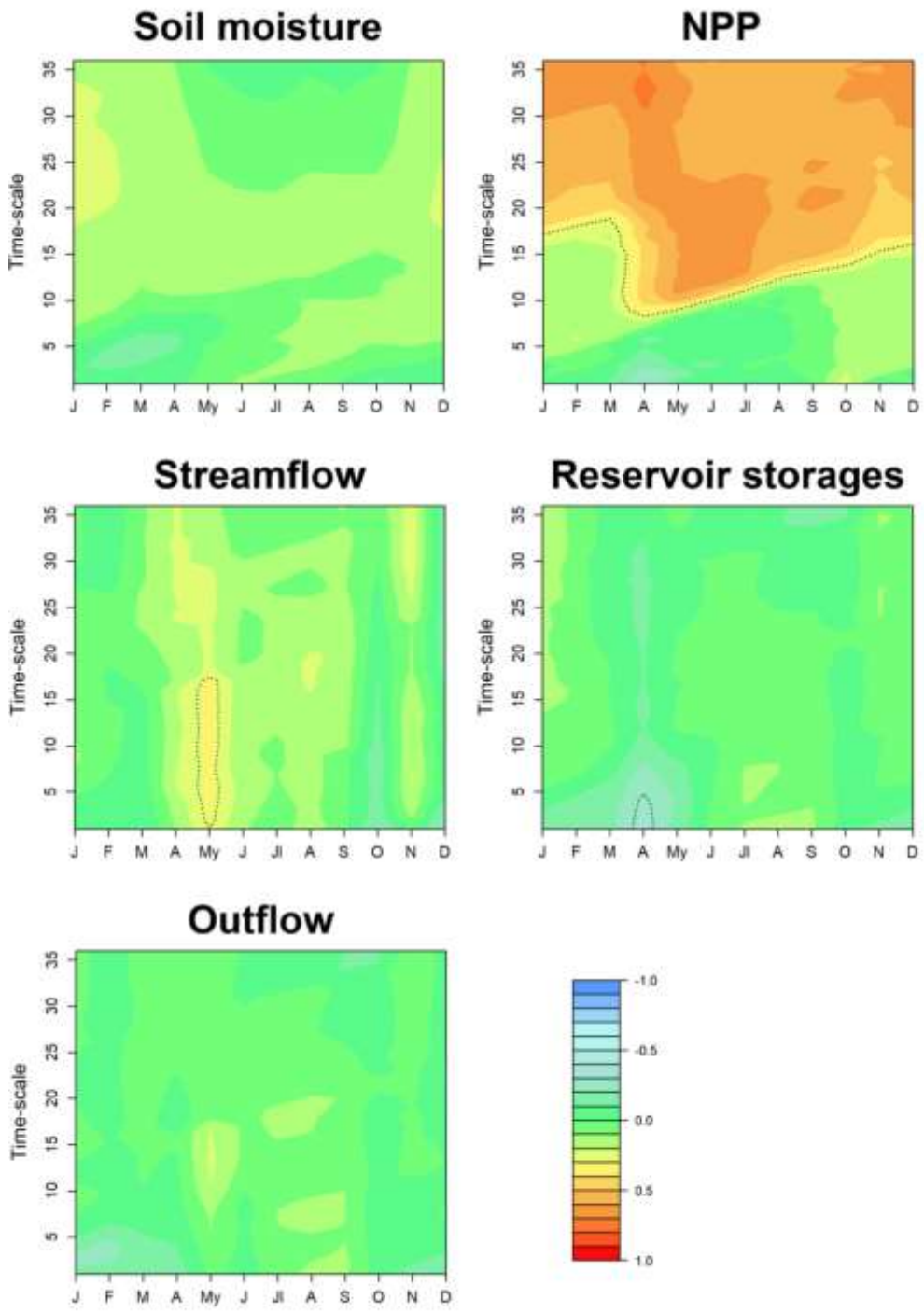

Figure 8: Monthly Pearson's r correlations between the basin Standardized LAI and the rest of hydrological and ecological variables. Dotted lines frame months and time-scales in which the correlations are statistically significant.

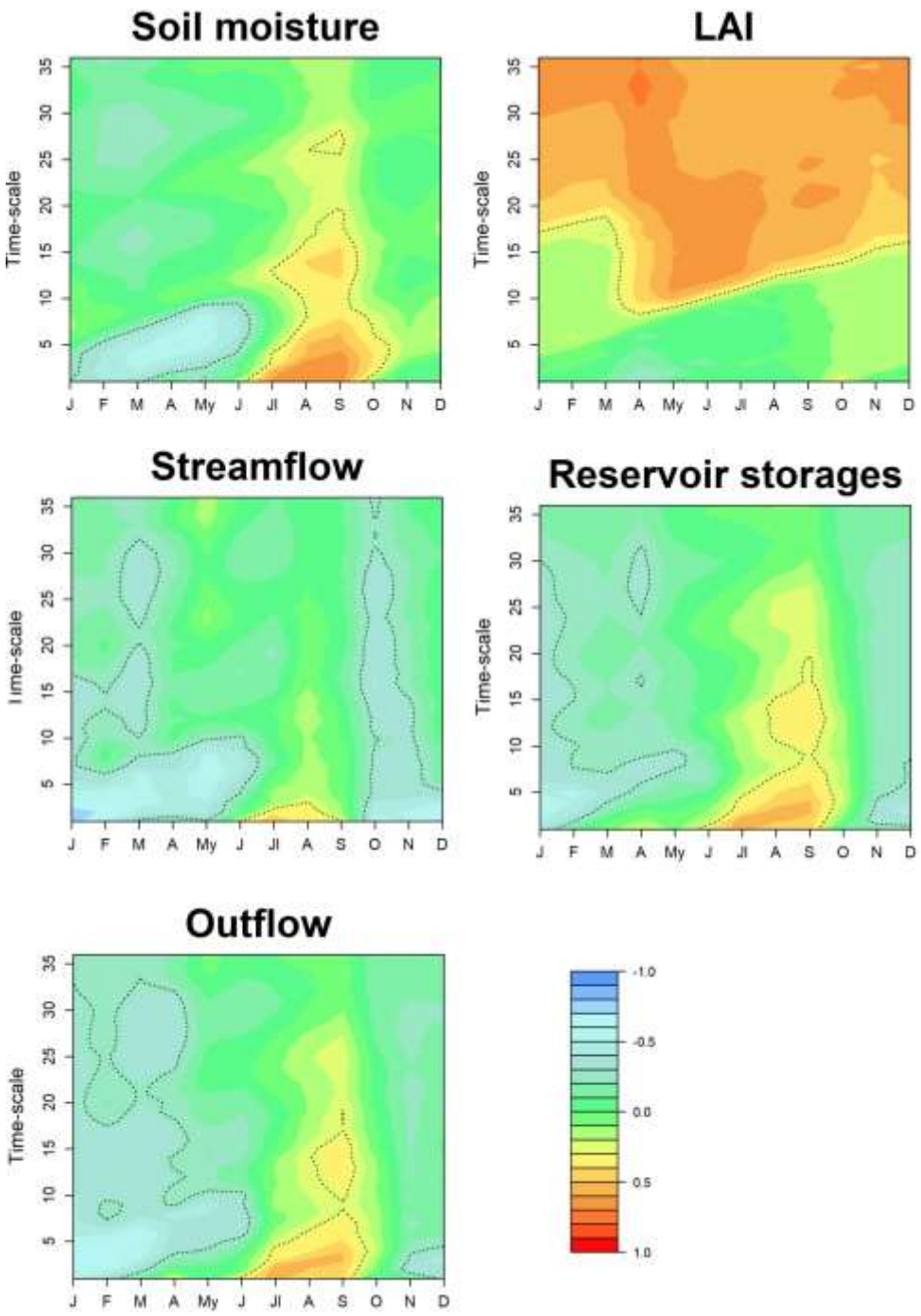

Figure 9: Monthly Pearson's r correlations between the basin Standardized NPP and the rest of hydrological and ecological variables. Dotted lines frame months and time-scales in which the correlations are statistically significant.

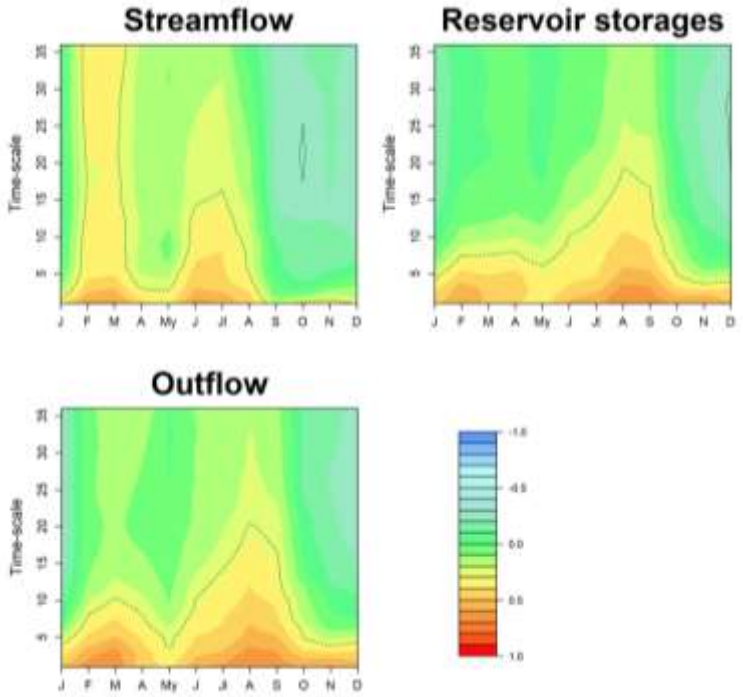

Figure 10: Monthly Pearson's r correlations between the basin Standardized Soil Moisture Index (SSMI) and the rest of hydrological variables. Dotted lines frame months and time-scales in which the correlations are statistically significant.

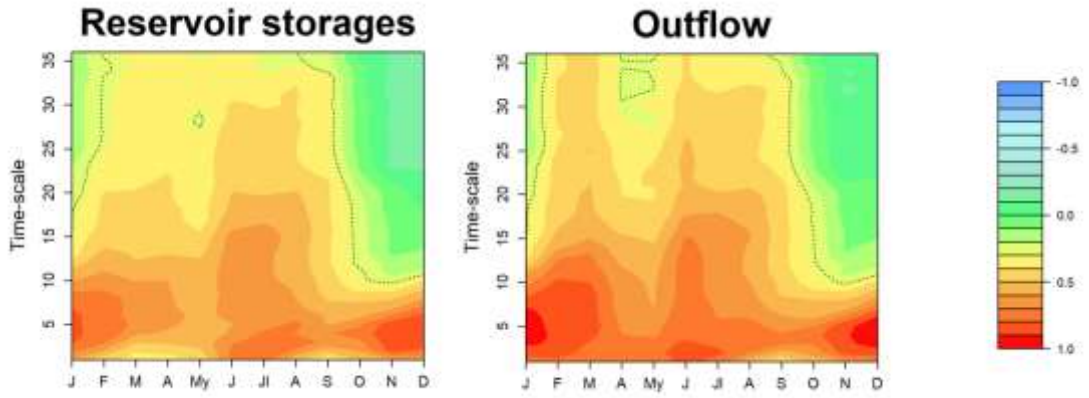

Figure 11: Monthly Pearson's r correlations between the basin Standardized Streamflow Index (SSI) and the rest of hydrological variables. Dotted lines frame months and time-scales in which the correlations are statistically significant.

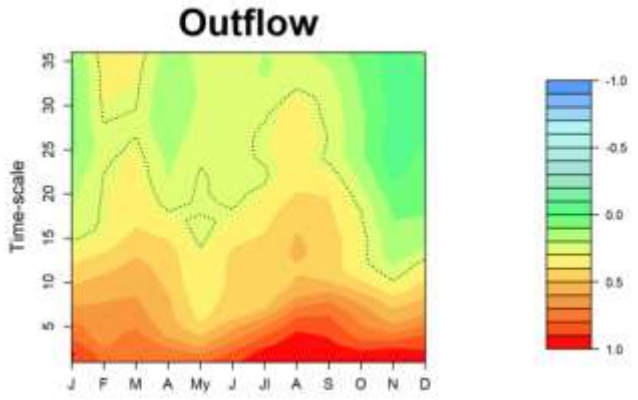

Figure 12: Monthly Pearson's r correlations between the basin Standardized reservoir storages calculated at time scales from 1 to 36 months and the standardized water outflows. Dotted lines frame months and time-scales in which the correlations are statistically significant.

4.3. Isolation of the role of different interactions

Partial correlations between EDDI, SPI, LAI, NPP and SSMI show that variations in soil moisture are mostly determined by precipitation variability, with a small role played by variability in AED and vegetation variables (NPP and LAI) (Figure 13). NPP is mostly dependent on soil moisture conditions during summer whereas the independent roles of AED, precipitation and LAI on NPP are small (Figure 14). LAI variability is most strongly connected with NPP at longer time scales, meaning that the previous year's NPP may have an important influence on LAI of the following year (Figure 15). The influence of climate, soil moisture, NPP and LAI variability on streamflow shows some interesting patterns. First, the ecological variables LAI and NPP do not appear to influence streamflow variability when the influence of other variables is removed. The main independent role is associated with precipitation, particularly from September to May. During the summer months SSMI is the most important variable of those considered in explaining interannual streamflow variability (Figure 16). For reservoir storage precipitation during the cold season is the primary control variable, principally at long time scales. By contrast, at shorter time scales reservoir storage is heavily influenced by streamflow and soil moisture (Figure 17). Finally, the outflows are mostly controlled by reservoir storages throughout the year, especially in summer months, but outflows are more affected by streamflow than by reservoir storages in some winter months. In addition, outflows are strongly determined by precipitation recorded over long time scales (Figure 18).

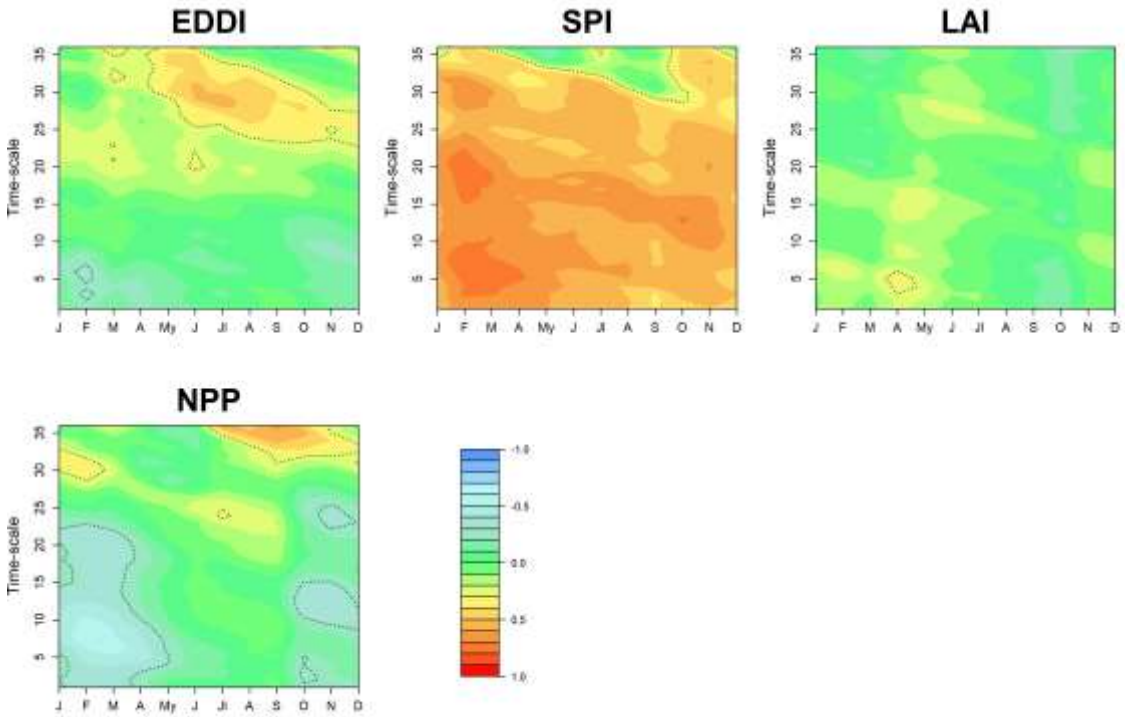

Figure 13: Monthly partial correlations between the basin Standardized Soil Moisture Index (SSMI) and the variables that may have a role on it (EDDI, SPI, LAI and NPP). Dotted lines frame months and time-scales in which the correlations are statistically significant.

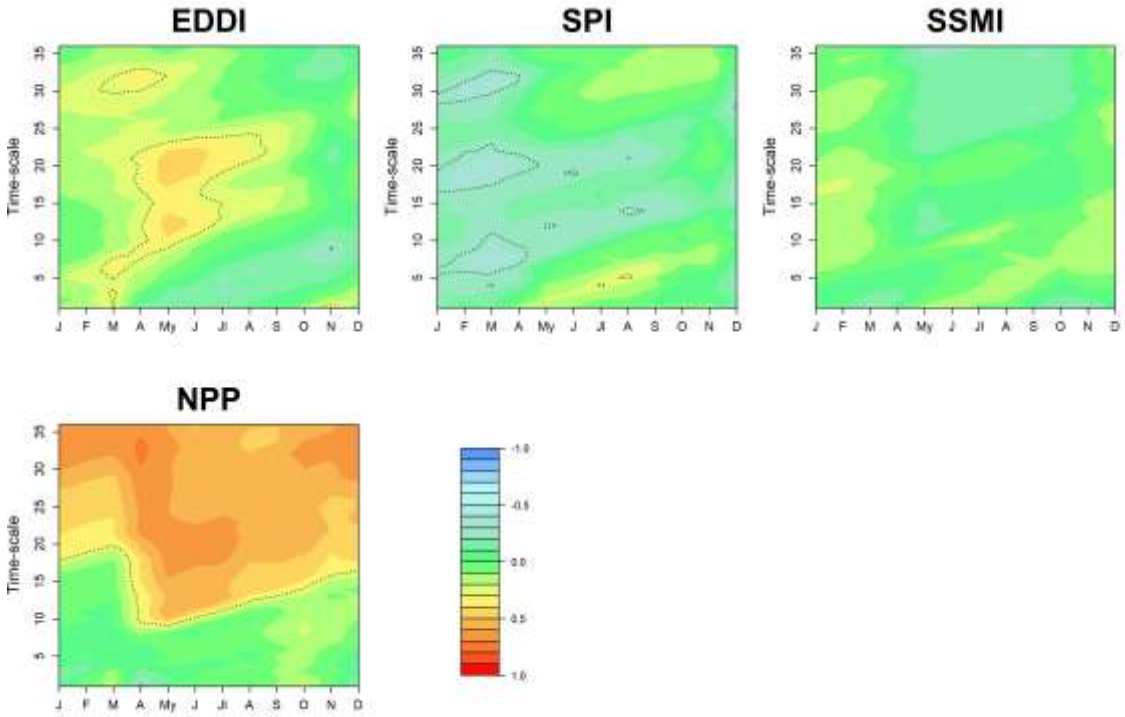

Figure 14: Monthly partial correlations between the basin Standardized NPP and the variables that may have a role on it (EDDI, SPI, SSMI and NPP). Dotted lines frame months and time-scales in which the correlations are statistically significant.

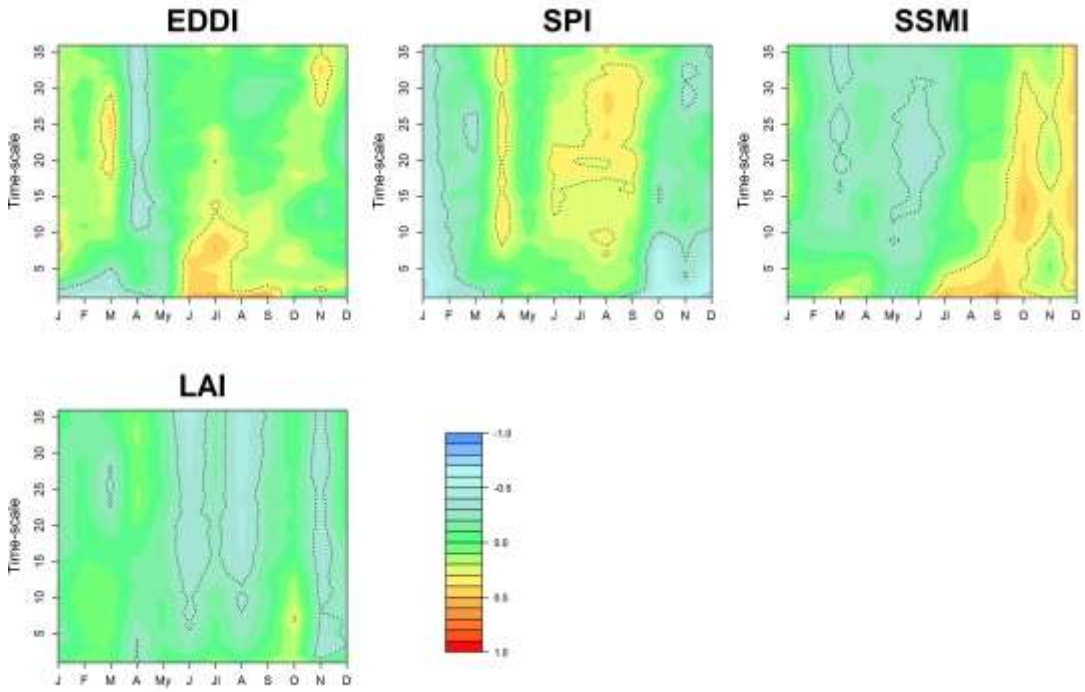

Figure 15: Monthly partial correlations between the basin Standardized NPP and the variables that may have a role on it (EDDI, SPI, SSMI and LAI). Dotted lines frame months and time-scales in which the correlations are statistically significant.

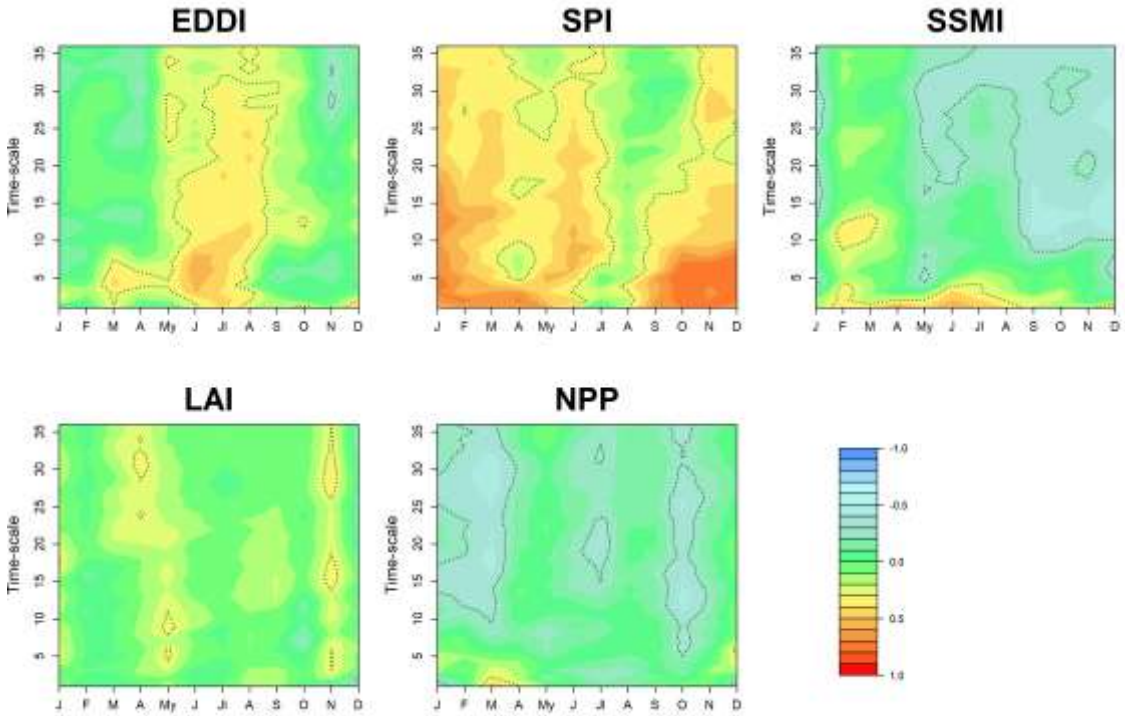

Figure 16: Monthly partial correlations between the basin Standardized Streamflow Index (SSI) and the variables that may have a role on it (EDDI, SPI, SSMI, LAI and NPP). Dotted lines frame months and time-scales in which the correlations are statistically significant.

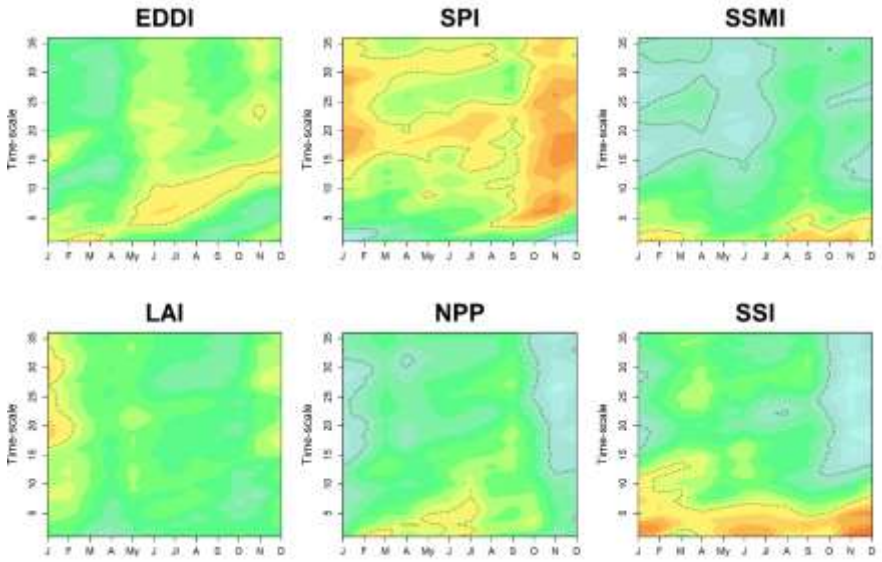

Figure 17: Monthly partial correlations between the standardized reservoir storages at Yesa reservoir and the variables that may have a role on it (EDDI, SPI, SSMI, SSI, LAI and NPP). Dotted lines frame months and time-scales in which the correlations are statistically significant.

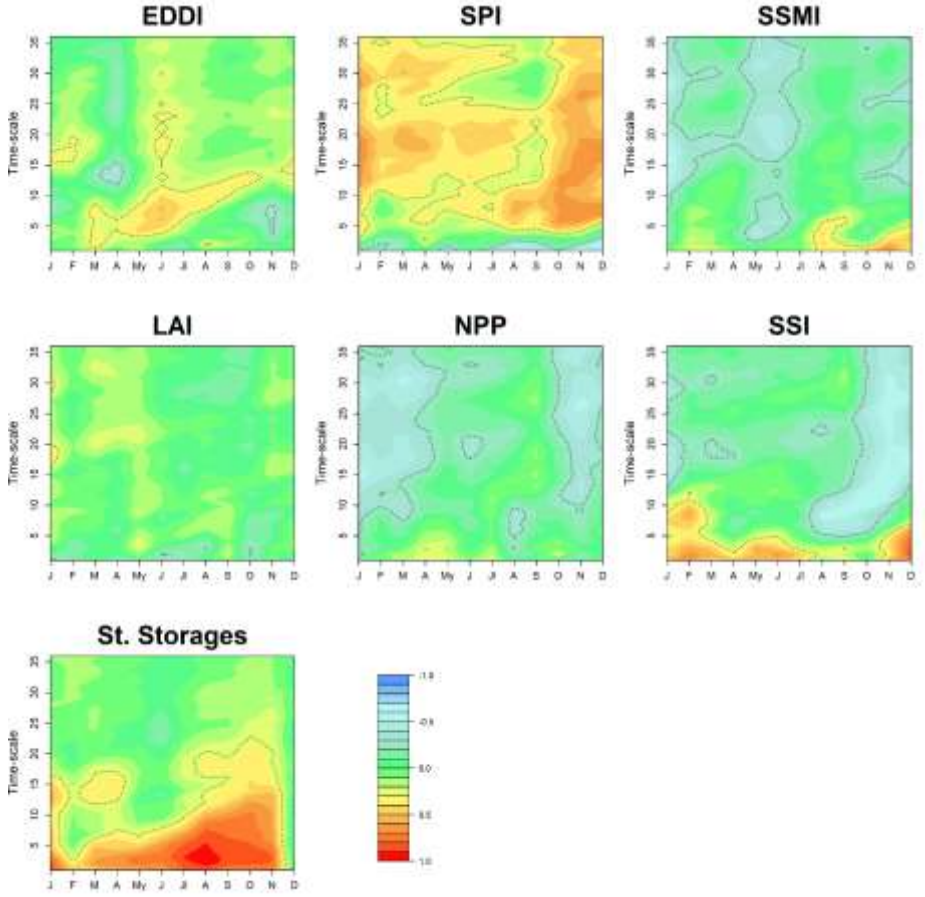

Figure 18. Monthly partial correlations between the basin Standardized OUTFLOWS and the variables that may have a role on it (EDDI, SPI, SSMI, SSI, LAI and NPP AND RESERVOIR STORAGES). Dotted lines frame months and time-scales in which the correlations are statistically significant.

5. Discussion and conclusions

This study analyzed the relationship between different drought metrics that provide information meteorological, hydrological and ecological drought severity in a mountain basin in the central Spanish Pyrenees with the purpose of determining: i) the possible propagation of drought conditions between systems and ii) to identify possible cross-interactions among hydrological and ecological drought conditions. Such assessments are important for the basin given that water resources generated are widely used downstream for irrigation agriculture and urban supply (López-Moreno *et al.*, 2004; Vicente-Serrano, 2021).

First, we analyzed the response of hydrological and ecological metrics to the variability in meteorological droughts, showing that the main response is recorded through precipitation with other variables (e.g., the actual evapotranspiration -Et-, and atmospheric evaporative demand –AED-) showing a smaller influence. This behavior is not specific to the Aragon basin, as different studies have shown that precipitation is the main meteorological variable controlling the temporal variability of streamflow worldwide (Berghuijs *et al.*, 2017; Vicente-Serrano *et al.*, 2019; Yang *et al.*, 2018). Although AED influences long term trends and temporal variability of surface water resources in Spain (Vicente-Serrano *et al.*, 2014), its role is still small in comparison to precipitation variability. An interesting finding of this study is that Et does not appear to be important in explaining variability in soil moisture and streamflow since the magnitude and seasonality of correlations using Precipitation minus Et are similar to those using SPI, which is only based on precipitation. Some studies in central Europe (Teuling *et al.*, 2013) have suggested that land ET could have an important role in depleting soil moisture and increasing the severity of hydrological droughts. Thus, Et can be very important in determining the partitioning of total precipitation between blue and green water during drought periods (Orth and Destouni, 2018). Et does play an important role in explaining the trend of water resources in the Pyrenees (Beguería *et al.*, 2003; López-Moreno *et al.*, 2011) as a consequence of rural abandonment and land cover changes characterized by natural revegetation (García-Ruiz *et al.*, 2015). Moreover, the influence of increased Et on streamflow is most relevant during the driest years (Vicente-Serrano *et al.*, 2021a). Nevertheless, in this study we found that in terms of explaining interannual variability of the hydrological and ecological metrics considered, Et plays a smaller role than precipitation, likely due to the fact that AED is smaller in this cold upland region (Vicente-Serrano *et al.*, 2007).

An important finding of our study is the very differential response of ecological and hydrological metrics to meteorological drought. Ecological metrics are less sensitive to meteorological drought in comparison to the hydrological metrics analysed. This is common in cool and humid areas where water availability is usually sufficient to maintain vegetation activity and growth even in the driest years (Vicente-Serrano, 2021). Although some previous studies have shown a response of tree growth to drought variability in some species of the upper Aragón basin (Camarero *et al.*, 2011; Gazol *et al.*, 2018a), the response is much less than found in the nearby semiarid areas of the Ebro basin (Pasho *et al.*, 2011), where tree species respond very differently (Vicente-Serrano, 2021). These results are not likely to be biased by model simulations since we find that summer NPP is correlated with precipitation recorded in the previous months. Nevertheless, the response of LAI to meteorological

drought is very small and not statistically significant and cannot be related to the variables obtained by the hydro-ecological simulation. Thus, using remote sensing measurements of vegetation activity, which are highly related to the leaf area (Carlson and Ripley, 1997), and tree-ring width measurements, as metric of tree growth and carbon uptake, the response is always greater between climate indices and tree growth, independent of the forest type considered (Gazol *et al.*, 2018b; Peña-Gallardo *et al.*, 2018). This suggests a low sensitivity of vegetation activity and leaf area to climate variability in the upper Aragón basin, with plants optimizing respiration and photosynthesis under periods of water deficit, while carbon uptake may be constrained by limited water conditions in summer months, as suggested by the response of NPP.

The influence of meteorological drought conditions is much greater on hydrological subsystems of the basin (including soil moisture), with water availability strongly determined by the interannual variability of precipitation, although the time-scales of response vary as expected (Barker *et al.*, 2016; Wang *et al.*, 2016).

A novel approach of our study has been the assessment of different meteorological, ecologic and hydrologic metrics in order to determine relationships and cross-interactions between them. Previous studies have suggested very important role for vegetation dynamics in explaining changes in runoff generation of Spain (Beguería *et al.*, 2003; Martínez-Fernández *et al.*, 2013). In our study domain, experimental studies have shown that runoff generation is strongly determined by the percentage of vegetation coverage (García-Ruiz *et al.*, 2008). Nevertheless, although long-term changes in vegetation plays a very important role in determining trends in water resources, the role of interannual variability in plant conditions seems to be small as our results suggest. This means that years characterized by high vegetation activity and growth do not have a negative effect on water availability in the basin. This is likely linked to the similar influence of climate variability on ecological and hydrological droughts, as higher precipitation cause positive anomalies in both metrics. Thus, although in humid years vegetation growth would be higher and Et would increase given higher photosynthesis, water availability would be sufficient to maintain positive anomalies in the surface water resources in the basin. The connection between different hydrological drought metrics in the basin is very strong and modulated by the seasonal response to precipitation and the reservoir management.

In conclusion, the effect of meteorological drought variability in the upper Aragón basin is much stronger in hydrological systems than in ecological systems. Indeed, we find little evidence for a strong role of vegetation in influencing hydrological drought variability in the basin at interannual timescales. These findings are highly relevant for evaluating how ecological and hydrological droughts are related in complex hydrological basins.

References

Baba K, Shibata R, Sibuya M. 2004. Partial correlation and conditional correlation as measures of conditional independence. *Australian & New Zealand Journal of Statistics*. John Wiley & Sons, Ltd **46**(4): 657–664. DOI: https://doi.org/10.1111/j.1467-842X.2004.00360.x.

Bachmair S, Svensson C, Hannaford J, Barker LJ, Stahl K. 2016. A quantitative analysis to objectively appraise drought indicators and model drought impacts. *Hydrology and Earth System Sciences* **20**(7): 2589–2609. DOI: 10.5194/hess-20-2589-2016.

Bachmair S, Tanguy M, Hannaford J, Stahl K. 2018. How well do meteorological indicators represent agricultural and forest drought across Europe? *Environmental Research Letters* **13**(3). DOI: 10.1088/1748-9326/aaafda.

Barker LJ, Hannaford J, Chiverton A, Svensson C. 2016. From meteorological to hydrological drought using standardised indicators. *Hydrology and Earth System Sciences* **20**(6): 2483–2505. DOI: 10.5194/hess-20-2483-2016.

Beguería S, López-Moreno JI, Lorente A, Seeger M, García-Ruiz JM. 2003. Assessing the effect of climate oscillations and land-use changes on streamflow in the Central Spanish Pyrenees. *Ambio* **32**(4): 283–286. DOI: 10.1579/0044-7447-32.4.283.

Berghuijs WR, Larsen JR, van Emmerik THM, Woods RA. 2017. A Global Assessment of Runoff Sensitivity to Changes in Precipitation, Potential Evaporation, and Other Factors. *Water Resources Research*. John Wiley & Sons, Ltd **53**(10): 8475–8486. DOI: https://doi.org/10.1002/2017WR021593.

Camarero JJ, Bigler C, Linares JC, Gil-Pelegrín E. 2011. Synergistic effects of past historical logging and drought on the decline of Pyrenean silver fir forests. *Forest Ecology and Management* **262**(5): 759–769. DOI: 10.1016/j.foreco.2011.05.009.

Carlson TN, Ripley DA. 1997. On the relation between NDVI, fractional vegetation cover, and leaf area index. *Remote Sensing of Environment* **62**(3): 241–252. DOI: 10.1016/S0034-4257(97)00104-1.

Chen B, Liu Z, He C, Peng H, Xia P, Nie Y. 2020. The Regional Hydro-Ecological Simulation System for 30 Years: A Systematic Review. *Water* **12**(10). DOI: 10.3390/w12102878.

Domínguez-Castro F, Vicente-Serrano SM, Tomás-Burguera M, Peña-Gallardo M, Beguería S, El Kenawy A, Luna Y, Morata A. 2019. High-spatial-resolution probability maps of drought duration and magnitude across Spain. *Natural Hazards and Earth System Sciences* **19**(3): 611–628. DOI: 10.5194/nhess-19-611-2019.

Filoso S, Bezerra MO, Weiss KCB, Palmer MA. 2017. Impacts of forest restoration on water yield: A systematic review. *PLoS ONE* **12**: e0183210.

Fritts HC. 1976. No Title. *Tree Rings and Climate*.

Garcia-Ruiz JM, Lasanta-Martinez T. 1990. Land-use changes in the Spanish Pyrenees. *Mountain Research & Development* **10**(3): 267–279. DOI: 10.2307/3673606.

García-Ruiz JM, López-Moreno JI, Lasanta T, Vicente-Serrano SM, González-Sampériz P, Valero-Garcés BL, Sanjuán Y, Beguería S, Nadal-Romero E, Lana-Renault N, Gómez-Villar A. 2015. Geo-ecological effects of global change in the Central Spanish Pyrenees: A review at different spatial and temporal scales [Los efectos geoecológicos del cambio global en el pirineo central español: Una revisión a distintas escalas espaciales y temporales. *Pirineos* **170**. DOI: 10.3989/Pirineos.2015.170005.

García-Ruiz JM, Regüés D, Alvera B, Lana-Renault N, Serrano-Muela P, Nadal-Romero E, Navas A, Latron J, Martí-Bono C, Arnáez J. 2008. Flood generation and sediment transport in experimental catchments affected by land use changes in the central Pyrenees. *Journal of Hydrology* **356**(1): 245–260. DOI: https://doi.org/10.1016/j.jhydrol.2008.04.013.

Gazol A, Camarero JJ, Sangüesa-Barreda G, Vicente-Serrano SM. 2018a. Post-drought Resilience After Forest Die-Off: Shifts in Regeneration, Composition, Growth and Productivity. *Frontiers in Plant Science* **9**: 1546. DOI: 10.3389/fpls.2018.01546.

Gazol A, Camarero JJ, Vicente-Serrano SM, Sánchez-Salguero R, Gutiérrez E, de Luis M, Sangüesa-Barreda G, Novak K, Rozas V, Tíscar PA, Linares JC, Martín-Hernández N, Martínez del Castillo E, Ribas M, García-González I, Silla F, Camisón A, Génova M, Olano JM, Longares LA, Hevia A, Tomás-Burguera M, Galván JD. 2018b. Forest resilience to drought varies across biomes. *Global Change Biology* **24**(5). DOI:

10.1111/gcb.14082.
Hobbins MT, Wood A, McEvoy DJ, Huntington JL, Morton C, Anderson M, Hain C. 2016. The evaporative demand drought index. Part I: Linking drought evolution to variations in evaporative demand. *Journal of Hydrometeorology* **17**(6): 1745–1761. DOI: 10.1175/JHM-D-15-0121.1.
Hoek van Dijke AJ, Herold M, Mallick K, Benedict I, Machwitz M, Schlerf M, Pranindita A, Theeuwen JJE, Bastin J-F, Teuling AJ. 2022. Shifts in regional water availability due to global tree restoration. *Nature Geoscience* **15**(5): 363–368. DOI: 10.1038/s41561-022-00935-0.
Hsiao TC. 1973. Plant Responses to Water Stress. *Annual Review of Plant Physiology*. Annual Reviews **24**(1): 519–570. DOI: 10.1146/annurev.pp.24.060173.002511.
Huete A, Didan K, Miura T, Rodriguez EP, Gao X, Ferreira LG. 2002. Overview of the radiometric and biophysical performance of the MODIS vegetation indices. *Remote Sensing of Environment* **83**(1–2): 195–213. DOI: 10.1016/S0034-4257(02)00096-2.
Kim D, Rhee J. 2016. A drought index based on actual evapotranspiration from the Bouchet hypothesis. *Geophysical Research Letters* **43**(19): 10,277-10,285. DOI: 10.1002/2016GL070302.
Lasanta-Martínez T, Vicente-Serrano SM, Cuadrat-Prats JM. 2005. Mountain Mediterranean landscape evolution caused by the abandonment of traditional primary activities: A study of the Spanish Central Pyrenees. *Applied Geography* **25**(1). DOI: 10.1016/j.apgeog.2004.11.001.
Lloyd-Hughes B. 2014. The impracticality of a universal drought definition. *Theoretical and Applied Climatology* **117**(3–4): 607–611. DOI: 10.1007/s00704-013-1025-7.
López-Moreno JI, Beguería S, García-Ruiz JM. 2004. The management of a large Mediterranean reservoir: Storage regimens of the Yesa Reservoir, Upper Aragon River basin, Central Spanish Pyrenees. *Environmental Management* **34**(4): 508–515. DOI: 10.1007/s00267-003-0249-1.
López-Moreno JI, García-Ruiz JM. 2004. Influence of snow accumulation and snowmelt on streamflow in the central Spanish Pyrenees | Influence de l'accumulation et de la fonte de la neige sur les écoulements dans les Pyrénées centrales espagnoles. *Hydrological Sciences Journal* **49**(5): 787–802.
López-Moreno JI, Soubeyroux JM, Gascoin S, Alonso-Gonzalez E, Durán-Gómez N, Lafaysse M, Vernay M, Carmagnola C, Morin S. 2020. Long-term trends (1958–2017) in snow cover duration and depth in the Pyrenees. *International Journal of Climatology*. John Wiley & Sons, Ltd **n/a**(n/a). DOI: 10.1002/joc.6571.
López-Moreno JI, Vicente-Serrano SM, Moran-Tejeda E, Zabalza J, Lorenzo-Lacruz J, García-Ruiz JM. 2011. Impact of climate evolution and land use changes on water yield in the ebro basin. *Hydrology and Earth System Sciences* **15**(1). DOI: 10.5194/hess-15-311-2011.
Martínez-Fernández J, Sánchez N, Herrero-Jiménez CM. 2013. Recent trends in rivers with near-natural flow regime: The case of the river headwaters in Spain. *Progress in Physical Geography* **37**(5): 685–700. DOI: 10.1177/0309133313496834.
McKee TB, Doesken NJ, Kleist J. 1993. The relationship of drought frequency and duration to time scales. *Eighth Conf. on Applied Climatology* 179–184.
Mukherjee S, Mishra A, Trenberth KE. 2018. Climate Change and Drought: a Perspective on Drought Indices. *Current Climate Change Reports* **4**(2): 145–163. DOI: 10.1007/s40641-018-0098-x.
O'Connor P, Murphy C, Matthews T, Wilby RL. 2022. Relating drought indices to impacts reported in newspaper articles. *International Journal of Climatology*. John Wiley & Sons, Ltd **n/a**(n/a). DOI: https://doi.org/10.1002/joc.7946.

Orth R, Destouni G. 2018. Drought reduces blue-water fluxes more strongly than green-water fluxes in Europe. *Nature Communications* **9**(1). DOI: 10.1038/s41467-018-06013-7.

Padrón RS, Gudmundsson L, Decharme B, Ducharne A, Lawrence DM, Mao J, Peano D, Krinner G, Kim H, Seneviratne SI. 2020. Observed changes in dry-season water availability attributed to human-induced climate change. *Nature Geoscience* **13**(7): 477–481. DOI: 10.1038/s41561-020-0594-1.

Pasho E, Camarero JJ, de Luis M, Vicente-Serrano SM. 2011. Impacts of drought at different time scales on forest growth across a wide climatic gradient in north-eastern Spain. *Agricultural and Forest Meteorology* **151**(12). DOI: 10.1016/j.agrformet.2011.07.018.

Peguero-Pina JJ, Camarero JJ, Abadía A, Martín E, González-Cascón R, Morales F, Gil-Pelegrín E. 2007. Physiological performance of silver-fir (Abies alba Mill.) populations under contrasting climates near the south-western distribution limit of the species. *Flora: Morphology, Distribution, Functional Ecology of Plants* **202**(3): 226–236. DOI: 10.1016/j.flora.2006.06.004.

Peña-Gallardo M, Vicente-Serrano SM, Camarero JJ, Gazol A, Sánchez-Salguero R, Domínguez-Castro F, El Kenawy A, Beguería-Portugés S, Gutiérrez E, de Luis M, Sangüesa-Barreda G, Novak K, Rozas V, Tíscar PA, Linares JC, del Castillo E, Ribas Matamoros M, García-González I, Silla F, Camisón Á, Génova M, Olano JM, Longares LA, Hevia A, Galván JD. 2018. Drought Sensitiveness on Forest Growth in Peninsular Spain and the Balearic Islands. *Forests* **9**(9).

Peña-Gallardo M, Vicente-Serrano SM, Hannaford J, Lorenzo-Lacruz J, Svoboda M, Domínguez-Castro F, Maneta M, Tomas-Burguera M, Kenawy AE. 2019. Complex influences of meteorological drought time-scales on hydrological droughts in natural basins of the contiguous Unites States. *Journal of Hydrology* **568**: 611–625. DOI: 10.1016/j.jhydrol.2018.11.026.

Pereira LS, Allen RG, Smith M, Raes D. 2015. Crop evapotranspiration estimation with FAO56: Past and future. *Agricultural Water Management* **147**: 4–20. DOI: 10.1016/j.agwat.2014.07.031.

Quiring SM, Papakryiakou TN. 2003. An evaluation of agricultural drought indices for the Canadian prairies. *Agricultural and Forest Meteorology* **118**(1): 49–62. DOI: 10.1016/S0168-1923(03)00072-8.

Sanjuán Y, Arnáez J, Beguería S, Lana-Renault N, Lasanta T, Gómez-Villar A, Álvarez-Martínez J, Coba-Pérez P, García-Ruiz JM. 2018. Woody plant encroachment following grazing abandonment in the subalpine belt: a case study in northern Spain. *Regional Environmental Change* **18**(4): 1103–1115. DOI: 10.1007/s10113-017-1245-y.

Shukla S, Wood AW. 2008. Use of a standardized runoff index for characterizing hydrologic drought. *Geophysical Research Letters* **35**(2). DOI: 10.1029/2007GL032487.

Tague CL, Band LE. 2004. RHESSys: Regional Hydro-Ecologic Simulation System—An Object-Oriented Approach to Spatially Distributed Modeling of Carbon, Water, and Nutrient Cycling. *Earth Interactions*. American Meteorological Society **8**(19): 1–42. DOI: 10.1175/1087-3562(2004)8<1:RRHSSO>2.0.CO;2.

Teuling AJ, de Badts E, Jansen FA, Fuchs R, Buitink J, van Dijke AJ, Sterling S. 2019. Climate change, re-/afforestation, and urbanisation impacts on evapotranspiration and streamflow in Europe. *Hydrology and Earth System Sciences Discussions* **2019**: 1–30. DOI: 10.5194/hess-2018-634.

Teuling AJ, Van Loon AF, Seneviratne SI, Lehner I, Aubinet M, Heinesch B, Bernhofer C, Grünwald T, Prasse H, Spank U. 2013. Evapotranspiration amplifies European summer drought. *Geophysical Research Letters* **40**(10): 2071–2075. DOI: 10.1002/grl.50495.

Tian L, Yuan S, Quiring SM. 2018. Evaluation of six indices for monitoring agricultural drought in the south-central United States. *Agricultural and Forest Meteorology*. Elsevier **249**: 107–119. DOI: 10.1016/J.AGRFORMET.2017.11.024.

Trnka M, Hlavinka P, Možný M, Semerádová D, Štěpánek P, Balek J, Bartošová L, Zahradníček P, Bláhová M, Skalák P, Farda A, Hayes M, Svoboda M, Wagner W, Eitzinger J, Fischer M, Žalud Z. 2020. Czech Drought Monitor System for monitoring and forecasting agricultural drought and drought impacts. *International Journal of Climatology*. John Wiley & Sons, Ltd **n/a**(n/a). DOI: 10.1002/joc.6557.

Tsakiris G, Pangalou D, Vangelis H. 2007. Regional Drought Assessment Based on the Reconnaissance Drought Index (RDI). *Water Resources Management* **21**(5): 821–833. DOI: 10.1007/s11269-006-9105-4.

Ukkola AM, Prentice IC, Keenan TF, Van Dijk AIJM, Viney NR, Myneni RB, Bi J. 2016. Reduced streamflow in water-stressed climates consistent with CO<inf>2</inf>effects on vegetation. *Nature Climate Change* **6**(1): 75–78. DOI: 10.1038/nclimate2831.

Vicente-Serrano SM. 2016. Foreword: Drought complexity and assessment under climate change conditions. *Cuadernos de Investigacion Geografica* **42**(1). DOI: 10.18172/cig.2961.

Vicente-Serrano SM, Beguería S, López-Moreno JI. 2010. A multiscalar drought index sensitive to global warming: The standardized precipitation evapotranspiration index. *Journal of Climate* **23**(7). DOI: 10.1175/2009JCLI2909.1.

Vicente-Serrano SM, Domínguez-Castro F, Murphy C, Peña-Angulo D, Tomas-Burguera M, Noguera I, López-Moreno JI, Juez C, Grainger S, Eklundh L, Conradt T, Azorin-Molina C, El Kenawy A. 2021a. Increased Vegetation in Mountainous Headwaters Amplifies Water Stress During Dry Periods. *Geophysical Research Letters*. John Wiley & Sons, Ltd **48**(18): e2021GL094672. DOI: https://doi.org/10.1029/2021GL094672.

Vicente-Serrano SM, Domínguez-Castro F, Reig F, Beguería S, Tomas-Burguera M, Latorre B, Peña-Angulo D, Noguera I, Rabanaque I, Luna Y, Morata A, El Kenawy A. 2022. A near real-time drought monitoring system for Spain using automatic weather station network. *Atmospheric Research* **271**. DOI: 10.1016/j.atmosres.2022.106095.

Vicente-Serrano SM, Lanjeri S, López-Moreno JI. 2007. Comparison of different procedures to map reference evapotranspiration using geographical information systems and regression-based techniques. *International Journal of Climatology* **27**(8). DOI: 10.1002/joc.1460.

Vicente-Serrano SM, Lopez-Moreno J-I, Beguería S, Lorenzo-Lacruz J, Sanchez-Lorenzo A, García-Ruiz JM, Azorin-Molina C, Morán-Tejeda E, Revuelto J, Trigo R, Coelho F, Espejo F. 2014. Evidence of increasing drought severity caused by temperature rise in southern Europe. *Environmental Research Letters* **9**(4): 044001. DOI: 10.1088/1748-9326/9/4/044001.

Vicente-Serrano SM, López-Moreno JI, Beguería S, Lorenzo-Lacruz J, Azorin-Molina C, Morán-Tejeda E. 2012. Accurate Computation of a Streamflow Drought Index. *Journal of Hydrologic Engineering* **17**(2). DOI: 10.1061/(ASCE)HE.1943-5584.0000433.

Vicente-Serrano SM, Peña-Angulo D, Murphy C, López-Moreno JI, Tomas-Burguera M, Domínguez-Castro F, Tian F, Eklundh L, Cai Z, Alvarez-Farizo B, Noguera I, Camarero JJ, Sánchez-Salguero R, Gazol A, Grainger S, Conradt T, Boincean B, El Kenawy A. 2021b. The complex multi-sectoral impacts of drought: Evidence from a mountainous basin in the Central Spanish Pyrenees. *Science of the Total Environment* **769**. DOI: 10.1016/j.scitotenv.2020.144702.

Vicente-Serrano SM, Peña-Gallardo M, Hannaford J, Murphy C, Lorenzo-Lacruz J, Dominguez-Castro F, López-Moreno JI, Beguería S, Noguera I, Harrigan S, Vidal J-P. 2019. Climate, Irrigation, and Land Cover Change Explain Streamflow Trends in Countries Bordering the Northeast Atlantic. *Geophysical Research Letters* **46**(19). DOI: 10.1029/2019GL084084.

Vicente-Serrano SM, Tomas-Burguera M, Beguería S, Reig F, Latorre B, Peña-Gallardo M, Luna MY, Morata A, González-Hidalgo JC. 2017. A High Resolution Dataset of Drought Indices for Spain. *Data* **2**(3).

Vicente-Serrano SMM, Martín-Hernández N, Reig F, Azorin-Molina C, Zabalza J, Beguería S, Domínguez-Castro F, El Kenawy A, Peña-Gallardo M, Noguera I, García M. 2020. Vegetation greening in Spain detected from long term data (1981–2015). *International Journal of Remote Sensing* **41**(5): 1709–1740. DOI: 10.1080/01431161.2019.1674460.

Vicente-Serrano SM. 2021. The complex multi-sectoral impacts of drought: Evidence from a mountainous basin in the Central Spanish Pyrenees. *Science of the Total Environment*.

Wang H, Vicente-serrano SM, Tao F, Zhang X, Wang P, Zhang C, Chen Y, Zhu D, Kenawy AE. 2016. Monitoring winter wheat drought threat in Northern China using multiple climate-based drought indices and soil moisture during 2000–2013. *Agricultural and Forest Meteorology* **228**–**229**. DOI: 10.1016/j.agrformet.2016.06.004.

Wilhite DA, Buchanan-Smith M. 2005. *Drought as hazard: Understanding the natural and social context*. *Drought and Water Crises: Science, Technology, and Management Issues*.

Wilhite DA, Pulwarty RS. 2017. Drought as Hazard: Understanding the Natural and Social Context. *Drought and Water Crises: Integrating Science, Management, and Policy*, 3–22.

Wilhite DA, Svoboda MD, Hayes MJ. 2007. Understanding the complex impacts of drought: A key to enhancing drought mitigation and preparedness. *Water Resources Management* **21**(5): 763–774. DOI: 10.1007/s11269-006-9076-5.

Yang Y, Zhang S, McVicar TR, Beck HE, Zhang Y, Liu B. 2018. Disconnection Between Trends of Atmospheric Drying and Continental Runoff. *Water Resources Research* **54**(7): 4700–4713. DOI: 10.1029/2018WR022593.

Yuan S, Quiring SM, Zhao C. 2020. Evaluating the Utility of Drought Indices as Soil Moisture Proxies for Drought Monitoring and Land–Atmosphere Interactions. *Journal of Hydrometeorology* **21**(9): 2157–2175. DOI: 10.1175/JHM-D-20-0022.1.

Zeng Z, Piao S, Li LZX, Wang T, Ciais P, Lian X, Yang Y, Mao J, Shi X, Myneni RB. 2018. Impact of Earth Greening on the Terrestrial Water Cycle. *Journal of Climate*. American Meteorological Society: Boston MA, USA **31**(7): 2633–2650. DOI: 10.1175/JCLI-D-17-0236.1.

Zhang X, Hao Z, Singh VP, Zhang Y, Feng S, Xu Y, Hao F. 2022. Drought propagation under global warming: Characteristics, approaches, processes, and controlling factors. *Science of The Total Environment* **838**: 156021. DOI: https://doi.org/10.1016/j.scitotenv.2022.156021.

Section ii)

Increased vegetation in mountainous headwaters amplifies water stress during dry periods

1. Introduction

The partitioning of precipitation between blue water, defined as runoff generation, and green water, representing water consumption by vegetation, determines the availability of surface water resources for human activities and freshwater ecosystems (Rulli et al., 2013). Green water is the largest fraction globally (Wang & Dickinson, 2012), but is challenging to quantify (Mueller et al., 2013). Modeling studies suggest a general increase in green water in recent decades, as a consequence of higher plant leaf area (Forzieri et al., 2020; Zeng et al., 2018), longer vegetative periods (Lian et al., 2020), and greater atmospheric evaporative demand (AED) (Vicente-Serrano et al., 2020).

The total vegetation coverage controls the relationship between total evaporation and total precipitation at the catchment scale (Zhang et al., 2001). This would explain how hydrological processes are impacted by changes in leaf area index and plant biomass (Forzieri et al., 2020; Zeng et al., 2018) and the replacement of plant species through secondary succession (Leuschner & Rode, 1999). Studies indicate that reduced tree coverage increases runoff generation after disturbances (Bosch & Hewlett, 1982) since after reduction of the dominant vegetation of a catchment, evaporation is usually reduced (Anderegg et al., 2016; Wine et al., 2017; Winkler et al., 2017). Overall, re-afforestation practices and natural secondary succession reduce runoff production (Filoso et al., 2017), although the magnitude of change is highly dependent on the vegetation types and the environmental conditions, such as average precipitation (Brown et al., 2005) and forest age (Teuling & van Dijke, 2020).

In southern Europe, different studies have shown a general reduction of streamflow in recent decades (Gudmundsson et al., 2017; Lorenzo-Lacruz et al., 2012; Stahl et al., 2010). Land abandonment and/or re-afforestation have resulted in a large increase in vegetation coverage in the region's headwaters (Lasanta-Martínez et al., 2005; Lasanta et al., 2017; Sanjuán et al., 2018) and different studies have stressed the fundamental role of higher plant transpiration in explaining streamflow trends in the region (García-Ruiz et al., 2011; Teuling et al., 2019; Vicente-Serrano et al., 2019). Thus, in the Mediterranean mountainous areas of Spain, the increase in the forest surface is the most plausible explanation for streamflow reductions in the headwaters (Beguería et al., 2003; Buendia et al., 2016; Martínez-Fernández et al., 2013; Morán-Tejeda et al., 2012).

Unraveling the interaction between vegetation and climate variability, as well as their impact on the partitioning of precipitation into blue and green water, is a high-priority research topic. While an increase in green water consumption has been linked to greening (Forzieri et al., 2020; Ukkola et al., 2016), it is unclear how water availability and seasonality affect the dependency between vegetation changes and precipitation partitioning. Although some studies have identified a dominance in the green water in response to drought events (Orth & Destouni, 2018), particularly during warm years (Mastrotheodoros et al., 2020), there is little understanding of the interaction between vegetation changes and the interannual and intraanual variability of climate conditions to explain anomalies and long-term streamflow trends.

We hypothesize that dominant re-vegetation changes in mountain Mediterranean areas of southern Europe have been the primary cause of the large decline in streamflow observed in recent decades. Nevertheless, the role of these vegetation changes in the partition of precipitation between blue and green water is dependent on interannual climate variability, with the role being stronger during dry years when the system has less available water. Moreover, the role of the vegetation changes in the blue and green partition would be seasonally dependent, with the role of vegetation being stronger in summer dry season, when vegetation is more active.

Here, we analyse the influence of vegetation changes on blue water generation in a humid natural basin (the upper Aragón basin,) over the last six decades (1962-2019). This basin, located in the Spanish Pyrenees (2181 km^2), is characterized by intense secondary succession toward more mature vegetation communities, representing a "typical" example of recent observed vegetation changes in mountainous areas of southern Europe (García-Ruiz et al., 2011; Lasanta et al., 2017). Accordingly, results of this work can be applied to a broad spatial region in Southern Europe, where water scarcity is a serious socioeconomic and environmental issue.

2. Description of the study area

The Upper Aragón River basin covers an area of 2181 km^2 (Figure 1), with the most elevated areas located in the north (Collarada Peak, 2886 m). The Aragón River flows north–south across the Paleozoic area (limestone, shale and clay), the Inner Sierras (limestone and sandstone) and the flysch sector before entering the Inner Depression (marls) and flowing westward. The average annual precipitation is 1303 mm, although it can reach 1500 mm in the most elevated sites and falls below 800 mm in the Inner Depression. Precipitation is mostly recorded between October and May with a summer dry season characterized by isolated rainstorm events caused by convective processes. Following the FAO-56 Penman-Monteith equation (Pereira et al., 2015), the annual atmospheric evaporative demand (AED) may reach 1045 mm. From December to April, snow cover is generally permanent above elevations of 1500 m a.s.l. (López-Moreno et al., 2020). Long-term annual streamflow is 1318 Hm^3. Winter flow is low due to snow accumulation, while the peak flow of 172.9 Hm^3 occurs in April, corresponding to the maximum precipitation and snowmelt. Rather, August is the month with the lowest river flow (29.3 Hm^3). The Yesa reservoir, with a capacity of 446.8 hm^3, is an important water management infrastructure because it supplies water for irrigation to the Bardenas region (81,000 ha) located 80 km to the south of the basin (López-Moreno et al., 2004; Vicente-Serrano, 2021). Also, it supplies water to Zaragoza, the most populated city (700,000 inhabitants) in the Ebro basin.

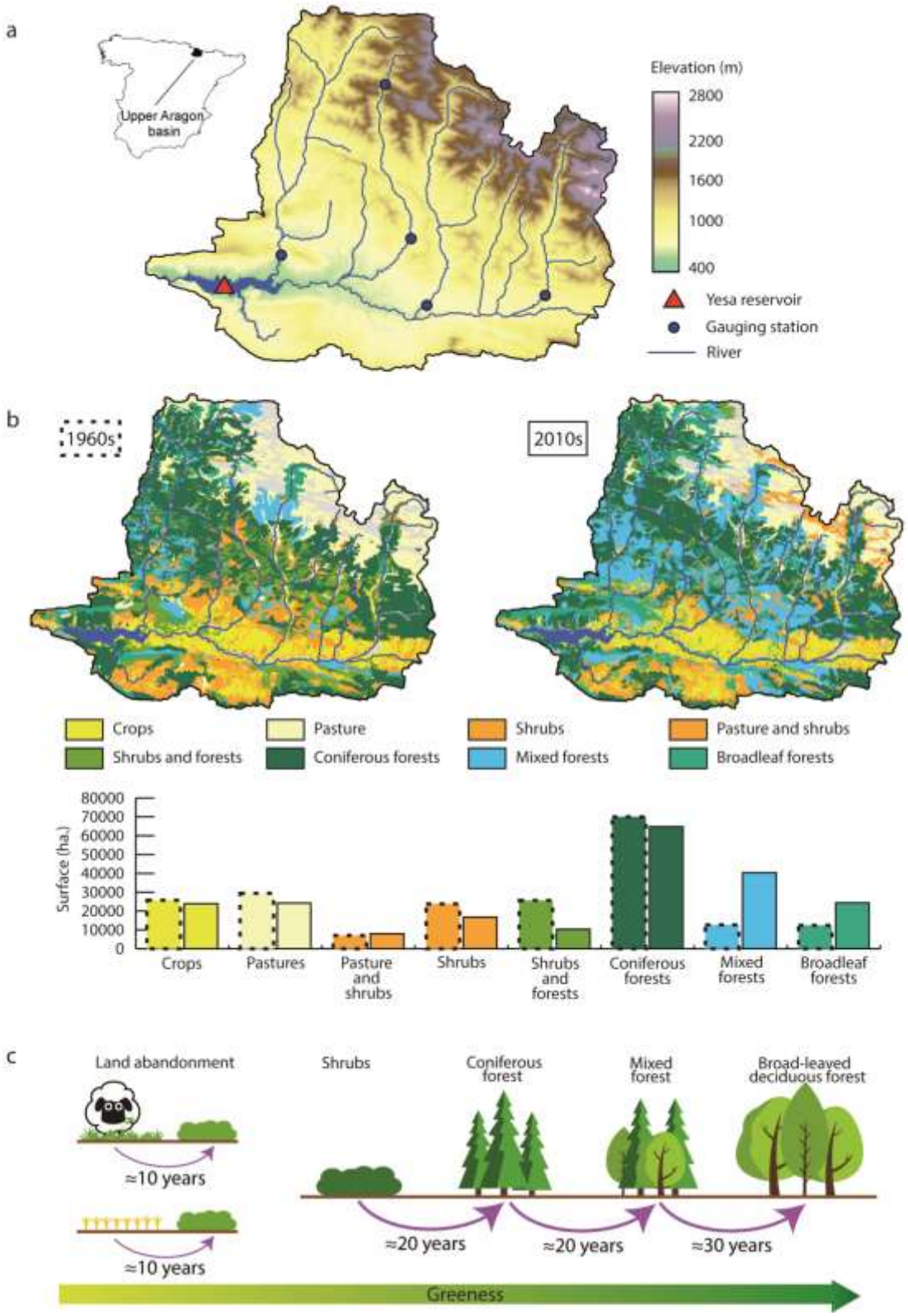

Figure 1: a) Physiography and main river network in the upper Aragón basin, b) land cover changes distribution and changes between the decades of 1960s and 2010s and c) dominant process of vegetation succession phases and lapse times in the study domain.

Vegetation cover in the upper Aragon basin is characterized by the dominance of conifers (e.g. *Pinus sylvestris L., Pinus uncinata Ram., Abies alba Mill., Pinus nigra J.F. Arn.)* and hardwood species (e.g. *Fagus sylvatica L., Quercus faginea Lam.*), while shrubs dominate the understory (e.g., *Buxus sempervirens L.*) or distributed over the surfaced slopes and in areas of poor soil (J.M. García-Ruiz et al., 2015). Winter cereals (mainly barley and wheat) dominate in the Inner depression. Vegetation cover in the basin has been strongly impacted by human activities. Historically, cultivated areas were found below 1600 m a.s.l. in valley bottoms, perched flats, and steep, south-facing hillslopes, which were managed even under shifting agriculture systems (Garcia-Ruiz & Lasanta-Martinez, 1990). The Aragón basin has undergone a land cover transformation in the 20th century, due to depopulation (Garcia-Ruiz & Lasanta-Martinez, 1990). The abandonment of agriculture, which represented 30% of the study area (Beguería et al., 2003), and livestock practices have resulted in a gradual natural revegetation process (Lasanta-Martínez et al., 2005; Sanjuán et al., 2018). This process was characterized by rapid changes between succession phases (Kouba et al., 2012; Lasanta-Martínez et al., 2005; Molinillo et al., 1997). In addition, some areas were reforested during the 1950s and 1960s (Ortigosa et al., 1990). Since the 1960s, vegetation changes have been characterized by dominant secondary succession, with coniferous forests being replaced by mixed and broadleaf forests. Currently, these biotas make up the main land cover types in the basin (Figure 1). This process has been accompanied by forest densification and foliar coverage increase (Vicente-Serrano et al., 2006), explaining a large increase in satellite photosynthetic activity since the 1980s (Figure 2) and representing a common change in the majority of the Mediterranean mountainous areas (J.M. García-Ruiz et al., 2011).

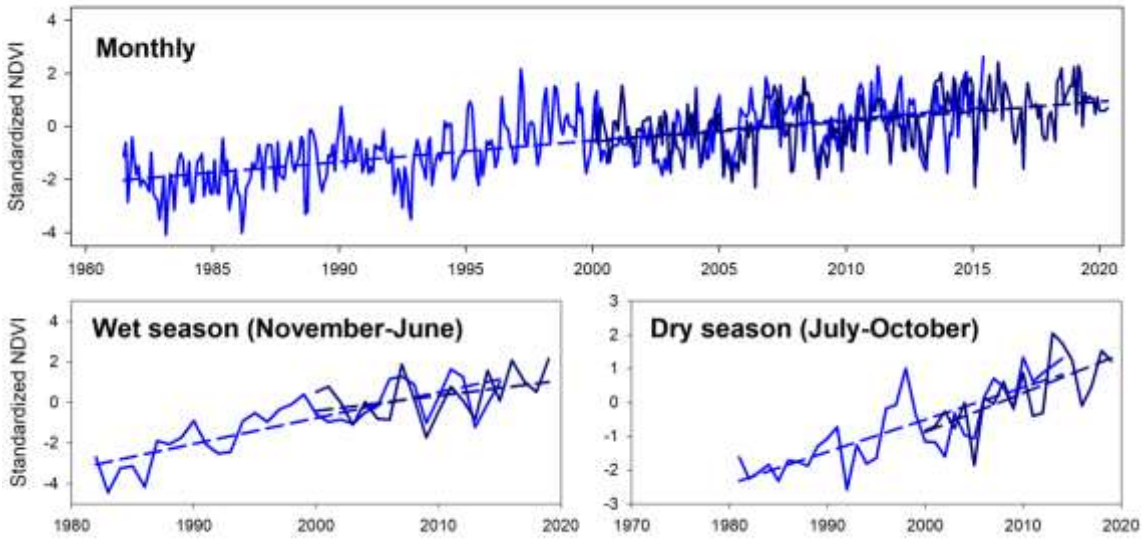

Figure 2: Evolution of the average standardized monthly and seasonal NDVI over the upper Aragón basin from 1981 to 2019. The reference period to obtain standardized values is the common 2000-2014. Blue solid lines represent the NOAA-AVHRR NDVI series and dark-blue solid lines the MODIS NDVI series. Dashed lines are the regression fits obtained by means of least-squares.

3. Material and methods

3.1. Data

Daily streamflow data for the basin was provided by the Ebro Basin Management Agency (CHE) (*Confederación Hidrográfica del Ebro*, http://www.chebro.es/; last accessed 1 February 2021). We derived the streamflow (in cubic hectometers, Hm^3) generated over the entire basin draining to the Yesa reservoir, which has been calculated by the CHE since 1962 by means of a mass balance using the reservoir data at the daily scale. The accuracy of this mass balance calculation was verified using monthly streamflow data from five available gauging stations spanning the study domain (Figure 3). Data were summarized for the wet (November-June) and dry (July-October) seasons, as well as annually (Figure 4). Herein, hydrological year spans the period between October and September.

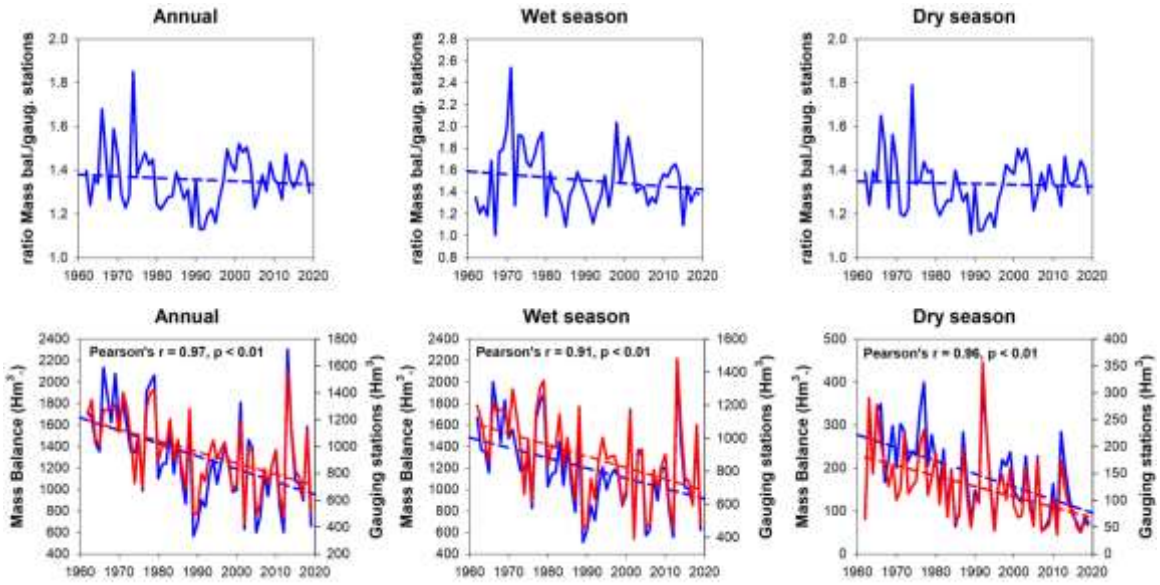

Figure 3: Top: evolution of the ratio of the sum of streamflow measured in the five available gauging stations together with the entire streamflow production obtained by the mass balance procedure with reservoir data. Bottom: evolution of the streamflow production generated by the mass balance procedure with reservoir data (blue) and the sum of streamflow measured at the five available gauging stations (red) (See locations in Fig 1). Dashed lines show linear regressions fitted using least-squares. The evolution of the ratio between the sum of streamflow data measured in the gauging stations and the total calculated streamflow does not show trends at the annual scale, and during both the wet (November-June) and dry (July-October) season. The water level of the reservoir and the outflows (in m^3/s) are monitored each minute by the Ebro Basin Management Agency. Given the sediment accumulation rates in the Yesa reservoir are very low and they have a clear decreasing trend (Navas et al., 2009) given small erosion processes as consequence of general agricultural abandonment and dominant natural revegetation processes in the basin (García-Ruiz et al., 2015; García-Ruiz et al., 2008; Lasanta et al., 2010), the method to assess water generation in the basin is very robust. Given that the annual and seasonal series have similar evolutions and trend magnitudes that the average steamflow series by different available gauging stations, the total streamflow provided by the Ebro Basin Management Agency is fully representative of the evolution of total streamflow production in the basin."

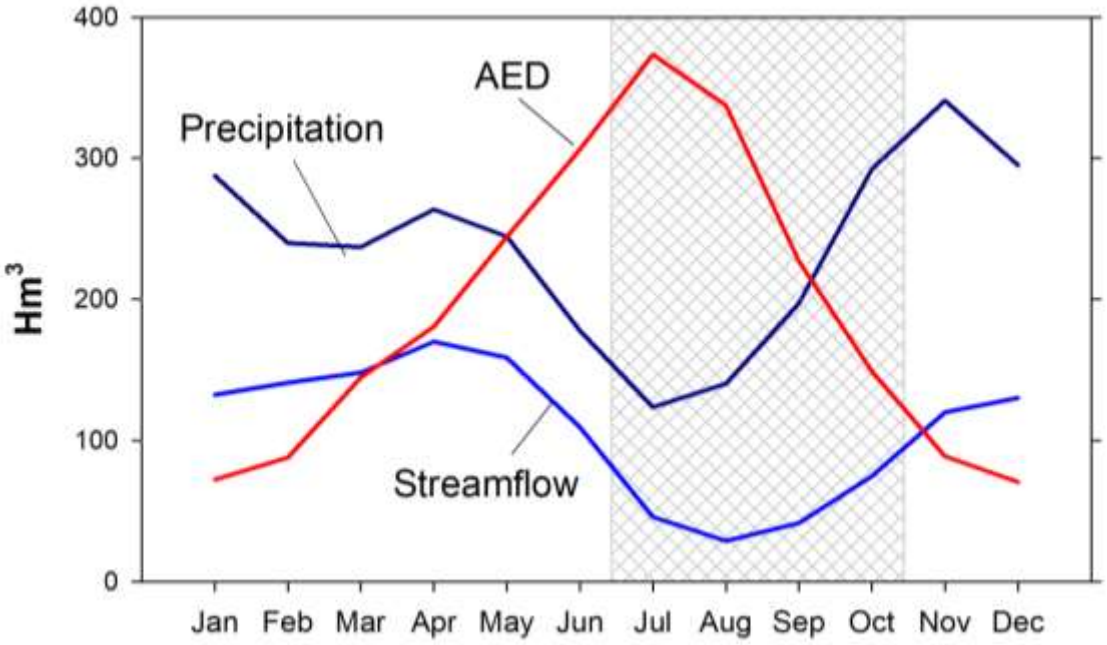

Figure 4: Average precipitation and streamflow over the basin. The low flow period is recorded between July and October (dry season) and marked with grey shading, while the high flow period occurs between November and June (wet season).

Climate data were obtained from a high-resolution (1.1 km) weekly gridded dataset for the whole of Spain from 1962 to 2019. This dataset was developed using the most complete register of meteorological data provided by the Spanish National Meteorological Service (AEMET) (Agencia Estatal de Meteorología, http://www.aemet.es/es/portada; last accessed 1 February 2021). The raw data were quality controlled, homogenized, and interpolated to a common grid resolution of 1.1 km. Further details about this dataset development are outlined in Vicente-Serrano et al. (2017). The gridded data of air temperature, relative humidity, sunshine duration (as a proxy for solar radiation), and wind speed were used to calculate atmospheric evaporative demand (AED) by means of the FAO-56 Penman-Monteith equation (Pereira et al., 2015). The complete drainage area, which was obtained from a digital elevation model at a spatial resolution of 100 m using ArcHydrotools in ArcGIS 10.2, was used to aggregate monthly precipitation and AED series over the entire basin. To be comparable with streamflow data, climate data were transformed to Hm^3 using the total basin area.

Land cover maps for the decades of 1960 and 2010 were provided by the Spanish Ministry of Agriculture (https: www.mapa.gob.es/es/cartografia-y-sig/publicaciones/agricultura/mac_2000_2009.aspx; last accessed 1 February 2021). Based on interpreting aerial photographs and conducting fieldwork, these maps were created at a spatial scale of 1:50000. To illustrate possible changes in greening conditions, the Normalized Difference Vegetation Index (NDVI) was calculated at a spatial resolution of 1.1 km using the NOAA-AVHRR images covering the period from 1981 to 2015 (Vicente-Serrano et al., 2020) combnined with MODIS NDVI (https://modis.gsfc.nasa.gov/data/dataprod/mod13.php) for the period 2000-2019. Both datasets were standardized using the reference period 2000-2015.

3.2. Methods

We have analyzed the magnitude of the trend in annual P, Q and AED to quantify the magnitude of the annual Q trend that may be associated to climate trends and vegetation changes. Significance of trends in hydrological and climatic variables was analysed by means of a modified Mann–Kendall trend test, which returns the corrected p values after accounting for temporal pseudoreplication (Hamed & Rao, 1998). To assess the magnitude of change in the different variables, we used a linear regression analysis between the series of time (independent variable) and the climatic and hydrological series (dependent variable). To quantify the magnitude of the annual Q trend that may be associated with climate trends and vegetation changes, we analyzed the annual trend magnitude of P, Q and AED. To figure out how climate and vegetation changes affect annual streamflow, we used multiple regression with streamflow as the dependent variable and precipitation, AED, and time as the independent variables (Beguería et al., 2003). Time was included in the models as a proxy for the progressive evolution of vegetation in the basin as a consequence of secondary succession. Due to the fact that the series only began in 1981, including NDVI was not possible; however, NDVI shows a clear linear increase (Figure 2), indicating that time can be used as a surrogate.

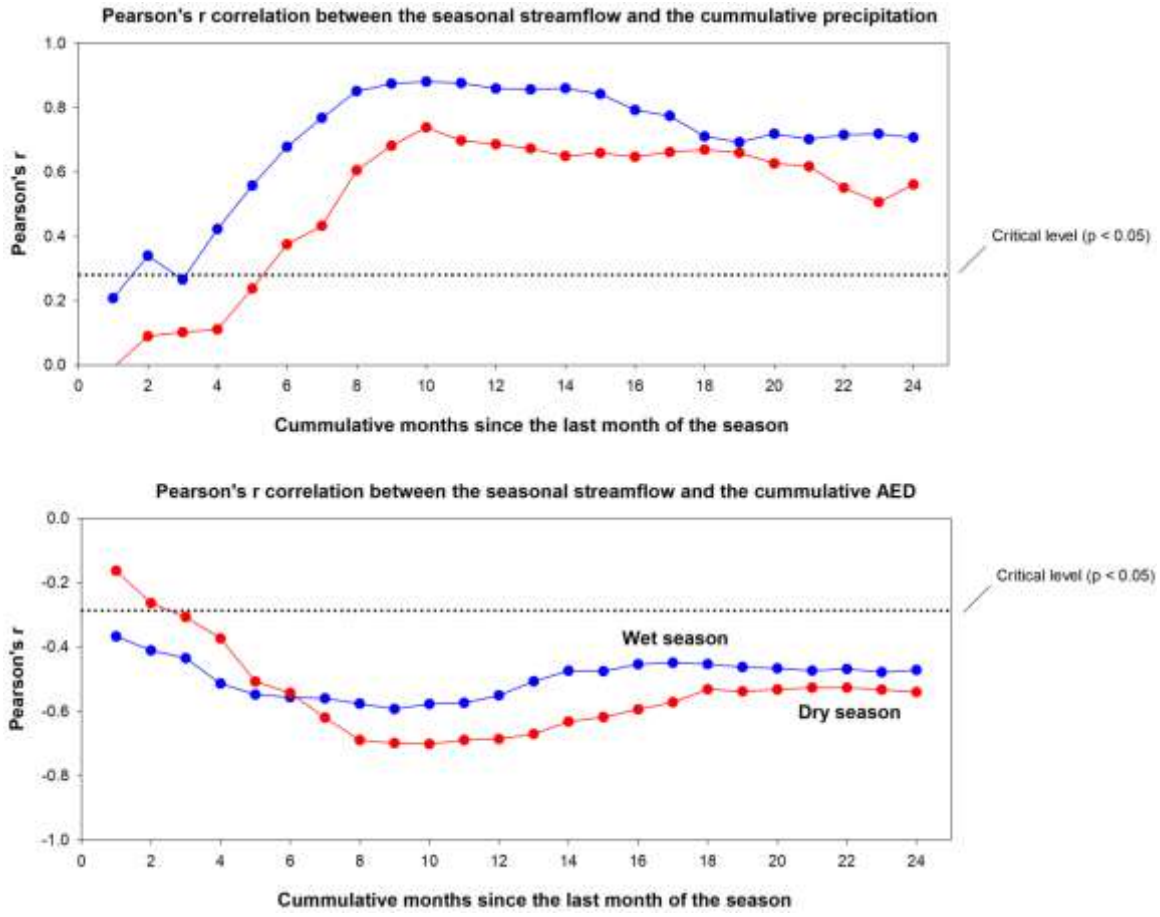

Figure 5: Pearson's r correlation coefficients between the streamflow series over the dry (red) and wet (blue) seasons and the monthly precipitation (top) and AED (bottom) accumulated for different periods.

The forward stepwise selection of predictors was used in the construction of regression models using a threshold of 0.05 (Hair et al., 1995). For the annual streamflow analysis,

annual precipitation totals and annual AED were considered as independent variables. Seasonally, there are large differences in the time windows in which climate variables are accumulated and affect streamflow, since they depend on physiographic and climatic variables (Barker et al., 2016; López-Moreno et al., 2013). For this reason, we first determined the precipitation and AED cumulative periods with the strongest correlations to streamflow (Figure 5). For the wet and dry seasons, higher correlations were obtained with precipitation accumulated for ten months before the end of the season. Therefore, the wet season precipitation totals from September to June were used as the independent variable in the regression model, while the dry season precipitation totals from January to October were used as the dependent variable. For the wet season, the maximum correlation between AED and streamflow was obtained for nine months, and for the dry season, the maximum correlation was obtained for ten months.

The ordinary least square regression method was used to assess trends for wet and dry years and seasons. Herein, wet years (seasons) were defined as those exceeding the 70th percentile of precipitation over the period of record. On the other hand, dry years (seasons) were determined as those with rainfall falling below the 30th percentile.

4. Results and discussion

Annual precipitation in the basin shows high variability, with a non-significant decrease of 8% in annual totals observed between 1962 and 2019 (Figure 6). Over the same time period, AED increased by 5.7%, which is statistically significant at the 95% level ($p<0.05$). From 1962 to 2019, the annual streamflow in the catchment decreased by more than 40%, which is consistent with the pattern observed in other natural non-managed basins in Spain (Martínez-Fernández et al., 2013). The decrease in annual streamflow is close to the increase (34.1%) in the estimated evaporation by means of the annual water balance. The decrease in streamflow cannot be attributed to changes in precipitation. Our findings indicate that annual precipitation decreased by 239.6 Hm^3 over the 58-year study period, while annual streamflow declined by 692.5 Hm^3. This difference (452.85 Hm^3) can be attributed to the net increase in evaporation. An assumption can be made that the amount of increase in AED between 1962 and 2019 corresponds to Evapotranspiration (E), as consequence of direct radiative forcing associated to warming. Nonetheless, this increase is only 130.9 Hm^3 and there are still 321 Hm^3 of streamflow decline between 1962 and 2019 that would not be explained by the observed climate trend. Moreover, it is important to note that the increase in observed AED cannot be completely associated to the increase in E since during summer months soil moisture deficits are common and there is an evaporation deficit (E-AED), which is the main driver controlling forest growth in the region (Vicente-Serrano et al., 2015). Thus drought has significant consequences on vegetation activity and growth in the study area (Camarero et al., 2011; Pasho et al., 2011; Peguero-Pina et al., 2007; Vicente-Serrano, 2021). After removing the role of precipitation, the non-climate-related streamflow decline would range between 321 Hm^3 (if AED increase is fully representing an increase in E) and 452.8 Hm^3 (assuming E changes are not driven by AED). These numbers represent between 46% and 65% of total streamflow decline, which would be explained primarily by the basin's secondary succession process.

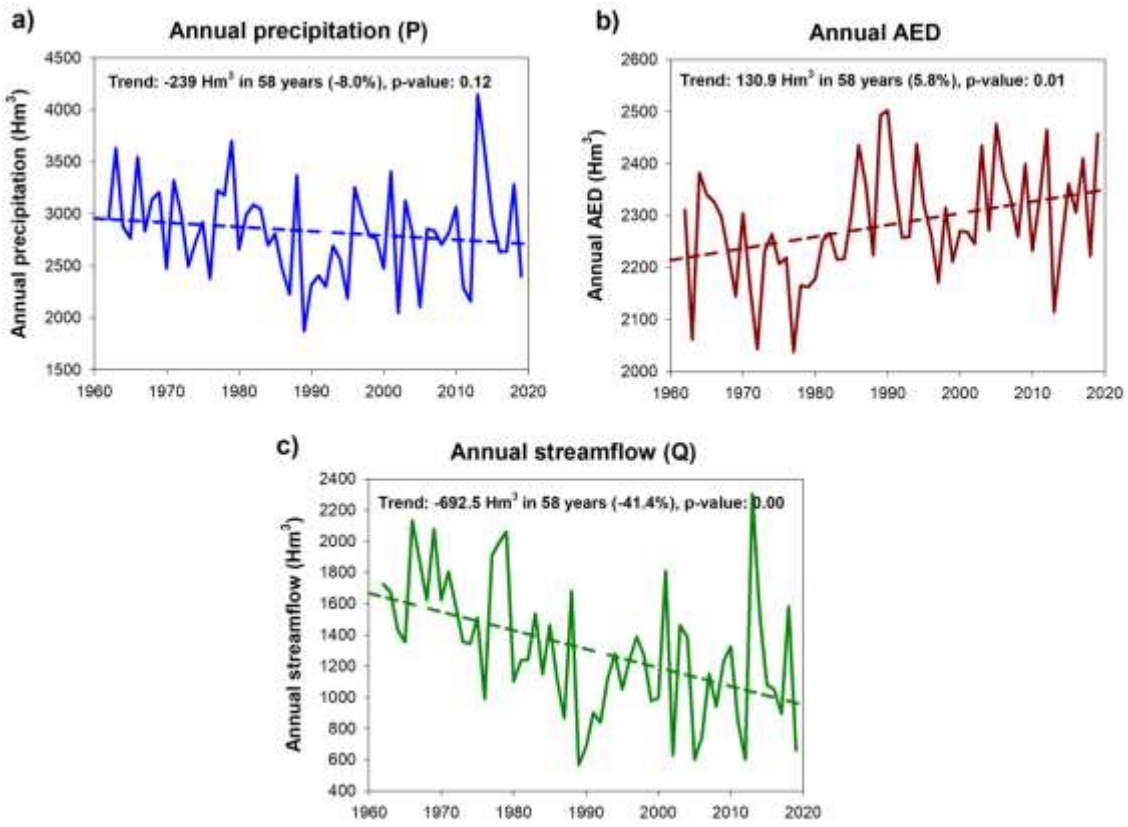

Figure 6: Temporal evolution of annual precipitation (a), atmospheric evaporative demand (AED) (b) and streamflow (c) in the upper Aragón basin for 1962-2019. Dashed lines represent the linear trend obtained by means of least-squares. The percentage changes between 1961 and 2019 are obtained from the regression lines. P-values are obtained by means of the modified Mann-Kendall test (See section 2.2).

The secondary role of the observed increase in AED in the streamflow reduction is confirmed by the regression analysis. Over the period 1962-2019, regression analysis using precipitation, AED, and time (in years, as a proxy for the effect of secondary succession and general greenness) as predictors of annual streamflow explains 82% of the variability in streamflow. However, AED was removed from our final model because it was not a significant predictor (Table 1). According to the partial correlation, precipitation has the largest (positive) influence on annual streamflow, while time exhibited a significant (negative) correlation. Annual precipitation showed a significant negative correlation with annual AED (Figure 7). The role of cloudiness in reducing solar radiation and air temperature can explain this negative relationship between precipitation and AED. Notably, the correlation between annual AED and streamflow was statistically non-significant after fixing (controlling) precipitation effect.

Table 1: Correlation coefficients of the linear stepwise regression analysis in which annual and seasonal streamflow was the dependent variable and precipitation, AED and Time (in years) were the independent predictors. R2 represents the percentage of total variance of the independent variable explained by the predictors. Partial correlations represent the role of each independent variable, removing the influence of the covariates. Predictors showing a non-significant (0.05 level) role in explaining streamflow variability were not included in the final models.

	R^2	Partial correlations		
		Precipitation	AED	Time
Annual	0.82	0.88	-0.09 (n.s.)	-0.64
Wet season (Nov.-Jun.)	0.87	0.92	-0.06 (n.s.)	-0.63
Dry season (Jul.-Oct.)	0.48	0.31	-0.21	-0.49

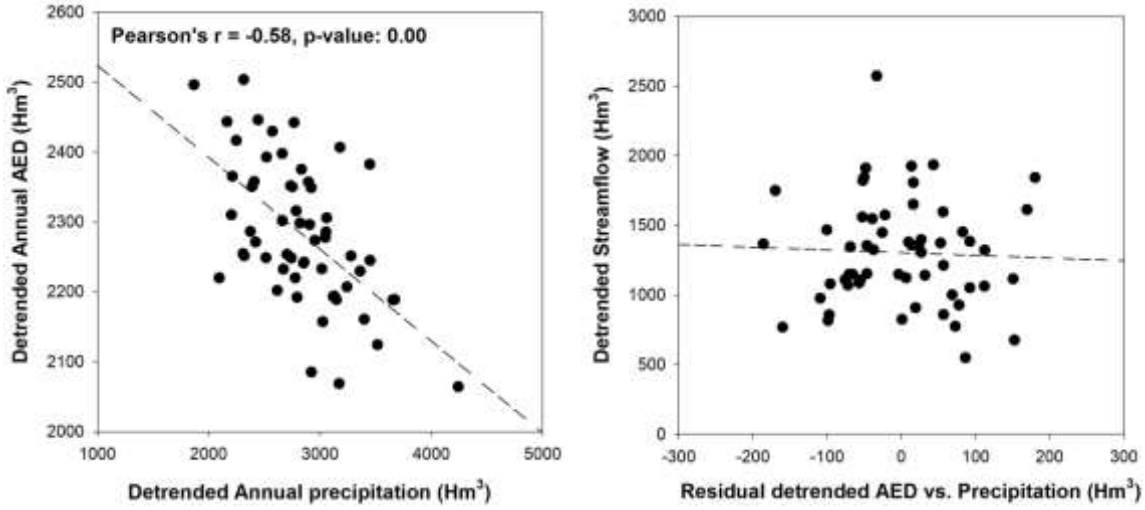

Figure 7: Left: relationship between the detrended annual precipitation and AED in the upper Aragón basin between 1962 and 2019. Right: relationship between detrended annual streamflow and the independent role of AED once the effect of precipitation is removed.

Seasonally, there is also a large decrease in streamflow, being much stronger (-63.7%) during the dry season (Figure 8). Again, this decrease can not be driven by precipitation, which showed a statistically non-significant decrease on the seasonal scale. During the dry season, AED showed a significant negative partial correlation with streamflow, but its influence on streamflow is minor compared to precipitation and time. In the dry season, the inclusion of AED in the linear model accounted only for 2.3% of the total variance in streamflow.

It can be concluded that while the interannual variability of streamflow is strongly correlated with annual precipitation totals, the decrease in streamflow cannot be explained by either precipitation decrease or enhanced AED. Rather, decreasing streamflow trends can be mostly associated with the progressive increase in vegetation cover and greenness over time. Previous studies suggested that the effect of increased greenness on precipitation partitioning between blue and green water is more pronounced in dry areas (Ukkola et al., 2016; Zeng et al., 2018). Based on empirical observations from the upper Aragón basin, where average precipitation is 1,300 mm $year^{-1}$, our findings suggest that in a humid region affected by secondary succession and increased greenness, vegetation changes can also play a key role in reducing blue water.

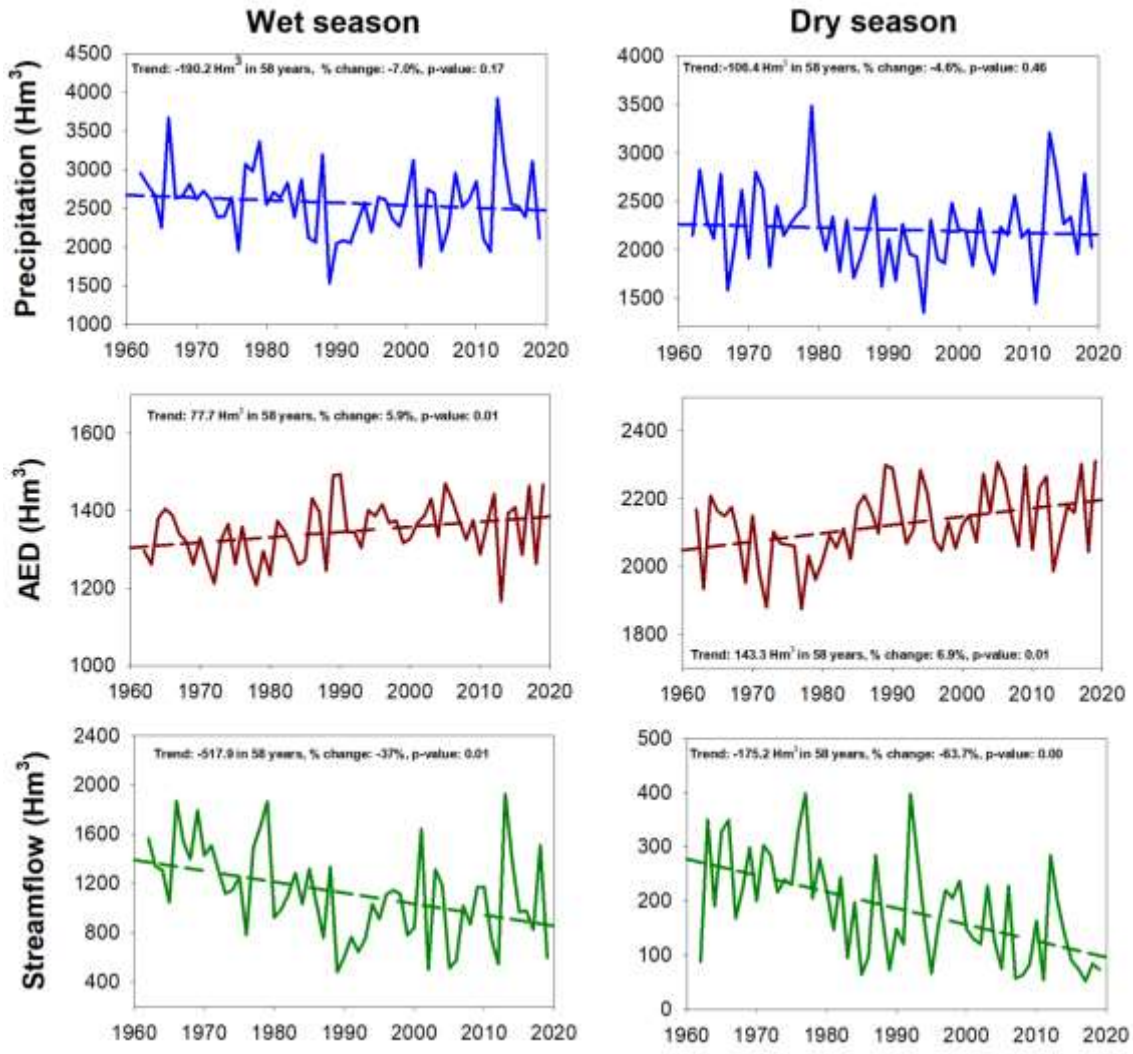

Figure 8: Temporal evolution of the dry (July-October) and wet (November-June) season streamflow. The values of precipitation and AED correspond to the periods having a stronger relationship with seasonal streamflow (see Figure S9) precipitation and AED

Furthermore, we found the effect of secondary succession on the partitioning of precipitation to be strongly differential between wet and dry years. Both precipitation and AED show similar non-significant trends during wet and dry years (Figure 9). However, a small (-15.4%) and non-significant decrease in annual streamflow was found in wet years, compared to a larger (-52.1%) and statistically significant decrease during dry years (Figure 10). The role of AED on streamflow evolution is non-statistically significant during either wet or dry years (Table 2). In wet years, green water increase is expected as a consequence of higher water consumption by more dense vegetation coverage but during these years, the abundance of precipitation makes that secondary succession and greenness have less impact on streamflow trend. In contrast, in dry years secondary succession tends to reduce blue water, in favor of increased green water use. Thus, blue water has been shown to decrease more during dry than wet years in Europe (Orth & Destouni, 2018), so it would be expected that the effect of secondary succession and increased greenness would be amplified during dry years. Vegetation tends to adapt maximum transpiration to available soil moisture (Grossiord et al., 2020), consuming water necessary for physiological processes as the first "ecosystems priority" by increasing water use efficiency (Peters et al., 2018) and, consequently, reducing

blue water generation. The differential effect of greenness on streamflow reduction between dry and humid regions (Ukkola et al., 2016; Zeng et al., 2018) identified by previous studies, is shown in the upper Aragón basin between wet and dry years; in wetter years the greater availability of water in the system, generates proportionally more blue water than during dry years.

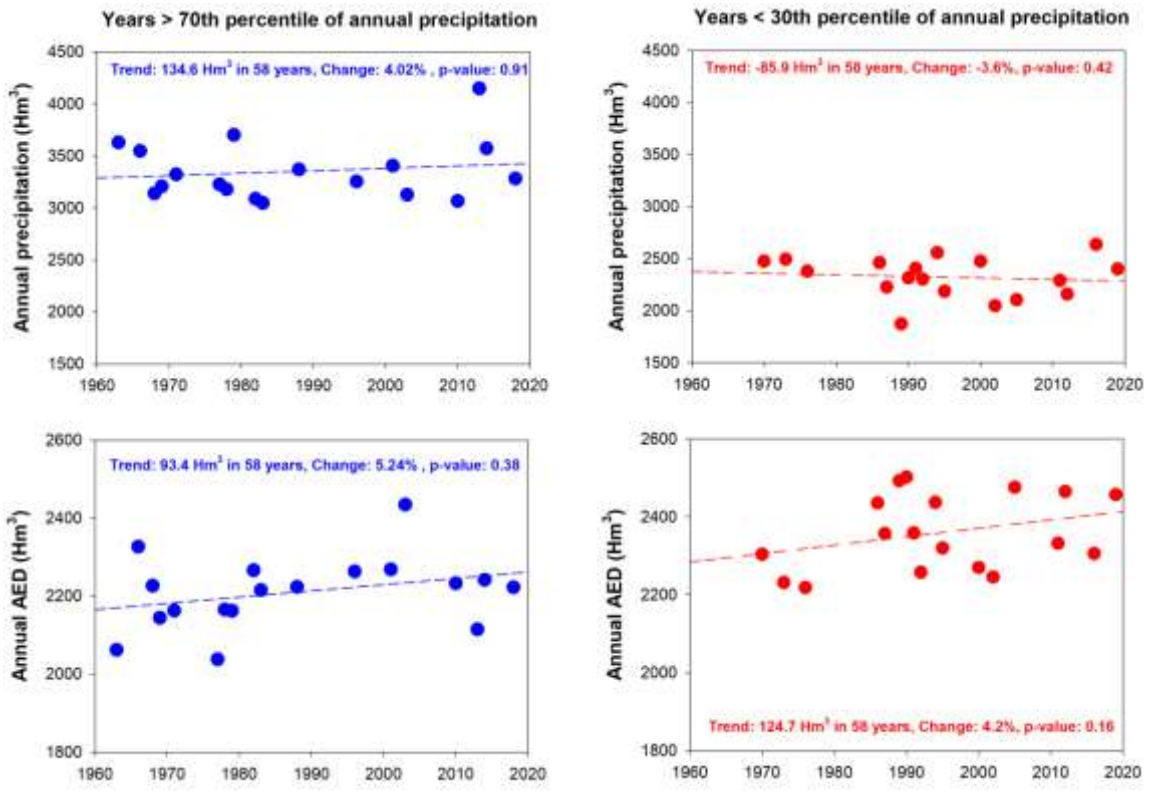

Figure 9: Evolution of precipitation and AED during wet (> 70% percentile) and dry (< 30% percentile) years.

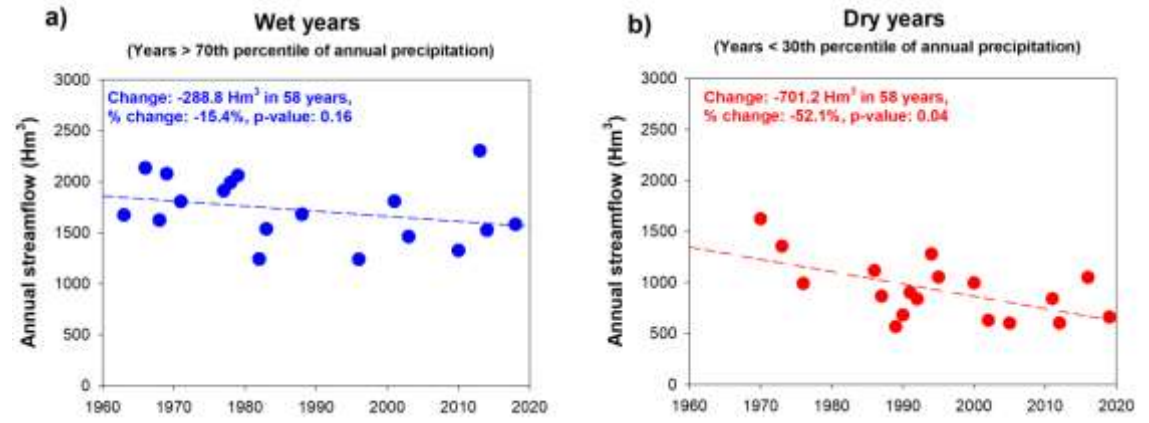

Figure 10: Evolution of annual streamflow during wet (a) and dry (b) precipitation years.

The influence of secondary succession also differs between wet and dry seasons (Figure 11). Precipitation and AED reveal non-significant changes in the wet season (November-June) in both wet and dry seasons (Figure 12). Similarly, no significant decrease in streamflow is found since the decrease of blue water during dry seasons is not statistically significant. In the upper Aragón basin vegetation activity shows strong seasonality. As a consequence of cold air temperatures and dominant snow coverage in winter, vegetation activity is low during these months. Therefore, although secondary succession contributes to some decrease in blue water generation in the wet season, particularly during dry periods (Table 2), the main effect is recorded during the warmer dry season (July-October), which is characterized by high vegetation activity, and consequently water consumption over the different altitudinal belts that characterize vegetation in the basin (García-Ruiz et al., 2015). A significant decrease in streamflow during the dry season is evident in both dry and wet periods, with declines being more pronounced in rainy periods. Even in wet periods, the decrease in blue water during the dry season has been significant, probably as consequence of increased plant coverage and greenness. Consequently the decrease in dry season blue water generation has been dramatic during both dry and wet periods. Increased plant water needs as a consequence of enhanced AED and competition for available soil moisture not only cause strong decreases in blue water but also episodes of plant stress, low plant growth and forest dieback in response to drought (Vicente-Serrano, 2021), which have become reinforced due to vegetation changes, climate variability and change in recent decades (Camarero et al., 2011; Macias et al., 2006).

Table 2: Correlation coefficients of the different regression models for annual and seasonal periods considering a subset of dry and wet years. In all models streamflow was the dependent variable and precipitation, AED and time (in years) were the independent predictors. The R^2 square coefficient represents the percentage of total variance of the independent variable explained by the predictors, while partial correlations represent the role of each independent variable after removing the influence of the covariates. non-significant (n.s.; 0.05 level) predictors were not included in the final models.

		R^2	**Partial correlations**		
			Precipitation	AED	Time
Annual	*Dry years*	0.76	0.80	-0.20 (n.s.)	-0.73
	Wet years	0.52	0.69	-0.15 (n.s.)	-0.49
Wet season (Nov.-Jun.)	*Dry years*	0.66	0.74	-0.00 (n.s.)	-0.63
	Wet years	0.59	0.74	-0.17 (n.s.)	-0.54
Dry season (Jul.-Oct.)	*Dry years*	0.42	0.55	-0.47	-0.49
	Wet years	0.70	0.18 (n.s.)	-0.19 (n.s)	-0.84

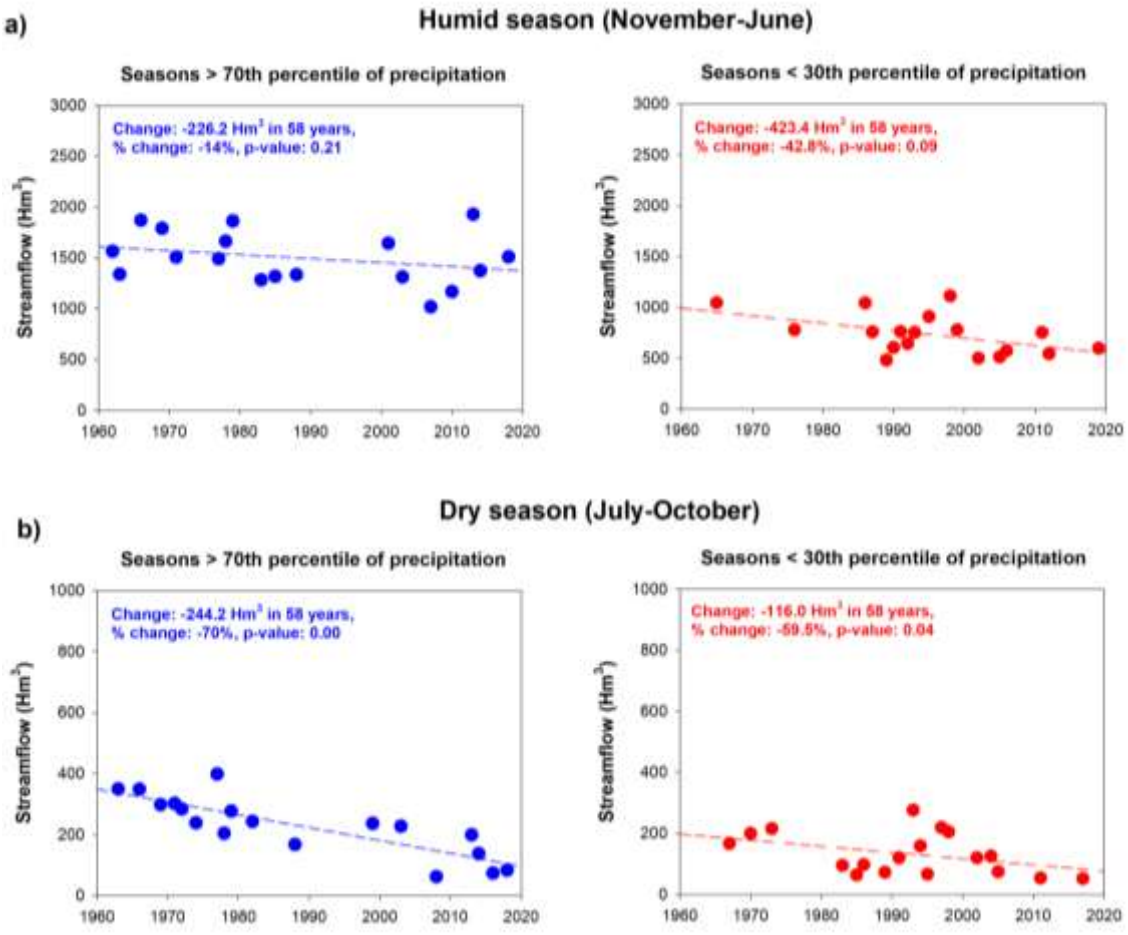

Figure 11: Evolution of annual streamflow during the wet (a) and dry (b) seasons during high and low precipitation periods.

Future climate change scenarios over the Mediterranean region show decreases in precipitation and more frequent droughts (Lionello & Scarascia, 2018). Large increases in AED are also projected (Vicente-Serrano et al., 2020). Under these scenarios, it is expected that blue water generation will decrease further in large areas of southern Europe affected by land abandonment (Lasanta et al., 2017), plant colonization and secondary succession (García-Ruiz et al., 2011). However, large uncertainties are associated with trends in future vegetation cover. While vegetation changes in the region have been considerable to date, potential remains for significant future changes, including the replacement of coniferous forests and shrublands by broadleaf forests below elevations of 1,600 m a.s.l., and the advance of shrublands and forests at elevations above 2,000 m a.s.l., as consequence of the pasture abandonment and increases in air temperature (Sanjuán et al., 2018). This evolution could affect future availability of water resources since once the current dominant young forests reach more mature levels they may demand more water, as old forests have a lower water yield response (Teuling & van Dijke, 2020). Although increased atmospheric CO_2 concentrations could have limited plant water needs (Swann, 2018), our results suggest that water availability for socio-economic activities have been highly affected by water demands from vegetation changes. This finding concur with modeling studies at larger scales (Mankin et al., 2019).

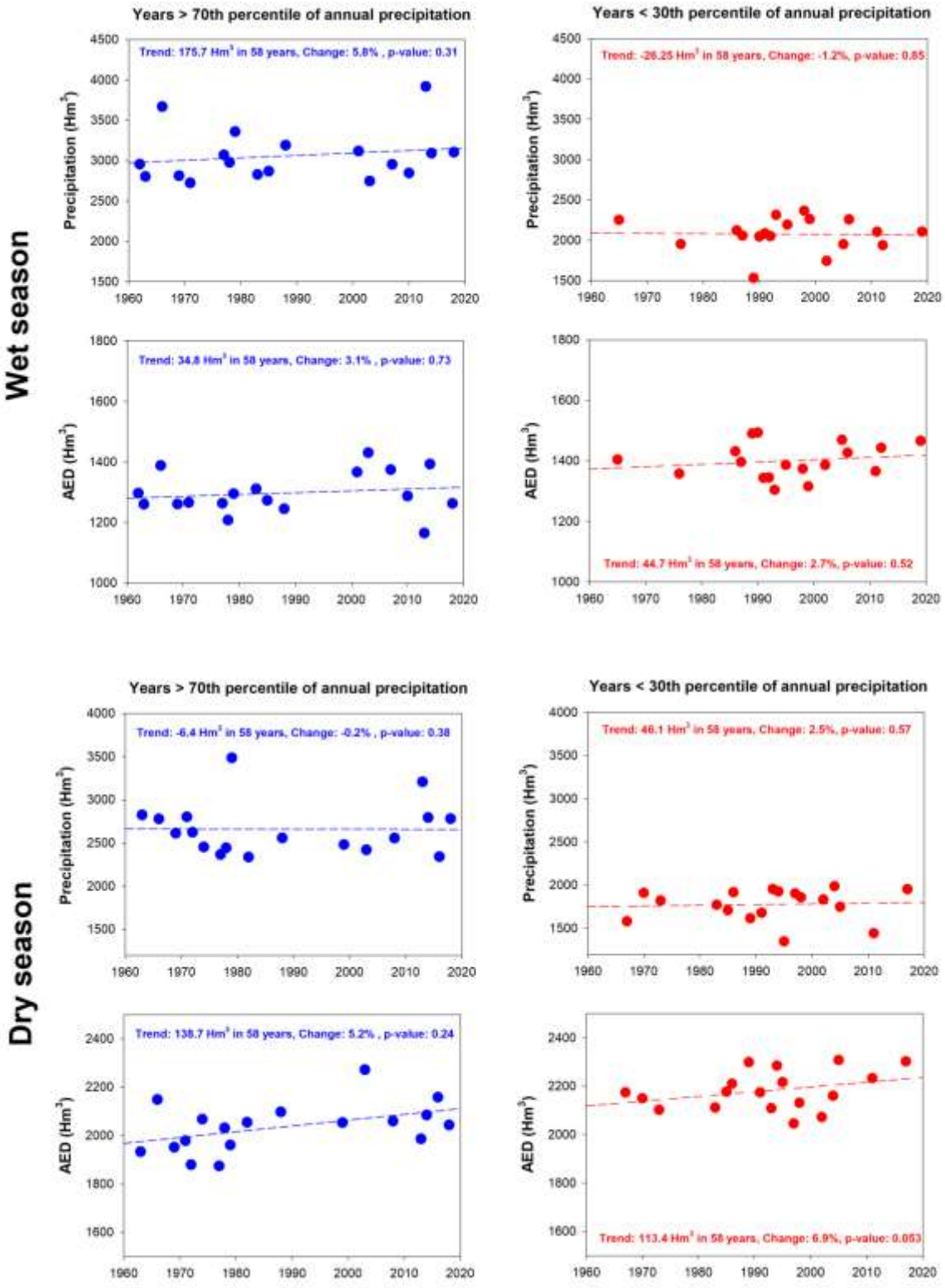

Figure 12: Evolution of precipitation and AED for wet (> 70% percentile) and dry (< 30% percentile) seasons and years.

Mountainous areas in southern Europe are the water towers (Viviroli & Weingartner, 2004) in which the usable water resources of the region are generated. Water supply to irrigated areas is already restricted during dry years in the study domain (Vicente-Serrano et al., 2017;

Vicente-Serrano, 2021). These findings, coupled with projected land use and climate change in southern Europe suggest that sustainable land management practices must be focused on limiting green water losses to enhance availability of blue water into the future. In this light, practices such as thinning (Manrique-Alba et al., 2020) and clearing shrublands for livestock (Lasanta et al., 2019) could be considered sustainable water management practices in southern Europe (García-Ruiz et al., 2020).

5. Conclusions

This study analysed the partition of the available water resources between blue and green water in a Spanish mountainous Mediterranean basin from 1960 to 2019. The study basisn is characterized by substantial plant secondary succession processes. Overall, the main conclusions of this study can be summarized: i)blue water has declined by 40% in the study domain over the last six decades, ii) climate trends accounted for a small portion of blue water reduction, iii) the strong decrease in streamflow can be explained largely by the process of plant secondary succession and increased vegetation, iv) the partition of precipitation trends between blue and green water trends differs between dry and wet years, v) there is stronger increase in the total basin evaporation during dry years, which drastically limits the production of blue water, posing major challenges to water availability during droughts episodes and vi) there are significant seasonal differences in the role of dry and humid years in precipitation partitioning between blue and green water. The most pronounced impacts can be noted during dry season, when vegetation is more active and consume more water, reducing dramatically water resources, even in wet summers.

References

Anderegg, W. R. L., Martinez-Vilalta, J., Cailleret, M., Camarero, J. J., Ewers, B. E., Galbraith, D., et al. (2016). When a Tree Dies in the Forest: Scaling Climate-Driven Tree Mortality to Ecosystem Water and Carbon Fluxes. *Ecosystems*, *19*(6), 1133–1147. https://doi.org/10.1007/s10021-016-9982-1

Barker, L. J., Hannaford, J., Chiverton, A., & Svensson, C. (2016). From meteorological to hydrological drought using standardised indicators. *Hydrology and Earth System Sciences*, *20*(6), 2483–2505. https://doi.org/10.5194/hess-20-2483-2016

Beguería, S., López-Moreno, J. I., Lorente, A., Seeger, M., & García-Ruiz, J. M. (2003). Assessing the effect of climate oscillations and land-use changes on streamflow in the Central Spanish Pyrenees. *Ambio*, *32*(4), 283–286. https://doi.org/10.1579/0044-7447-32.4.283

Bosch, J. M., & Hewlett, J. D. (1982). A review of catchment experiments to determine the effect of vegetation changes on water yield and evapotranspiration. *Journal of Hydrology*, *55*(1), 3–23. https://doi.org/https://doi.org/10.1016/0022-1694(82)90117-2

Brown, A. E., Zhang, L., McMahon, T. A., Western, A. W., & Vertessy, R. A. (2005). A review of paired catchment studies for determining changes in water yield resulting from alterations in vegetation. *Journal of Hydrology*, *310*(1), 28–61. https://doi.org/https://doi.org/10.1016/j.jhydrol.2004.12.010

Buendia, C., Bussi, G., Tuset, J., Vericat, D., Sabater, S., Palau, A., & Batalla, R. J. (2016). Effects of afforestation on runoff and sediment load in an upland Mediterranean catchment. *Science of The Total Environment*, *540*, 144–157. https://doi.org/https://doi.org/10.1016/j.scitotenv.2015.07.005

Camarero, J. J., Bigler, C., Linares, J. C., & Gil-Pelegrín, E. (2011). Synergistic effects of past historical logging and drought on the decline of Pyrenean silver fir forests. *Forest Ecology and Management*, *262*(5), 759–769. https://doi.org/10.1016/j.foreco.2011.05.009

Filoso, S., Bezerra, M. O., Weiss, K. C. B., & Palmer, M. A. (2017). Impacts of forest restoration on water yield: A systematic review. *PLoS ONE*, *12*, e0183210.

Forzieri, G., Miralles, D. G., Ciais, P., Alkama, R., Ryu, Y., Duveiller, G., et al. (2020). Increased control of vegetation on global terrestrial energy fluxes. *Nature Climate Change*, *10*(4), 356–362. https://doi.org/10.1038/s41558-020-0717-0

García-Ruiz, J. M., López-Moreno, J. I., Vicente-Serrano, S. M., Lasanta-Martínez, T., & Beguería, S. (2011). Mediterranean water resources in a global change scenario. *Earth-Science Reviews*, *105*(3–4). https://doi.org/10.1016/j.earscirev.2011.01.006

García-Ruiz, J. M., López-Moreno, J. I., Lasanta, T., Vicente-Serrano, S. M., González-Sampériz, P., Valero-Garcés, B. L., et al. (2015). Geo-ecological effects of global change in the Central Spanish Pyrenees: A review at different spatial and temporal scales [Los efectos geoecológicos del cambio global en el pirineo central español: Una revisión a distintas escalas espaciales y temporales. *Pirineos*, *170*. https://doi.org/10.3989/Pirineos.2015.170005

Garcia-Ruiz, J. M., & Lasanta-Martinez, T. (1990). Land-use changes in the Spanish Pyrenees. *Mountain Research & Development*, *10*(3), 267–279. https://doi.org/10.2307/3673606

García-Ruiz, J.M., López-Moreno, J. I., Vicente-Serrano, S. M., Lasanta-Martínez, T., & Beguería, S. (2011). Mediterranean water resources in a global change scenario. *Earth-Science Reviews*, *105*(3–4). https://doi.org/10.1016/j.earscirev.2011.01.006

García-Ruiz, J.M., López-Moreno, J. I., Lasanta, T., Vicente-Serrano, S. M., González-Sampériz, P., Valero-Garcés, B. L., et al. (2015). Geo-ecological effects of global change in the Central Spanish Pyrenees: A review at different spatial and temporal scales. *Pirineos*, *170*. https://doi.org/10.3989/Pirineos.2015.170005

García-Ruiz, José M, Regüés, D., Alvera, B., Lana-Renault, N., Serrano-Muela, P., Nadal-Romero, E., et al. (2008). Flood generation and sediment transport in experimental catchments affected by land use changes in the central Pyrenees. *Journal of Hydrology*, *356*(1), 245–260. https://doi.org/https://doi.org/10.1016/j.jhydrol.2008.04.013

García-Ruiz, J. M., Lasanta, T., Nadal-Romero, E., Lana-Renault, N., & Álvarez-Farizo, B. (2020). Rewilding and restoring cultural landscapes in Mediterranean mountains: Opportunities and challenges. *Land Use Policy*. https://doi.org/10.1016/j.landusepol.2020.104850

Grossiord, C., Buckley, T. N., Cernusak, L. A., Novick, K. A., Poulter, B., Siegwolf, R. T. W., et al. (2020). Plant responses to rising vapor pressure deficit. *New Phytologist*, *226*(6), 1550–1566. https://doi.org/10.1111/nph.16485

Gudmundsson, L., Seneviratne, S. I., & Zhang, X. (2017). Anthropogenic climate change detected in European renewable freshwater resources. *Nature Climate Change*, *7*(11), 813–816. https://doi.org/10.1038/nclimate3416

Hair, J. F., Anderson, R. E., Tatham, R. L., & Black, W. C. (1995). No Title. *Multivariate Data Analysis*.

Hamed, K. H., & Ramachandra Rao, A. (1998). A modified Mann-Kendall trend test for autocorrelated data. *Journal of Hydrology*, *204*(1–4), 182–196. https://doi.org/10.1016/S0022-1694(97)00125-X

Kouba, Y., Camarero, J. J., & Alados, C. L. (2012). Roles of land-use and climate change on the establishment and regeneration dynamics of Mediterranean semi-deciduous oak forests. *Forest Ecology and Management*, *274*, 143–150.

https://doi.org/10.1016/j.foreco.2012.02.033
Lasanta-Martínez, T., Vicente-Serrano, S. M., & Cuadrat-Prats, J. M. (2005). Mountain Mediterranean landscape evolution caused by the abandonment of traditional primary activities: A study of the Spanish Central Pyrenees. *Applied Geography*, *25*(1). https://doi.org/10.1016/j.apgeog.2004.11.001
Lasanta, T., Arnáez, J., Pascual, N., Ruiz-Flaño, P., Errea, M. P., & Lana-Renault, N. (2017). Space–time process and drivers of land abandonment in Europe. *Catena*, *149*, 810–823. https://doi.org/10.1016/j.catena.2016.02.024
Lasanta, T., Nadal-Romero, E., & García-Ruiz, J. M. (2019). Clearing shrubland as a strategy to encourage extensive livestock farming in the Mediterranean Mountains. *Geographical Research Letters*, *45*(2), 487–513. https://doi.org/10.18172/cig.3616
Lasanta, T., Nadal-Romero, E., Serrano-Muela, P., Vicente-Serrano, S. M., & García-Ruiz, J. M. (2010). Runoff and erosion after farmland abandonment in mountain areas: Results from the Aísa valley experimental station. *Pirineos*, (165). https://doi.org/10.3989/Pirineos.2010.165006
Leuschner, C., & Rode, M. W. (1999). The role of plant resources in forest succession: Changes in radiation, water and nutrient fluxes, and plant productivity over a 300-yr-long chronosequence in NW-Germany. *Perspectives in Plant Ecology, Evolution and Systematics*. https://doi.org/10.1078/1433-8319-00067
Lian, X., Piao, S., Li, L. Z. X., Li, Y., Huntingford, C., Ciais, P., et al. (2020). Summer soil drying exacerbated by earlier spring greening of northern vegetation. *Science Advances*, *6*(1), eaax0255. https://doi.org/10.1126/sciadv.aax0255
Lionello, P., & Scarascia, L. (2018). The relation between climate change in the Mediterranean region and global warming. *Regional Environmental Change*, *18*(5), 1481–1493. https://doi.org/10.1007/s10113-018-1290-1
López-Moreno, J. I., Vicente-Serrano, S. M., Zabalza, J., Beguería, S., Lorenzo-Lacruz, J., Azorin-Molina, C., & Morán-Tejeda, E. (2013). Hydrological response to climate variability at different time scales: A study in the Ebro basin. *Journal of Hydrology*, *477*, 175–188. https://doi.org/10.1016/j.jhydrol.2012.11.028
López-Moreno, J. I., Beguería, S., & García-Ruiz, J. M. (2004). The management of a large Mediterranean reservoir: Storage regimens of the Yesa Reservoir, Upper Aragon River basin, Central Spanish Pyrenees. *Environmental Management*, *34*(4), 508–515. https://doi.org/10.1007/s00267-003-0249-1
López-Moreno, J. I., Soubeyroux, J. M., Gascoin, S., Alonso-Gonzalez, E., Durán-Gómez, N., Lafaysse, M., et al. (2020). Long-term trends (1958–2017) in snow cover duration and depth in the Pyrenees. *International Journal of Climatology*, *n/a*(n/a). https://doi.org/10.1002/joc.6571
Lorenzo-Lacruz, J., Vicente-Serrano, S. M., López-Moreno, J. I., Morán-Tejeda, E., & Zabalza, J. (2012). Recent trends in Iberian streamflows (1945-2005). *Journal of Hydrology*, *414–415*. https://doi.org/10.1016/j.jhydrol.2011.11.023
Macias, M., Andreu, L., Bosch, O., Camarero, J. J., & Gutiérrez, E. (2006). Increasing aridity is enhancing silver fir (Abies alba Mill.) water stress in its south-western distribution limit. *Climatic Change*, *79*(3–4), 289–313. https://doi.org/10.1007/s10584-006-9071-0
Mankin, J. S., Seager, R., Smerdon, J. E., Cook, B. I., & Williams, A. P. (2019). Mid-latitude freshwater availability reduced by projected vegetation responses to climate change. *Nature Geoscience*, *12*(12), 983–988. https://doi.org/10.1038/s41561-019-0480-x
Manrique-Alba, À., Beguería, S., Molina, A. J., González-Sanchis, M., Tomàs-Burguera, M., del Campo, A. D., et al. (2020). Long-term thinning effects on tree growth, drought response and water use efficiency at two Aleppo pine plantations in Spain. *Science of the Total Environment*. https://doi.org/10.1016/j.scitotenv.2020.138536

Martínez-Fernández, J., Sánchez, N., & Herrero-Jiménez, C. M. (2013). Recent trends in rivers with near-natural flow regime: The case of the river headwaters in Spain. *Progress in Physical Geography*, *37*(5), 685–700. https://doi.org/10.1177/0309133313496834

Mastrotheodoros, T., Pappas, C., Molnar, P., Burlando, P., Manoli, G., Parajka, J., et al. (2020). More green and less blue water in the Alps during warmer summers. *Nature Climate Change*, *10*(2), 155–161. https://doi.org/10.1038/s41558-019-0676-5

Molinillo, M., Lasanta, T., & García-Ruiz, J. M. (1997). Managing mountainous degraded landscapes after farmland abandonment in the Central Spanish Pyrenees. *Environmental Management*, *21*(4), 587–598. https://doi.org/10.1007/s002679900051

Morán-Tejeda, E., Ceballos-Barbancho, A., Llorente-Pinto, J. M., & López-Moreno, J. I. (2012). Land-cover changes and recent hydrological evolution in the Duero Basin (Spain). *Regional Environmental Change*, *12*(1), 17–33. https://doi.org/10.1007/s10113-011-0236-7

Mueller, B., Hirschi, M., Jimenez, C., Ciais, P., Dirmeyer, P. A., Dolman, A. J., et al. (2013). Benchmark products for land evapotranspiration: LandFlux-EVAL multi-data set synthesis. *Hydrology and Earth System Sciences*. https://doi.org/10.5194/hess-17-3707-2013

Navas, A., Valero-Garcés, B., Gaspar, L., & Machín, J. (2009). Reconstructing the history of sediment accumulation in the Yesa reservoir: an approach for management of mountain reservoirs. *Lake and Reservoir Management*, *25*(1), 15–27. https://doi.org/10.1080/07438140802714304

Orth, R., & Destouni, G. (2018). Drought reduces blue-water fluxes more strongly than green-water fluxes in Europe. *Nature Communications*, *9*(1). https://doi.org/10.1038/s41467-018-06013-7

Ortigosa, L. M., Garcia-Ruiz, J. M., & Gil-Pelegrin, E. (1990). Land reclamation by reforestation in the Central Pyrenees. *Mountain Research & Development*, *10*(3), 281–288. https://doi.org/10.2307/3673607

Pasho, E., Camarero, J. J., de Luis, M., & Vicente-Serrano, S. M. (2011). Impacts of drought at different time scales on forest growth across a wide climatic gradient in north-eastern Spain. *Agricultural and Forest Meteorology*, *151*(12). https://doi.org/10.1016/j.agrformet.2011.07.018

Peguero-Pina, J. J., Camarero, J. J., Abadía, A., Martín, E., González-Cascón, R., Morales, F., & Gil-Pelegrín, E. (2007). Physiological performance of silver-fir (Abies alba Mill.) populations under contrasting climates near the south-western distribution limit of the species. *Flora: Morphology, Distribution, Functional Ecology of Plants*, *202*(3), 226–236. https://doi.org/10.1016/j.flora.2006.06.004

Pereira, L. S., Allen, R. G., Smith, M., & Raes, D. (2015). Crop evapotranspiration estimation with FAO56: Past and future. *Agricultural Water Management*, *147*, 4–20. https://doi.org/10.1016/j.agwat.2014.07.031

Peters, W., van der Velde, I. R., van Schaik, E., Miller, J. B., Ciais, P., Duarte, H. F., et al. (2018). Increased water-use efficiency and reduced CO<inf>2</inf> uptake by plants during droughts at a continental scale. *Nature Geoscience*, *11*(10), 744–748. https://doi.org/10.1038/s41561-018-0212-7

Rulli, M. C., Saviori, A., & D'Odorico, P. (2013). Global land and water grabbing. *Proceedings of the National Academy of Sciences of the United States of America*. https://doi.org/10.1073/pnas.1213163110

Sanjuán, Y., Arnáez, J., Beguería, S., Lana-Renault, N., Lasanta, T., Gómez-Villar, A., et al. (2018). Woody plant encroachment following grazing abandonment in the subalpine belt: a case study in northern Spain. *Regional Environmental Change*, *18*(4), 1103–

1115. https://doi.org/10.1007/s10113-017-1245-y

Stahl, K., Hisdal, H., Hannaford, J., Tallaksen, L. M., Van Lanen, H. A. J., Sauquet, E., et al. (2010). Streamflow trends in Europe: Evidence from a dataset of near-natural catchments. *Hydrology and Earth System Sciences*, *14*(12), 2367–2382. https://doi.org/10.5194/hess-14-2367-2010

Swann, A. L. S. (2018). Plants and Drought in a Changing Climate. *Current Climate Change Reports*, *4*(2), 192–201. https://doi.org/10.1007/s40641-018-0097-y

Teuling, A J, de Badts, E., Jansen, F. A., Fuchs, R., Buitink, J., van Dijke, A. J., & Sterling, S. (2019). Climate change, re-/afforestation, and urbanisation impacts on evapotranspiration and streamflow in Europe. *Hydrology and Earth System Sciences Discussions*, *2019*, 1–30. https://doi.org/10.5194/hess-2018-634

Teuling, Adriaan J, & Hoek van Dijke, A. J. (2020). Forest age and water yield. *Nature*, *578*(7794), E16–E18. https://doi.org/10.1038/s41586-020-1941-5

Ukkola, A. M., Prentice, I. C., Keenan, T. F., Van Dijk, A. I. J. M., Viney, N. R., Myneni, R. B., & Bi, J. (2016). Reduced streamflow in water-stressed climates consistent with CO<inf>2</inf>effects on vegetation. *Nature Climate Change*, *6*(1), 75–78. https://doi.org/10.1038/nclimate2831

Vicente-Serrano, S. M., Beguería, S., & Lasanta, T. (2006). Spatial diversity of vegetal activity in abandoned fields of the central Spanish Pyrenees: Analysis of the processes of succession by means of Landsat imagery (1984-2001). *Pirineos*, (161).

Vicente-Serrano, S. M. M., Martín-Hernández, N., Reig, F., Azorin-Molina, C., Zabalza, J., Beguería, S., et al. (2020). Vegetation greening in Spain detected from long term data (1981–2015). *International Journal of Remote Sensing*, *41*(5), 1709–1740. https://doi.org/10.1080/01431161.2019.1674460

Vicente-Serrano, S.M., Camarero, J. J., Zabalza, J., Sangüesa-Barreda, G., López-Moreno, J. I., & Tague, C. L. (2015). Evapotranspiration deficit controls net primary production and growth of silver fir: Implications for Circum-Mediterranean forests under forecasted warmer and drier conditions. *Agricultural and Forest Meteorology*, *206*. https://doi.org/10.1016/j.agrformet.2015.02.017

Vicente-Serrano, S.M., Peña-Gallardo, M., Hannaford, J., Murphy, C., Lorenzo-Lacruz, J., Dominguez-Castro, F., et al. (2019). Climate, irrigation, and land-cover change explain streamflow trends in countries bordering the Northeast Atlantic. *Geophysical Research Letters*, *46*(19), 10821–10833. https://doi.org/10.1029/2019GL084084

Vicente-Serrano, S M, Zabalza-Martínez, J., Borràs, G., López-Moreno, J. I., Pla, E., Pascual, D., et al. (2017). Extreme hydrological events and the influence of reservoirs in a highly regulated river basin of northeastern Spain. *Journal of Hydrology: Regional Studies*, *12*, 13–32. https://doi.org/10.1016/j.ejrh.2017.01.004

Vicente-Serrano, Sergio M, Tomas-Burguera, M., Beguería, S., Reig, F., Latorre, B., Peña-Gallardo, M., et al. (2017). A High Resolution Dataset of Drought Indices for Spain. *Data*, *2*(3).

Vicente-Serrano, Sergio M, McVicar, T. R., Miralles, D. G., Yang, Y., & Tomas-Burguera, M. (2020). Unraveling the influence of atmospheric evaporative demand on drought and its response to climate change. *WIREs Climate Change*, *11*(2), e632. https://doi.org/10.1002/wcc.632

Vicente-Serrano, S. M. (2021). The complex multi-sectoral impacts of drought: Evidence from a mountainous basin in the Central Spanish Pyrenees. *Science of the Total Environment*.

Viviroli, D., & Weingartner, R. (2004). The hydrological signifance of mountains: From regional to global scale. *Hydrology and Earth System Sciences*, *8*(6), 1016–1029. Retrieved from https://www.scopus.com/inward/record.uri?eid=2-s2.0-

18944381972&partnerID=40&md5=abd0b3b972e7ba32f6b56823f291fdcd
Wang, K., & Dickinson, R. E. (2012). A review of global terrestrial evapotranspiration: Observation, modeling, climatology, and climatic variability. *Reviews of Geophysics*, *50*(2), RG2005. https://doi.org/10.1029/2011RG000373
Wine, M., Cadol, D., & Makhnin, O. (2017). In ecoregions across western USA streamflow increases during post-wildfire recovery. *Environmental Research Letters*, *13*. https://doi.org/10.1088/1748-9326/aa9c5a
Winkler, R., Spittlehouse, D., & Boon, S. (2017). Streamflow response to clear-cut logging on British Columbia's Okanagan Plateau. *Ecohydrology*, *10*(2), e1836. https://doi.org/https://doi.org/10.1002/eco.1836
Zeng, Z., Piao, S., Li, L. Z. X., Wang, T., Ciais, P., Lian, X., et al. (2018). Impact of Earth Greening on the Terrestrial Water Cycle. *Journal of Climate*, *31*(7), 2633–2650. https://doi.org/10.1175/JCLI-D-17-0236.1
Zhang, L., Dawes, W. R., & Walker, G. R. (2001). Response of mean annual evapotranspiration to vegetation changes at catchment scale. *Water Resources Research*, *37*(3), 701–708. https://doi.org/https://doi.org/10.1029/2000WR900325

Section iii)

The impact of arterial and land drainage on low flows and drought in the Boyne Catchment, Ireland

1. Introduction

Arterial drainage comprises the artificial widening and deepening of main river channels and important tributaries to improve discharge conveyance (O'Kelly, 1955). Following arterial works peak flows have been noted to increase and the time to peak and duration of flood hydrographs to shorten (O' Kelly, 1955; Bree and Cunnane, 1979; Bailey and Bree, 1981). The Boyne catchment experienced widespread arterial drainage over the period 1969-1986 (OPW, 2014) with more than 60 % of the river network affected. According to Harrigan et al. (2014) most works were competed between 1977 and 1979 with works on the main channel of the Boyne completed in 1984 (Figure 2). Coincident with arterial drainage, the catchment was also subject to extensive field drainage works. This involves the installation of pipes and ditches to remove surplus water from waterlogged agricultural lands, resulting in shorter transmission times of water to river channels (Harrigan et al., 2014). Previous studies have indicated that field drainage likely increases runoff in winter and spring (Burdon, 1986).

Little is known about the impact of arterial and land drainage on drought and low flows. Even international reviews have tended to concentrate on impacts on high flows and highlight the lack of catchment based studies investigating low flow and drought response (Blann et al, 2009; Gramlich et al., 2018). In Ireland Essery and Wilcock (1991) found that low flows were increased following drainage of the upper River Maine in Northern Ireland, though the highlight uncertainty as to whether this change was due to climate variability or drainage impacts. Other than this single study we know of no other previous research investigating low flow response to drainage, despite the fact that such schemes have been widely implemented not just in Ireland, but across Europe.

Therefore, in this study we attempt to use simulation-based methods to reconstruct river flows in the Boyne catchment to create a 'virtual' world in which drainage did not take place. Our reconstructions include climate variability, with only internal catchment change not included in the model. We calibrate our model on the pre drainage period and use it to simulate the post drainage record. We then evaluate evidence of change in key low flow metrics and drought events to examine any impact of drainage on flows in the Boyne.

2. Description of the study area

The Boyne catchment located in east Ireland has an annual average total precipitation of 897 mm (1952-2009). The catchment drains a total land area of 2,694 km^2 (Figure 1). A long-term river flow gauging site (1941-present) of good quality is located at Slane Castle in Co. Meath (lat 53.706870^{o}N, long 6.562389^{o}W) and used in this study to represent flows in the catchment. The catchment area to Slane Castle is 2,460 km^2 and the main channel length is 94 km. There are several lakes in the catchment, to the north, the most significant being Lough Ramor and Mullagh lake in Co. Cavan. The catchment can be characterised as being predominantly flat to undulating lowland with elevation ranging between 16 and 338 m. Land-use is dominated by agricultural pastures (87 %) with dairy farming being the predominant agricultural enterprise. Other significant land use types comprise arable agriculture (~10 %), forestry (~5 %) and bogs (~5 %). The catchment is classified as

essentially rural with approximately 1.5 % of the catchment containing urbanised areas. The main towns in the catchment include Drogheda, Navan, Trim, Kells, Virginia, Bailieborough, Athboy, Kinnegad, Edenderry and Enfield. The total population of the catchment is approximately 196,400, with a population density of circa 73 people per km^2. Water supplies in the catchment for human consumption comprise 89 abstractions, including six group water schemes, eight public supplies serving major urban centres and five private supplies.

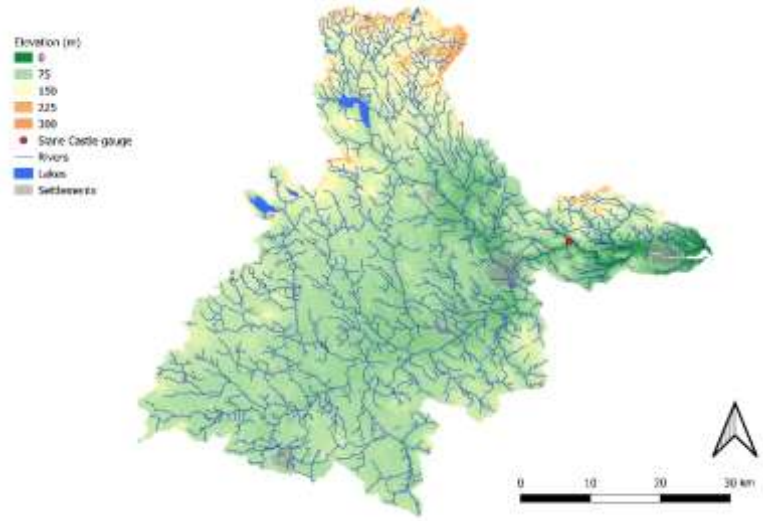

Figure 1 The Boyne catchment in eastern Ireland. The red dot marks the location of the river flow gauge at Slane Castle.

The catchment is underlain by metamorphic rocks in the north and limestone bedrock in the centre and south of the catchment. Extensive sand and gravel areas are found in the upper reaches of the catchment. Geology and soil types show a similar pattern with the southern and central parts of the catchment dominated by grey brown podzolics and gleys with significant peat deposits. In the north of the catchment soils are typically acid brown earths and gleys. More than 35 percent of the catchment is comprised of poorly drained soils, including basin peat and gleys. Given the importance of agriculture in the catchment and the presence of poorly drained soils, the catchment has been subject to extensive arterial and field drainage works. Harrigan et al. (2014) estimate that more than 30 percent of the catchment has been subjected to field drainage, however neither exact figures, nor the location of field drainage works are available due to a lack of records on implementation.

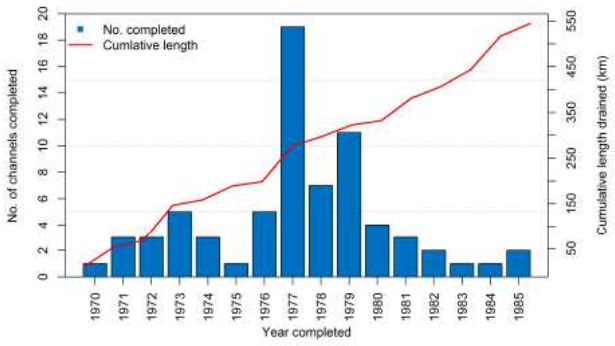

Figure 2 Number of major watercourses per year in which arterial drainage was completed in the Boyne. The cumulative length (km) completed is shown by the red line (Source: Harrigan et al., 2014).

3. Data and methods

3.1 Data

Daily streamflow data for the Boyne at Slane Castle for the period 1942-2019 were obtained from the OPW hydrometric website (https://waterlevel.ie/hydro-data/). Before use metadata codes were evaluated to ascertain the quality of flow measurements during critical low flow periods. For the earliest record a high proportion of data for summer and autumn were flagged as poor data as so daily streamflow data from 1960 on onwards were employed. Catchment average precipitation was estimated from five rainfall gauges maintained by Met Éireann and distributed throughout the catchment, namely Kells, Warrentown, Navan, Mulligar and Ballivor. Catchment average rainfall was derived as a simple average across stations for each day. As the number of gauges contributing to the catchment average varies through time, checks were made to ensure that no breaks in the series were associated with the changing number of contributing gauges. Finally, potential evapotranspiration (PET) losses for the catchment were obtained from Dublin Airport using the Penman Monteith method. While located outside the catchment this series is assumed to be representative and no direct measurements of PET are available within the catchment concurrent with time period of observed rainfall.

3.2 Methods

3.2.1 Hydrological Model

We employ the GR4J (Perrin et al., 2003) daily lumped conceptual rainfall-runoff model to model daily streamflow. GR4J has a parsimonious structure consisting of four parameters (x_1–x_4) that require calibration. The model takes input of observed daily runoff, precipitation and potential evaporation. Observed daily discharge (m^3/s) was converted to runoff in mm/day. We chose GR4J as it has undergone extensive testing in several countries and has been shown to accurately simulate the hydrology of diverse catchment types, with comparatively good results versus other models (e.g. Coron et al., 2012; Perrin et al., 2003; Vaze et al., 2011). It has also been successfully applied to Irish conditions (Broderick et al., 2016; 2019, Donegan et al., 2021) where it was found to perform well across a wide range of catchments, with respect to both temporal transitioning between wet and dry periods and the reproduction of various hydrological signatures. GR4J was implemented using the AirGR R package (Coron et al., 2017).

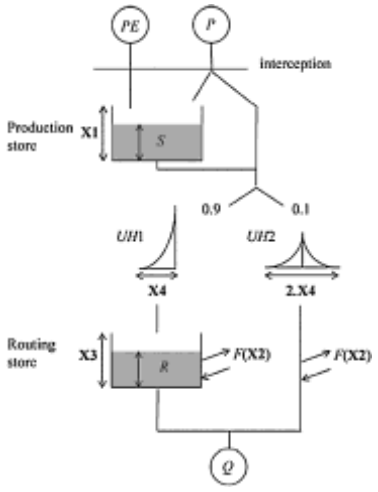

Figure 3 Structure of the GR4J model and four parameters (x1-x4) (Source: Drogue and Khediri, 2016).

The GR4J model structure is shown in Figure 3. Water is partitioned between the production (soil moisture accounting) store and the routing store. The production store (capacity x_1 mm) gains water from effective rainfall and loses water from evaporation and percolation. Ninety percent of the total quantity of water reaching the routing component is routed by a unit hydrograph (time base x_4 d) and a non-linear routing store (capacity x_3 mm). The remaining 10% is routed by a single unit hydrograph (time base $2(x_4)$ d). A groundwater exchange function (rate x_2 mm d^{-1}) operates on both routing channels and can be positive, negative, or zero.

We calibrate the model in the pre-drainage period before simulating runoff for the period 1960-2019. We assume that the calibrated model, which implicitly contains information of climate variability and change can be used as an estimate of flows in the absence of arterial drainage. For a range of low flow indices, comparing observed (including drainage) with simulations (absence of drainage) allows us to isolate the impact of drainage interventions in the catchment. Calibration was undertaken for the period 1/1/1960 to 31/12/1969 before being used to simulate runoff for the entire period 1/1/1960 to 31/12/2019. Two years of data (1958-1959) were used for model warmup.

Uncertainty in simulations due to model parameters was evaluated by sampling 10,000 parameter sets using a uniform distribution representing plausible ranges for each parameter (X1: 100-300; X2: -1.5-0.5; X3: 50-150; X4: 1.5-2.9). Simulations for each parameter set were assessed using two criteria during the calibration period. First, given our focus on low flows we used the Nash Sutcliffe Efficiency criteria derived on the log of runoff. Second, the ability each parameter set to capture observed baseflow was assessed. To this end we employed the baseflow separation technique from the 'lfstat' R package (Koffler and Laaha, 2012), which implements the techniques for low flow analysis recommended by the World Meteorological Organisation (Gustard and Demuth, 2009). Parameter sets were deemed behavioural and retained if they achieved a LogNS ≥ 0.80 and a percent bias $\geq \pm 2.5$ percent during the calibration period. Behavioural parameter sets were further evaluated for the evaluation and full simulation periods to examine loss in performance. In addition to evaluating individual model runs we also derived a median simulation across all retained parameter sets, and upper (0.975) and lower (0.025) quantile-based confidence intervals.

3.2.2 Low flow indices examined

Indices representing low flow conditions were extracted for observed and simulated runoff for the period 1952-2019. These include Q95, Q90, and Q70, annual minimum 1-, 7- and 15-day runoff. In addition, we examine annual mean flow together with annual mean baseflow and runoff derived using the baseflow separation technique described above. Finally runs analysis was undertaken to identify individual drought events defined as those in which runoff falls below Q70. Statistics on the number of events, their duration and accumulated deficits were extracted from observed and median simulated runoff.

3.2.3 Statistical tests

Different tests for change (break) points in observed and simulated flows were deployed. We are particularly interested in whether change points were detected in observed flows around the period of drainage implementation in 1970s and whether any changes detected were evident in both the observed and simulated flows. The null hypothesis of no evidence of a change point was evaluated at the 0.05 level. Four tests for change points were implemented, namely; the non-parametric Pettitt test (Pettitt, 1979), and the parametric Buishand Range test (Buishand, 1982), Buishand U test (Buishand, 1982) and Standard Normal Homogeneity Test

(SNHT) (Alexandersson, 1986). For parametric tests significance was evaluated using 20,000 Monte-Carlo replicates. All indices were checked for evidence of autocorrelation before application of statistical tests, with no significant autocorrelation detected at the 0.05 level using the Durbin Watson test. We also tested for monotonic trend using the Sen's Slope (Sen, 1968) and Mann Kendall test (Mann, 1945; Kendall, 1975). All statistical testing was implemented using the 'trend' R package (Pohlert et al, 2016).

4. Results and discussion

4.1 Model performance

GR4J performed well during calibration with medial logNS score of 0.935 with 835 behavioural parameter sets identified and retained. Figure 4 shows boxplots for calibration and associated performance for the simulation period 1970-2019. In the post drainage simulation period, there is a decrease in the performance of behavioural parameters sets, with the median score falling to 0.91. Figure 4 b and c also shows scatter plots of the median simulation for both the calibration and simulation period. For calibration the scatter plot is tightly clustered across the range of flows, indicating the ability of the model to capture high and low flows. For the post drainage simulation period there is increased scatter, particularly at high flow, where the model tends to under estimate the high flows.

This consistent with the findings of Harrigan et al. (2014) who show an increase in high flows following drainage and an inability of their three models, calibrated for a similar pre-drainage period, to capture high flows following drainage. They hypothesised that drainage increases the rainfall runoff response, decreasing storage and producing a quicker response to rainfall (Harrigan et al., 2014). Other empirical work also indicates the impact of drainage on enhanced high flows (REFS).

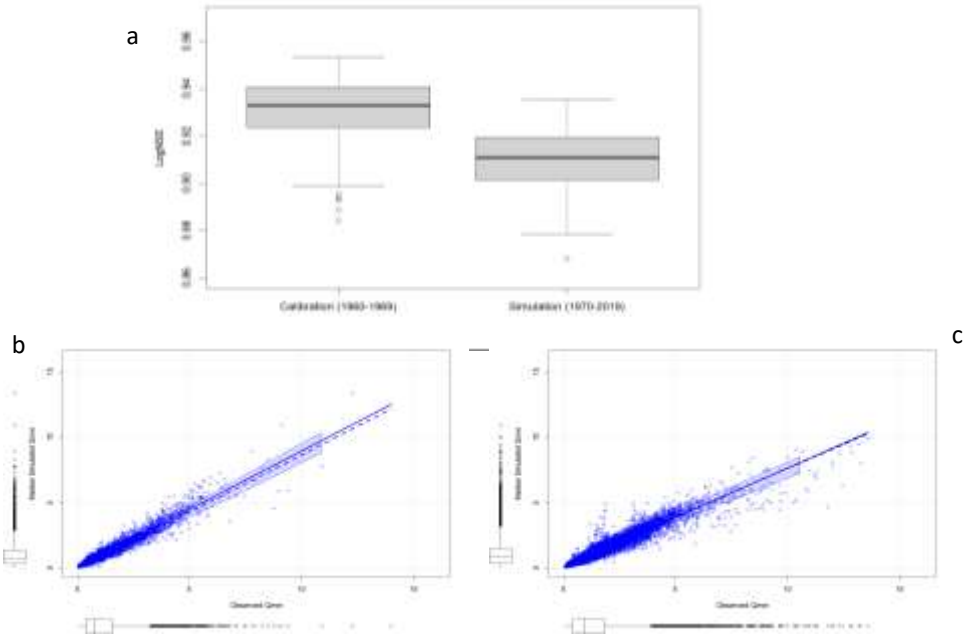

Figure 4 Calibration and simulation results for the Boyne at Slane castle a) shows boxplots of LogNSE results for behavioural simulations for the calibration and simulation periods. b) scatter plot of observed and median simulated runoff for the calibration period and c) for the simulation period.

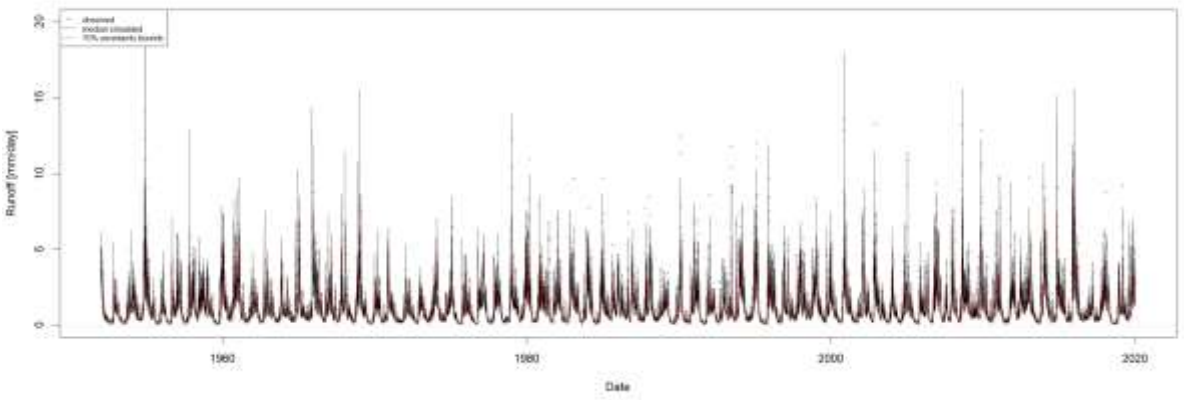

Figure 5 Comparison of observed (grey dots), median simulated (red line) runoff and 95 percent confidence intervals (black dashed line) for the full simulation period 1960-2019.

Figure 5 shows the observed, median simulation and uncertainty bounds of daily flows produced using behavioural parameter sets for the entire period. Again, the good fit of simulated and observed flows is evident for the pre-drainage period, with observations in high agreement with the median and well contained within the 95 percent confidence intervals of simulations. In the post drainage period, high flows in particular frequently fall outside the model confidence intervals. However, it is noted that performance for low flows is hard to discern from this plot, we return to results for low flows in more detail below.

4.2 Drainage impact on baseflow, runoff and total flow

To further investigate the possible impact of drainage on the hydrological regime of the Boyne catchment we apply a baseflow separation routine to daily flows to investigate if any impacts on baseflow, runoff and total flows are evident across the simulation period. Figure 6 shows the results for the median and behavioural parameter sets relative to the observed annual mean flows for the full simulation period. For baseflow, the model performs well in the pre-drainage period with close coherence between observed and simulated baseflow up to the mid-1970s, when drainage works were being implemented. In addition, observations fall well withing the confidence intervals estimated across all 835 behavioural parameter sets. From the mid-1970s, a particularly from the 1980s onwards, there is a a large increase in baseflow contributions to total flows, that is not captured by the model simulations. For the post drainage period baseflow falls well outside even the upper confidence interval of simulations. Therefore, an increase in baseflow is apparent as drainage works were proceedings, likely as the proportion of the catchment impacted increased beyond a certain threshold. It is evident that the installation of field drains and the deepening and widening of river channels may have cut through aquifers in the catchment, increasing baseflow contributions to the overall flow. Notably, the increase the enhanced baseflow in the post drainage period persists through the entire record, with little evidence of return to pre-drainage conditions. This finding contrasts with the work of Bhattari and O'Connor (2004) who investigated rainfall runoff response to drainage in the Brosna catchment finding an initial response to drainage, but a return to pre-drainage rainfall-runoff conditions after a decade and a half.

Figure 6 also shows the simulations for annual mean runoff (again identified using a baseflow separation routine). Notably, uncertainty in runoff derived from model parameters is larger

for runoff that for baseflow. Nonetheless, the model performs well for the pre-drainage calibration period. There is a slight tendency for the median simulation to underestimate runoff. Following drainage, the discrepancy between observed and simulated runoff is enhanced, particularly for the period after 1980, after which there is a persistent and large under estimation of runoff by the model. The timing of this deviation in performance is a little later that identified for baseflow and is likely due to the fact that the late 1970s were a particularly drought rich period. Once wetter conditions were experienced in the early 1980s, the impact of drainage on runoff becomes more obvious.

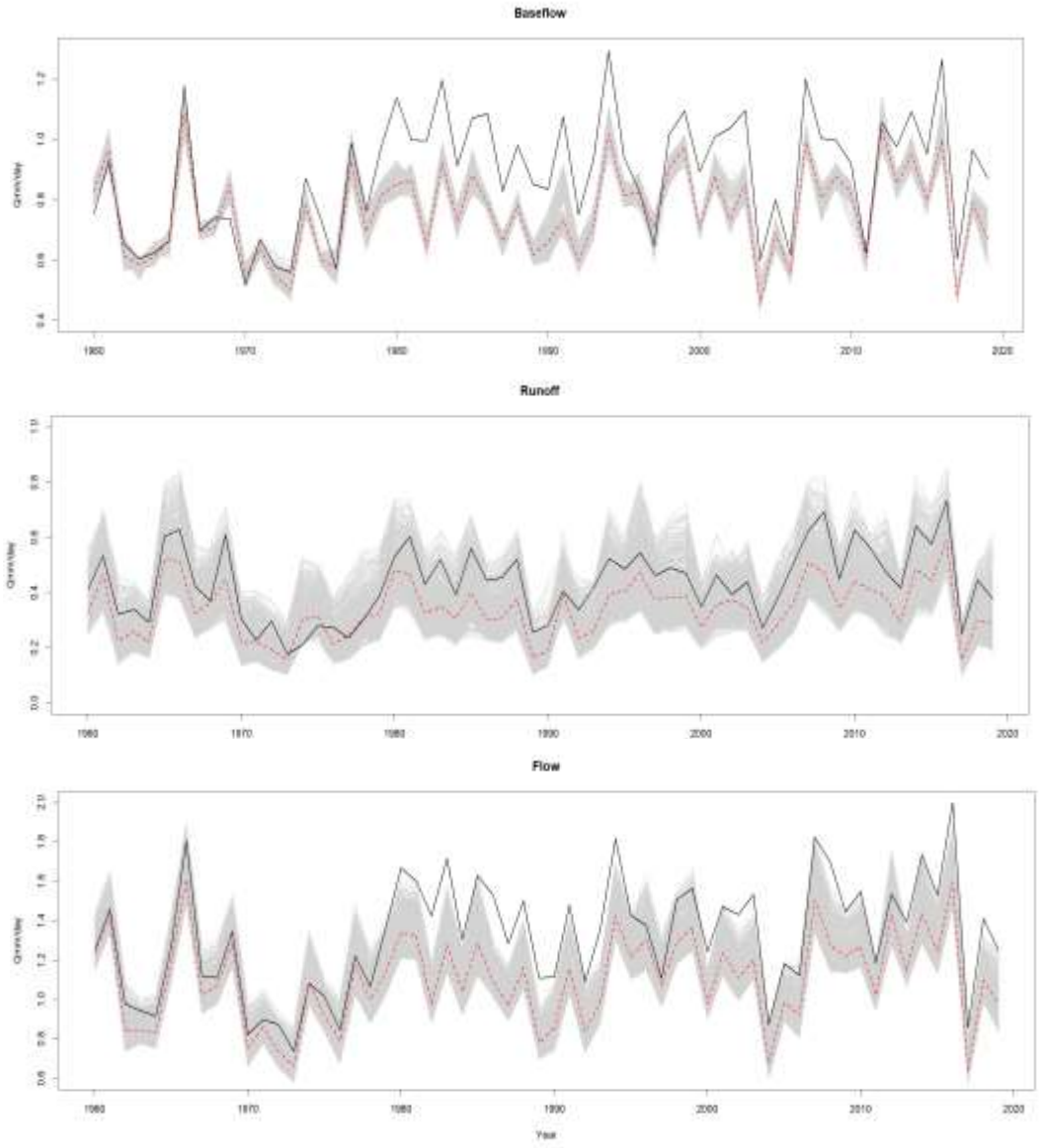

Figure 6 Observed (black line) and simulated baseflow, runoff and total flow for the full simulation period 1960-2019. Red dashed line is the median simulation across behavioural simulations (grey).

Finally, Figure 6 shows the overall impact of drainage (combined changes in baseflow and runoff) for annual mean flows in the catchment. As expected, there is good agreement between model simulations and observations in the pre-drainage period, with the model substantially underestimating flows in the post drainage period, with this persisting through the entirety of the remaining dataset. Our analysis indicates that the largest contribution to

increased flows post drainage is through enhanced baseflow contributions which adds a different perspective to previous research which has tended to focus on floods and high flows. This research had tended to conclude that arterial drainage works in Ireland has increased flows through enhanced runoff efficiency and resulted in higher peaks. Higher peaks in the post drainage period, together with elevated annual mean flows are evident in our results for the Boyne. However, in contrast to previous work, this analysis indicates that the largest contribution to enhanced flows post drainage in the Boyne catchment comes not from runoff but from elevated baseflow. Next, we evaluate changes pre and post drainage for low flow indices and drought events.

4.3 Drainage impact on low flow percentiles

To evaluate the impact of drainage on low flows we extract the annual Q95 (flow exceeded 95 percent of the time), Q90 and Q70 from observed and simulated runoff. The results are shown in Figure 7. For both Q95 and Q90 only modest differences between observed and simulated flows are evident throughout the series. Greatest differences are apparent for the wetter years, with little difference discerned for drier or average years, where for the most part, model simulations and observations are in close agreement for the pre and post drainage record. Previous work for the river Maine in Northern Ireland highlighted that drainage in that catchment increased low flows (Essery and Wilcock, 1990). In addition, this result is somewhat surprising given the increase in baseflow identified above. However, we find no such evidence for Q95 and Q90. That said, while volumetric flows may not be increased, widening of channels after drainage works would mean shallower water levels for the same flows, pre and post drainage, with knock on effects for sensitive ecosystems and fisheries.

Notably, differences in Q70 are apparent between the pre and post drainage periods, with the latter showing an increase in this flow percentile, consistent with the timing of increases in baseflow. Despite close agreement between median simulated and observed annual Q70 in the pre drainage period, model simulations consistently, with the exception of the wettest years, underestimate observed Q70 with the observed series falling well above the upper bound of the confidence intervals from the late 1970s onwards. These results suggest that while increases in baseflow do not seem to impact on the lowest flow percentiles, it does impact on less extreme low flows. This is also seen when the flow duration curve is examined for the median simulated and observed flow quantiles across the post drainage record, with notable divergence commencing at Q70 and extending to the highest flows (not shown). That little evidence for drainage impact is evident below Q70 suggests that increases in baseflow contribution are more limited at lower flows and that the impact of drainage may be limited for drought events (see section 4.5).

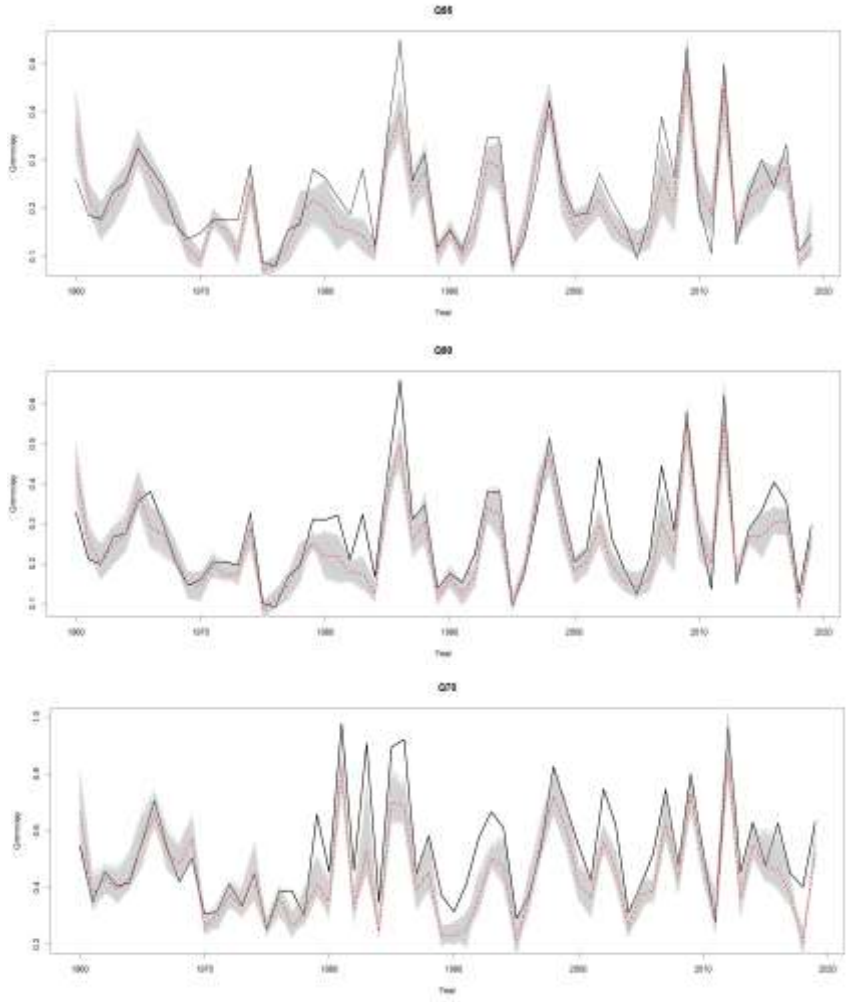

Figure 7 Annual observed (black line) and simulated Q95, Q90 and Q70 runoff. Red dashed line is median simulation across behavioural parameter sets (grey).

4.4 Statistical significance of observed and simulated changes

Statistical tests for change points and monotonic trends were evaluated for catchment precipitation, PET together with different observed and simulated flow metrics to examine if the changes identified above are significant at the 0.05 level. No significant changes were identified for catchment precipitation, while results for each flow metric are provided in Figure 8, where box plots show the range of p-values for each statistical test from behavioural simulation and the red dots show the resultant p-values for observations. In agreement with earlier analyses no significant changes are evident for the lowest flows (annual Q95, Q90, min-7 and min-15 day flows). For Q70 a possible change point in observations is identified for 1978 (consistent in timing across all tests). While not significant at the 0.05 level, this change point is significant at the 0.10 level. None of the behavioural simulations return p-values even close to the critical threshold. Observed annual baseflow, runoff and flows show a significant breakpoint (0.05 level) in late 1970s, coincident with implementation of drainage. Simulations do not show evidence of significant breakpoint, consistent with findings for observed precipitation. These results quantify findings presented in previous sections, while the timing of observed breaks, together with the nature of changes in rainfall runoff processes add confidence that the observed changes are due to arterial drainage and

not other potential drivers of change not considered. It is worth noting however, that the purpose of drainage works was to improve agricultural land and therefore drainage is likely to have been accompanied by changes in land use. However, we do not consider those changes here.

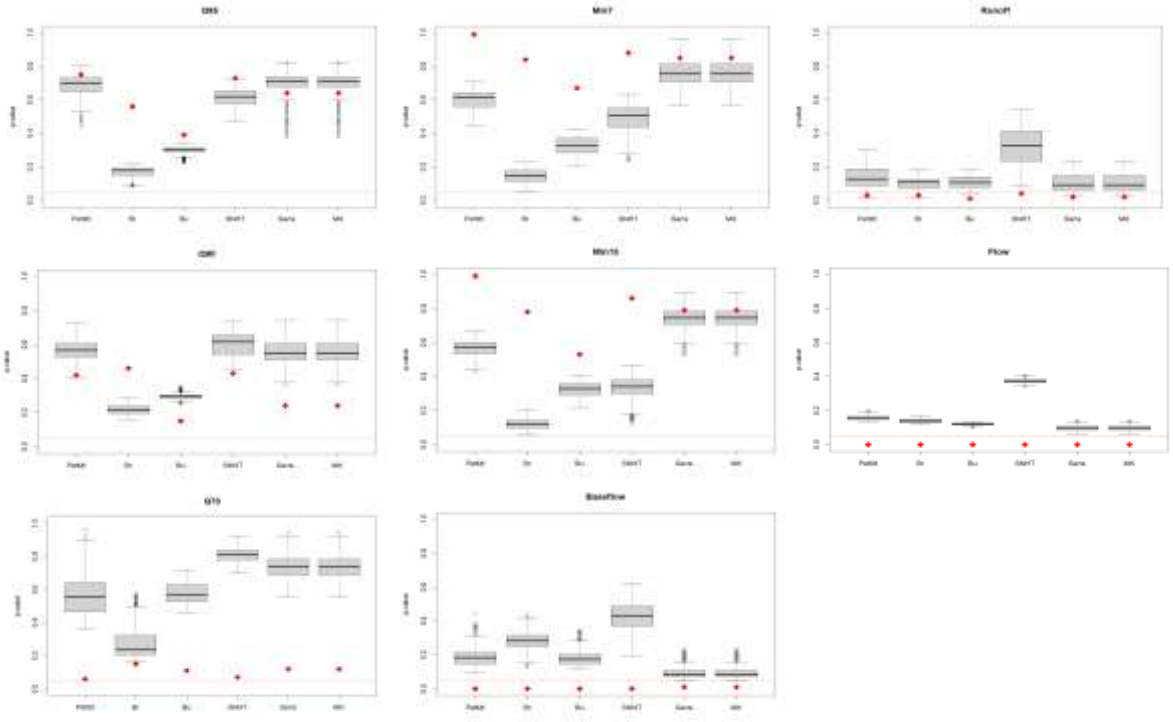

Figure 8 P-values of tests for step and monotonic change in observed (red dot) and simulated (boxplots) indices. The red dashed line marks the 0.05 threshold for rejecting the null hypothesis of no step change/trend.

4.5 Drainage impact on hydrological drought events

Lastly, we deploy runs analysis to identify individual drought events in the post drainage record to examine for any changes in drought frequency and their characteristics. We use Q70 as the threshold for identifying droughts, whereby drought commences once flows fall below Q70 identified over the entire period of record, and end once flows recover/exceed Q70. Figure 9 shows density plots constructed for minimum flows, duration (days) and accumulated deficits of all droughts identified using the observed and median simulated series. No significant difference in the frequency of drought events is found. Similarly, no significant differences in drought duration or accumulated deficits are evident between observed and simulated flows in the post drainage record.

However, differences in the minimum flows reached during drought events are apparent with minimum flows in the observed series tending to be more extreme than those returned for the median simulated series. This suggests that drainage may be increasing drought severity. Given the increases in baseflow following drainage highlighted above, it is not clear why this may be so. Perhaps it is the case that while drainage increases the connectivity of local aquifers with the river, this becomes impeded at the lower flow range as the water table falls, resulting in more severe droughts through more severe minimum flows. However, we note that no significance changes are found for our assessment of observed changes in the

minimum annual flow, nor for extended low flow metrics (min-7 and min-15 day events). It may be, therefore that the differences found for minimum flows during drought events are an artefact of the hydrological model used. Future research should prioritise investigation of these contradictory findings.

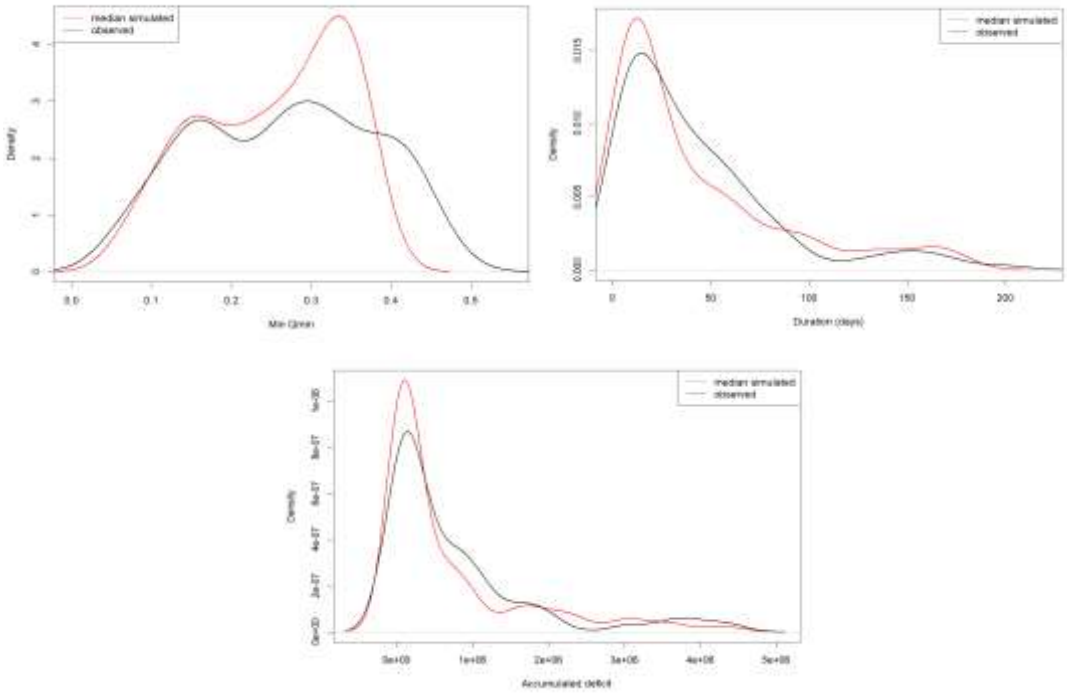

Figure 9 Density plots of observed (black) and median simulated (red) drought characteristics for the post drainage period (1970-2019) for minimum flow, duration and accumulated deficits of each drought event identified.

5. Conclusions

This research investigated the impact of arterial and land drainage on low flows and droughts in the Boyne catchment, Ireland. Little previous research has investigated the impact of drainage on low flows and drought, with most focusing on high flows and floods. We find evidence of changes in flows consistent with the timing of arterial drainage works. In line with previous research high flows are greater in magnitude following drainage, while we find that drainage results in an increase in baseflow and to a lesser extent an increase in runoff, resulting in enhanced annual mean flows relative to the pre drainage record. Despite the increase in baseflow we find limited evidence for change in low flow metrics below Q70 (the flow exceeded 70 percent of the time) in the post drainage period. Moreover, for individual drought events, we find little difference between model simulated drought duration and accumulated deficits in the post drainage period. However, we do find some evidence that arterial drainage may increase the severity of minimum flows during drought events, although we highlight this result as tentative and suggest that future research should examine the robustness of our result.

Overall, our findings contrast with one of the few studies to examine drainage impacts on low flows, whereby increases in low flows were found for the river Maine in Northern Ireland following implementation of drainage works. This highlights the importance of local scale hydrology, catchment characteristics and the specifics of the drainage installation works

themselves in determining overall rainfall runoff responses. It is therefore difficult to extrapolate the above findings beyond the Boyne catchment. Valuable ongoing research is attempting to rescue hydrometric data for arterially drained catchments in Ireland (de Smeth et al., 2023) to extend available observations for implementation of simulation-based approaches to attribution, as implemented here. These data will facilitate a greater sample of drained catchments with pre and post drainage records to further investigate impacts across the flow regime.

References

Alexandersson, H. (1986), A homogeneity test applied to precipitation data, Journal of Climatology 6, 661–675.

Bailey, A. D. and Bree, T. 1981. Effect of improved land drainage on river flow, in: Flood Studies Report – five Years on, Thomas Telford, London, 131–142.

Bhattarai, K.P. and O'Connor, K.M., 2004. The effects over time of an arterial drainage scheme on the rainfall-runoff transformation in the Brosna catchment. *Physics and Chemistry of the Earth, Parts A/B/C*, *29*(11-12), pp.787-794.

Blann, K.L., Anderson, J.L., Sands, G.R. and Vondracek, B., 2009. Effects of agricultural drainage on aquatic ecosystems: a review. *Critical reviews in environmental science and technology*, *39*(11), pp.909-1001.

Bree, T. and Cunnane, C. 1979. Evaluating the effects of arterial drainage on river flood discharges, Annexe 1, Office of the Public Works, Dublin, Ireland.

Broderick, C., Matthews, T., Wilby, R.L., Bastola, S. and Murphy, C., 2016. Transferability of hydrological models and ensemble averaging methods between contrasting climatic periods. *Water Resources Research*, *52*(10), pp.8343-8373.

Broderick, C., Murphy, C., Wilby, R.L., Matthews, T., Prudhomme, C. and Adamson, M., 2019. Using a scenario-neutral framework to avoid potential maladaptation to future flood risk. *Water resources research*, *55*(2), pp.1079-1104.

Buishand, T.A. (1982), Some Methods for Testing the Homogeneity of Rainfall Records, Journal of Hydrology 58, 11–27

Burdon, D.J., 1986. Hydrogeological aspects of agricultural drainage in Ireland. *Environmental Geology and Water Sciences*, *9*(1), pp.41-65.

Coron, L., Andréassian, V., Perrin, C., Lerat, J., Vaze, J., Bourqui, M. and Hendrickx, F., 2012. Crash testing hydrological models in contrasted climate conditions: An experiment on 216 Australian catchments. *Water Resources Research*, *48*(5).

Coron, L., Thirel, G., Delaigue, O., Perrin, C. and Andréassian, V., 2017. The suite of lumped GR hydrological models in an R package. *Environmental modelling & software*, *94*, pp.166-171.

De Smeth, K., Comer, J, Murphy, C., 2023. Hydrometric data rescue and extension of river flow records: Method development and application to catchments modified by arterial drainage. *Geosciences Data Journal*. Submitted.

Donegan, S., Murphy, C., Harrigan, S., Broderick, C., Foran Quinn, D., Golian, S., Knight, J., Matthews, T., Prudhomme, C., Scaife, A.A. and Stringer, N., 2021. Conditioning ensemble streamflow prediction with the North Atlantic Oscillation improves skill at longer lead times. *Hydrology and Earth System Sciences*, *25*(7), pp.4159-4183.

Drogue, G. and Khediri, W.B., 2016. Catchment model regionalization approach based on spatial proximity: Does a neighbor catchment-based rainfall input strengthen the method?. *Journal of Hydrology: Regional Studies*, *8*, pp.26-42.

Essery, C.I. and Wilcock, D.N., 1990. The impact of channelization on the hydrology of the upper river main, county antrim, northern Ireland—a long term case study. *Regulated Rivers: Research & Management*, *5*(1), pp.17-34.

Gramlich, A., Stoll, S., Stamm, C., Walter, T. and Prasuhn, V., 2018. Effects of artificial land drainage on hydrology, nutrient and pesticide fluxes from agricultural fields–A review. *Agriculture, Ecosystems & Environment*, *266*, pp.84-99.

Gustard, A. and Demuth, S., 2009. Manual on low-flow estimation and prediction. Operational hydrology report, No. 50 WMO-No. 1029. *World Meteorological Organization, Geneva, Switzerland*, *136*.

Harrigan, S., Murphy, C., Hall, J., Wilby, R.L. and Sweeney, J., 2014. Attribution of detected changes in streamflow using multiple working hypotheses. *Hydrology and Earth System Sciences*, *18*(5), pp.1935-1952.

Kendall, M. G.: Rank correlation methods, Charles Griffin, London, 1975

Koffler, D. and Laaha, G., 2012, April. LFSTAT-an R-package for low-flow analysis. In *EGU General Assembly Conference Abstracts* (p. 8940).

Mann, H. B.: Nonparametric tests against trend, Econometrica, 13, 245–259, 1945

O KELLY, J.J., 1955. The employment of unit hydrographs to determine the flows of irish arterial drainage channels. *Proceedings of the Institution of Civil Engineers*, *4*(4), pp.365-412.

Perrin, C., Michel, C. and Andréassian, V., 2003. Improvement of a parsimonious model for streamflow simulation. *Journal of hydrology*, *279*(1-4), pp.275-289.

Pettitt, A. N. (1979), A non-parametric approach to the change point problem. Journal of the Royal Statistical Society Series C, Applied Statistics 28, 126-135.

Pohlert, T., Pohlert, M.T. and Kendall, S., 2016. Package 'trend'. *Title non-parametric trend tests and change-point detection*.

Sen, P.K. (1968), Estimates of the regression coefficient based on Kendall's tau, Journal of the American Statistical Association 63, 1379–1389.

Section iv)

Relating drought indices to impacts reported in newspaper articles

Previous deliverables highlighted the utility of newspaper records for examining drought impacts in the Boyne catchment. In this work we expand the analysis of newspaper impact reports to a larger number of catchments in Ireland. In doing so we explored the link between standardised drought metrics representing meteorological and hydrological droughts and associated thresholds typically associated with reporting of drought impacts in newspapers. These findings show the value of newspaper archives for understanding regional sensitivities to drought and have potential to inform the development of a drought monitoring and warning system in Ireland.

1. Introduction

Drought is one of the most damaging natural hazards, arising from extended periods of reduced precipitation, often covering large areas for periods of months to years, or even decades (Mishra and Singh, 2010; Van Loon and Laaha, 2015). Impacts may be experienced at local, regional and national scales (Wilhite *et al*., 2007), including reduced agricultural output, freshwater shortages, ecosystem degradation, reduced energy and industrial productivity (Gil *et al*., 2013; Mosely, 2015; Van Vliet *et al*., 2016; García-León *et al*., 2021). Given their effects, understanding drought events and their links to impacts is crucial to successful management (Wilhite *et al*., 2007). Typically, drought assessments involve analysing the features of historic drought – in terms of their occurrence, duration, intensity and accumulated moisture deficits, expressed through drought indicators. Studies linking indicators to impacts, however, have been relatively rare, primarily due to the limited availability and spatial coverage of historical impact data (Bachmair *et al*., 2015). Studies undertaken typically relate to agricultural drought and linking indices to crop yields, with multi-sectoral impact assessments much sparser (Wang *et al*., 2020b). As such studies are of fundamental importance in gaining a better understanding of drought impacts, further research is warranted in this area (Bachmair *et al*., 2016).

Indices are widely employed to quantify historic and future drought (Steinemann *et al*., 2015; Ekström *et al*., 2018). For meteorological drought, indices such as the Standardised Precipitation Index (SPI), Standardised Precipitation Evapotranspiration Index (SPEI), Effective Drought Index (EDI), Reconnaissance Drought Index (RDI) and Palmer Drought Severity Index (PDSI) are often used (e.g., Erfurt *et al*., 2019; Erfurt *et al*., 2020; Deo *et al*., 2017; Tsakiris *et al*., 2007; Lloyd-Hughes and Saunders 2002). For hydrological drought, indices such as the Standardised Streamflow Index (SSI), Total Storage Deficit Index (TSDI) and Palmer Hydrological Drought Index (PHDI) can be applied (e.g. Vicente-Serrano *et al*.,

2012b; Nie *et al*., 2018; Karl, 1986). Although indicators provide a means of quantifying and comparing droughts (Vicente-Serrano *et al*., 2011) their usefulness and representativeness of extreme events can be limited when derived from short series (Wu *et al*., 2005). Furthermore, drought indices may not always reflect actual impacts on society and/or the environment (Bachmair *et al*., 2016), particularly in cases of modulation and propagation of hydrological droughts by catchment properties (Barker *et al*., 2016; Rust *et al*., 2021).

Good quality, long-term precipitation and flow records are essential for drought analysis (Brigode *et al*., 2016). However, most precipitation datasets are short, with observations typically commencing in the second half of the 20th century in many regions (Brunet and Jones, 2011). For river flows, available records are often even shorter (Mediero *et al*., 2015). Data rescue efforts are continually extending the availability of observed meteorological variables including precipitation (e.g. Ashcroft *et al*., 2018; Hawkins *et al*., 2019; Ryan *et al*., 2021a), however historical records for river flow are not as readily available. One means of addressing this is by reconstructing historic river flows using rainfall-runoff models forced with long-term temperature and precipitation series (e.g. Jones, 1984; Spraggs *et al*., 2015; Crooks and Kay, 2015; Rudd *et al*., 2017; Hanel *et al*., 2018; Smith *et al*., 2019; Noone and Murphy, 2020; O'Connor *et al*., 2021b).

Drought indicators have been extracted from reconstructed flows to assess historical droughts in a number of studies (e.g. Caillouet *et al*., 2017; Hanel *et al*., 2018; Erfurt *et al*., 2020; Rudd *et al*., 2017; Moravec *et al*., 2019; O'Connor *et al*., 2022a). However, knowledge of drought characteristics alone does not necessarily translate into socio-economic impacts. Establishing robust links between indicators and impacts is important for evaluating and communicating drought risks. Methods have been developed to do this by associating meteorological drought indices with historic records (e.g. Vicente-Serrano *et al*., 2012a; Gudmundsson *et al*., 2014; Bachmair *et al*., 2015; Blauhut *et al*., 2015; Stagge *et al*., 2015a; Bachmair *et al*., 2018; Parsons *et al*., 2019; Salmoral *et al*., 2020). Others have related hydrological drought to impact metrics (e.g. Bachmair *et al*., 2016; Sutanto and Van Lanen, 2020) by drawing on centralised databases (e.g., the European Drought Impact Report Inventory: Stahl *et al*., 2012). National-level databases also exist, such as the UK Drought Inventory (UKCEH, 2021) and US Drought Impact Reporter (Wilhite *et al*., 2007). In Ireland, historic monastic writings, including the Irish annals, have been used to evaluate extreme weather events and their impacts over the last two millennia (e.g. Hickey, 2011; Ludlow 2006). More recently, Murphy *et al*. (2017) demonstrated the value of historical newspaper archives in an analysis of drought impacts over the past 250 years. Noone *et al*. (2017) also used newspaper archives to verify the occurrence and duration of historical droughts. The utility of newspaper articles as a source of information on drought impacts has also been demonstrated in the UK (e.g. Dayrell *et al*., 2022) and elsewhere (e.g. Llasat *et al*., 2009; Linés *et al*., 2017; Brázdil *et al*., 2019).

The SPI has been shown to be effective in generating strong links between drought occurrence and agricultural impacts (Vincente-Serrano *et al*., 2012a). Similarly, the SSI has demonstrable utility for linking hydrological drought with groundwater levels, vegetative growth, and agricultural yields (Vicente-Serrano *et al*., 2021). Most studies explore such

associations using correlation analysis, but other methods have been trialled. For example, Bachmair *et al*. (2017) found that random forest and logistic regression models predicted text-based reports of a range of drought impacts well. Similarly, Blauhut *et al*. (2015), Parsons *et al*. (2019), Stagge *et al*. (2015a) and Sutanto *et al*. (2019) concluded that logistic regression could generate valuable information on localised impacts.

Although many studies have demonstrated the utility of indices in drought assessments (Kchouk *et al*., 2021), impacts are often evaluated within a static framework under assumed stationarity. However, population change, demographic profiles, technological developments, water and land management policies, environmental conditions, water demand and social behaviour are all dynamic factors affecting drought vulnerability (Wilhite *et al*., 2014). Recent studies have begun to address this knowledge gap. For example, Parsons *et al*. (2019) found an increasing likelihood of agricultural related drought impact reports in the UK, which they equate to increases in actual or perceived vulnerability as a result of changing farming and reporting practices. Stagge *et al*. (2015a) attributed inter-annual variations in agricultural drought impacts across Europe to sampling and reporting bias, impact awareness, changes in coping capacity, economic stressors and political effects. Erfurt *et al*. (2019) found that, despite meteorological drought propagation and types of impacts remaining consistent over time in southwest Germany, impacts and vulnerability have fallen.

In this paper, we related monthly drought indicators and reported impacts for 51 catchments in Ireland. We use reconstructed catchment precipitation and river flows, alongside drought impacts derived from newspaper archives covering the period 1900-2016. Section 2 provides an overview of the datasets and methods employed, Section 3 presents the results of our analysis, then Section 4 provides a discussion of key results and insights. Finally, conclusions are drawn and suggestions for further research are offered in Section 5.

2. Data and Methods

2.1 Meteorological and hydrological data

Meteorological and hydrological data consist of monthly precipitation and river flow reconstructions (1767-2016), produced by O'Connor *et al.* (2021a) for 51 catchments across Ireland[1]. Catchment specific monthly precipitation reconstructions were extracted from the gridded (0.5° x 0.5°) precipitation dataset developed by Casty et al. (2007) and bias-corrected to observed catchment data. O'Connor *et al*. (2021a) also produced uncertainty estimates for flow reconstructions by applying different model structures and parameter sets; here we use the available ensemble median flow reconstruction for each catchment. Previous hierarchical cluster analysis of the SSI-1, 3, 6 and 12 during 1767-2016 identified three dominant catchment clusters for Ireland from the same 51 test catchments (O'Connor *et al.*, 2022a). To allow for a comparison of results between both studies, we conduct our analysis using the same cluster groupings (see Figure 1a). Cluster 1 catchments, located in the wetter northwest of the island, have relatively small areas, low groundwater content, and most frequent hydrological droughts. Cluster 3 catchments, located in the drier east/southeast, have

[1] https://doi.org/10.1594/PANGAEA.914306

relatively large groundwater contributions, large areas and the lowest frequency of hydrological droughts that, once established, result in the longest durations and greatest accumulated deficits. Cluster 2 catchments, located in the southwest, have a drought frequency intermediate between Cluster 1 and 3, with short durations and relatively low accumulated deficits. Median monthly flow and precipitation were extracted for catchments comprising each identified cluster. As per O'Connor *et al.* (2022a), standardised drought indices for 1767-2016 were applied to median monthly precipitation and flow data in each cluster. These were the Standardised Precipitation Index (SPI; McKee *et al*., 1993) and Standardised Streamflow Index (SSI; Vicente-Serrano *et al*., 2012b) over accumulations of 1, 2, 3, 4, 5, 6, 9, 12 and 18 months. These were generated using the "SCI" package in R (Gudmundsson and Stagge, 2016). The 70-year reference period (1930-2000) and the Tweedie distribution, both found by O'Connor et al. (2022a) to perform best at fitting SPI and SSI in Irish catchments, were employed to generate indices. Extracted monthly SPI and SSI series for 1767-2016 were subsequently truncated to 1900-2016, concurrent with the derived drought impact data discussed next.

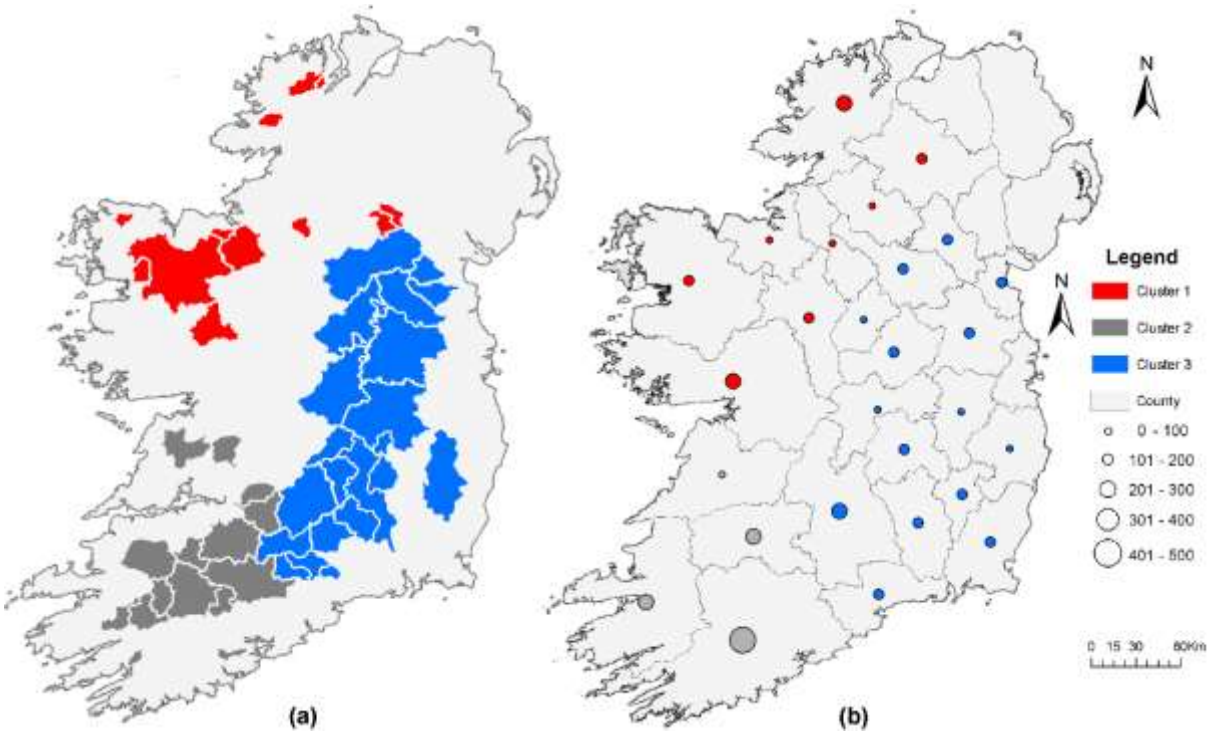

Figure 1. Spatial distribution of (a) clusters of catchments used in the analysis and (b) counties and corresponding drought impact article numbers (combined land-based and hydrological-based) over the period 1900-2016.

2.2 Drought Impact Data

Jobbová *et al*. (2022b) developed an Irish Drought Impacts Database (IDID; Jobbová *et al*., 2022a) from the Irish Newspaper Archive (INA) spanning the period 1738-2019. The INA is

an online newspaper database consisting of over six million pages of searchable content from 100 titles for the Island of Ireland. A number of search terms were trialled (e.g. “dryness”, “dry spell”, etc.) with the terms ‘drought’ and ‘droughts’ finally chosen to identify relevant newspaper articles. All search results were assessed so as to remove articles that used the term for descriptive or other purposes resulting in a total of 6,309 drought related articles. Using a modification of European Drought Impact report Inventory (EDII; Stahl *et al*., 2012) adapted to cater for the nature of the Irish newspaper data, returned articles were assigned to 15 drought impact categories (i.e. agriculture and livestock farming; forestry; freshwater aquaculture and fisheries; energy and industry; waterborne transportation; tourism and recreation; public water supply; water quality; freshwater ecosystem: habitats, plants and wildlife; terrestrial ecosystem: habitats, plants and wildlife; soil systems; wildfires; air quality; human health and public safety; conflicts), with the possibility of each article being assigned to one or more categories depending on impacts described. Where the described impact could be categorised under multiple categories the final decision on the associated grouping was determined by the authors to ensure consistency in classifications across the entire dataset. For each drought impact, i.e. the occurrence of an article that references a specific impact related to a drought event and fitting to one of the pre-defined impact types, information including the date of publication, date of impact, location, newspaper title and a quote from the article were all included in the database.

In total, more than 11,500 individual drought impact reports are included in the IDID dataset. The number of titles contributing to the INA remains relatively stable for the period post-1900, while having good spatial coverage across Irish counties. Therefore, we employ output from the IDID for the period 1900-2016, concurrent with the last year of available meteorological and hydrological data. Of the 15 drought impact categories we retain all but the Human Health and Public Safety and Conflicts categories due to a lack of articles in those categories. The resulting 13 drought impact categories were further grouped into two simple categories signified as land-based impact reports (related to agriculture and livestock farming, terrestrial ecosystems, soil systems, wildfires, air quality, and forestry) and hydrological-based impact reports (related to aquaculture and fisheries, waterborne transport, energy and industry, tourism and recreation, public water supply, water quality and freshwater ecosystems). We matched the associated year and month of each reported impact in the IDID to the drought indices on that date. Impact reports which did not include a year and month of impact were excluded from the analysis. Impact reports in the IDID are not systematically compiled for catchments, therefore, we tallied reports for each county, the boundaries of which have remained largely unchanged over the period of assessment and assigned them to one of our three clusters of catchments (see Figure 1b). Impact reports that did not provide a specific location or from which the relevant county could not be derived were excluded from the analysis. When a county straddles two clusters of catchments, impact reports are associated with the cluster overlapping the largest area of that county. Counties with no study catchment(s) contained within their boundaries (five in total) were excluded from the assessment. An inventory of article numbers, by county, allocated cluster and drought impact sub-category is given in Table S1. For each cluster, the cumulative number of drought impact reports were then calculated for each month from 1900-2016.

2.3 Model generation and analysis

Logistic regression and Generalised Additive Models (GAMS) have been previously used to link drought indices to impacts (Bachmair *et al*., 2017; Parsons *et al*., 2019; Stagge *et al*., 2015a). We take a similar approach by applying binomial logistic regression models to establish relationships between SPI and SSI indices with drought impact occurrence (based on article counts). First, we transform the dependent variable (impact articles) into a binary series by noting the occurrence/non-occurrence of articles. Logistic regression was then used to determine the odds of event occurrence (impact article), by relating the conditional expectation of the response variable to a combination of linear predictor variables (drought indices). This link was obtained using a logit, or log odds function typically applied to derive the probability of occurrence from regression models (see Morgan *et al*., 1988). Logistic regressions were fit using the Generalised Additive Model (GAM) framework which enables logistic regressions to be applied with a smoothing function for selected predictor variables (month values) to account for non-linear components in series (e.g. the seasonal components of monthly SPI/SSI values). To convert the log-odds predicted output to a simple probability output (i.e. to generate impact probability values in the range from 0 to 1) the inverse logit of the predicted values were found. Values could then be easily categorised by their probability of impact and assessed for each model.

Model fitting and subsequent predictions were carried out in the R environment using the 'mgcv' package (Wood, 2012). Individual models were generated for each cluster linking SPI values to land- and SSI values to hydrological-based articles. Model predictor variables included standardised drought indices, smoothed month values and year values. Month values account for seasonal variations in drought impact reporting probability, whilst year values allow for any trends in the data (cf. Parsons *et al*., 2019).

Weights were derived and then applied to each model to account for cases where more than one drought impact article occurred in a given month. For each model we determined the weights by reciprocally ranking the total monthly article numbers. The procedure was as follows: Step 1, the date (month/year) with the highest number of articles was ranked as one (rank1 = 1), the second highest as two (rank2 = 2), etc., until all dates were assigned a rank. Dates with the same number of articles were given the same rank, including dates with zero articles which were assigned the lowest rank. Step 2, the Reciprocal Rank was found for this series of ranked values, as shown in equation 1, with i representing the rank number, Q representing the total number of distinct article values. Step 3, the resultant series of values was then applied as the weighting factor in the final model, in the order of the original time-series.

$$Reciprocal\ Rank = \sum_{i=1}^{Q} \frac{1}{rank_i} \qquad (1)$$

Reciprocal ranked weights were determined separately for each model. Dependent variable values for each model were represented by the binary occurrence/non-occurrence of monthly

drought impact articles (land- or hydrological-based) for each cluster, with final model output returning the probability of occurrence of articles for given SI values.

Following Parsons *et al*. (2019), we test the model by initially generating logistic regression models with a single predictor consisting of either SPI or SSI at accumulations of 1, 2, 3, 4, 5, 6, 9, 12 or 18 months. Only one drought index accumulation period was considered in each model as indices for overlapping periods tend to be highly correlated. Model performances were assessed using the different accumulation periods, with best performing accumulation periods for each cluster identified for the 1900-2016 period and retained. Model performance was assessed by evaluating the amount of explained variance, adjusted for sample size (R2adj). Subsequently, models were regenerated with the inclusion of smoothed monthly values (to account for seasonality of reported impacts) as well as year (to account for any trend). Smoothing was carried out using the Restricted Maximum Likelihood (REML) approach to estimate components of variance resulting from the unbalancing caused by the nonlinear, seasonal impacts of the monthly data. Models were then re-evaluated to examine improvement in skill.

For each cluster, models were used to relate SPI and SSI to predicted impact report probabilities, i.e., the likelihood of a drought related newspaper article for a given SPI or SSI value. To aid interpretation, we classify reported impact probability scores as follows: 'very low' (0-0.19), 'low' (0.20-0.39), 'medium' (0.40-0.59), 'high' (0.60-0.79), and 'very high' (0.80-1.00). We primarily focus on the high probability of reported impacts threshold (≥0.60) as it represents an above average likelihood of impact report occurrence. We identify temporal and spatial variations in drought impact reports for each catchment cluster over the full 116 years using SPI and SSI values at that threshold and at the lower limit of -3 SI, matching that used by Parsons *et al*., 2019. We also investigate the variation in reported impact probabilities at annual and monthly timescales with the latter allowing for assessment of how reported impact likelihood changes within clusters over the course of a year. Annual probabilities were derived by finding the mean of the monthly probabilities for each year across the 1900-2016 period. Finally, we assess homogeneity in reported drought impact likelihoods by identifying any significant change points in the drought impact report series for each cluster, using the non-parametric Pettitt (1979) test. Theil-Sen slope estimates (Sen, 1968) were also calculated to identify significant trends in the series. We subsequently investigate how impact report likelihoods (for SPI and SSI values of -3) and SPI and SSI values required to exceed the high likelihood (0.6) threshold have changed in each cluster pre/post break point.

3. Results

3.1 Indices and impact data

SPI and SSI were derived for each cluster for the period 1900-2016 for accumulations of 1, 2, 3, 4, 5, 6, 9, 12 and 18 months (sample plots are shown in Figures S1 and S2). Across the period there are several extreme events identifiable in both the SPI and SSI series, and over multiple accumulation periods. These include the 1933-1935, 1953-1954, 1971-1972 and

1975-1977 droughts. Other prominent events in the SPI series are less notable in the SSI equivalent, such as the 1911-1912 and 1983-1984 droughts, whilst events such as the 2003-2004 drought show greater prominence in the SSI series. Figure 2 plots the annual number of articles by cluster over the period 1900-2016. Notable are the high number of articles for Cluster 3 and the large decrease in land-based drought reports in both Clusters 1 and 2 during recent decades. Some of the largest meteorological and hydrological drought article numbers occur in 1921, 1938, 1940, 1949, 1959, 1975 and 1984. Differences in article numbers for certain events are identifiable between clusters and article types. Although most droughts coincide with article occurrence (e.g. the 1911-1912 and 1975 droughts) others show fewer impact reports, despite being classified as severe or extreme droughts by the standardised indices (e.g. the 1933-1934 and 1972-1973 droughts). Conversely, events such as the 1921 and 1949 droughts do not rank as significant droughts in SPI- and SSI-12 series despite producing some of the highest number of drought impact reports. It should be noted however that the level of agreement between drought impact reports and indices is dependent on the accumulation period applied.

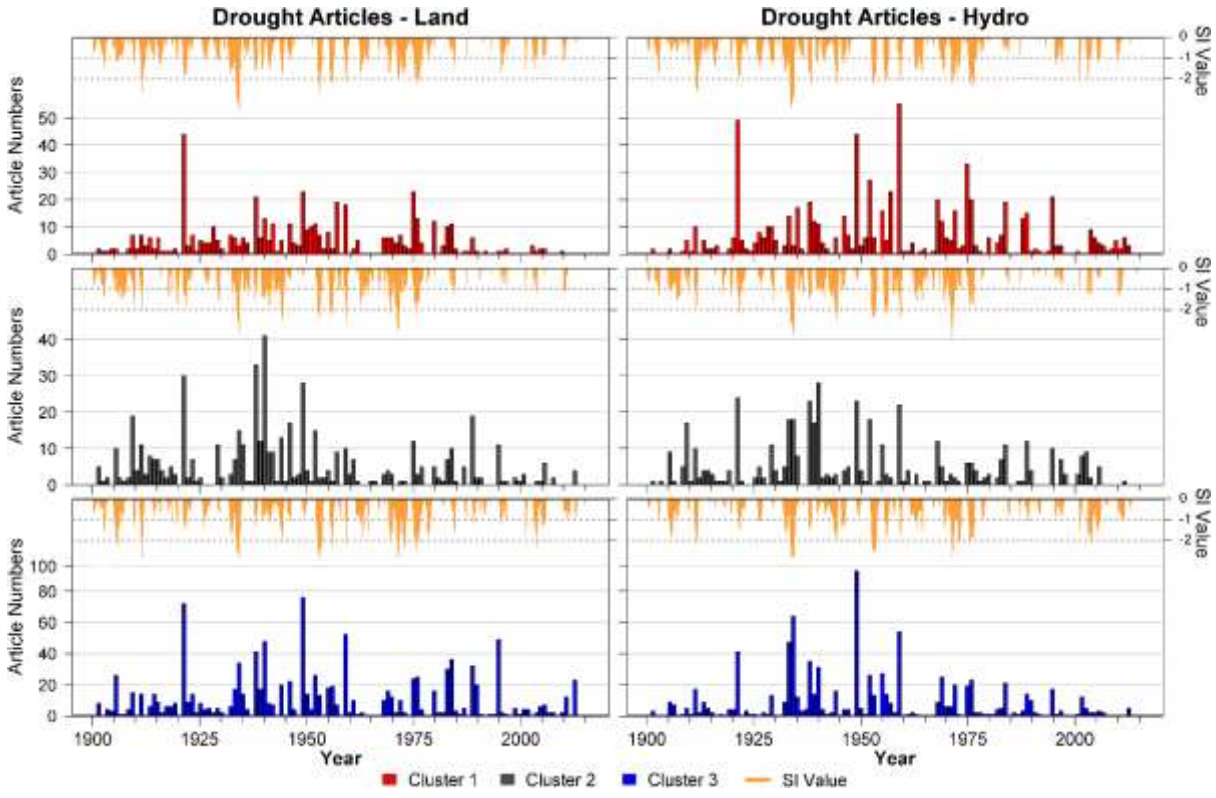

Figure 2. Distribution of land-based (left) and hydrological-based (right) drought impact reports (annual totals) for each cluster (bottom of each panel) are displayed for the period 1900-2016. Also displayed are related SI values (top of each panel; SPI-12 on the left and SSI-12 on the right).

3.2 Model performance analysis

Logistic regression and GAMs show the relationship between SPI/SSI and land-/hydrological-based impact reports in each cluster. Figure 3 displays results of this assessment with R2adj values for different SPI/SSI accumulation periods plotted for land-

and hydrological-based impact reports (lighter coloured bars). For hydrological-based impact reports SSI-2 performed best across all three clusters (R2adj values of 0.14 ($p<0.05$; Cluster 1), 0.18 ($p< 0.05$; Cluster 2) and 0.25 ($p< 0.05$; Cluster 3)). For land-based impact reports SPI-3 performed best having the highest R2adj score for Cluster 1 (0.10; $p<0.05$) and 3 (0.17; $p<0.05$). For Cluster 2, SPI-2 performed marginally better than SPI-3 (0.11; $p<0.05$ versus 0.10 ($p<0.05$). For simplicity, SPI-3 was adopted as the best predictor of land-based drought impact reports in all clusters.

Following Parson *et al*. (2019) both month and year predictor variables were added to each of the best performing single variable models (i.e. SPI-3 and SSI-2), with monthly smoothing implemented using the REML method (see Section 2.3). Model performance was again assessed using R2adj, with results presented in Figure 3 (darker coloured bars). Across all clusters, inclusion of month led to significant model improvements. Final model structures for land- and hydrological-based drought impact reports are given in Equations 2 and 3, with additional performance metrics provided in Table 1. For reported land-based impacts (Eq. 1) model performance is best for Cluster 3 (R2adj = 0.49; $p<0.05$), with Cluster 1 and 2 having R2adj values of 0.34 ($p<0.05$). For reported hydrological-based impacts (Eq. 2) model performance is greater than the land-based equivalent for Cluster 1, 2 whilst for Cluster 3 it is lower, with R2adj values of 0.38, 0.35 and 0.42 respectively (all with p-values of <0.05).

$$\mathrm{SPI}-3 + s(\mathrm{month}) + \mathrm{year} \quad (2)$$

$$\mathrm{SSI}-2 + s(\mathrm{month}) + \mathrm{year} \quad (3)$$

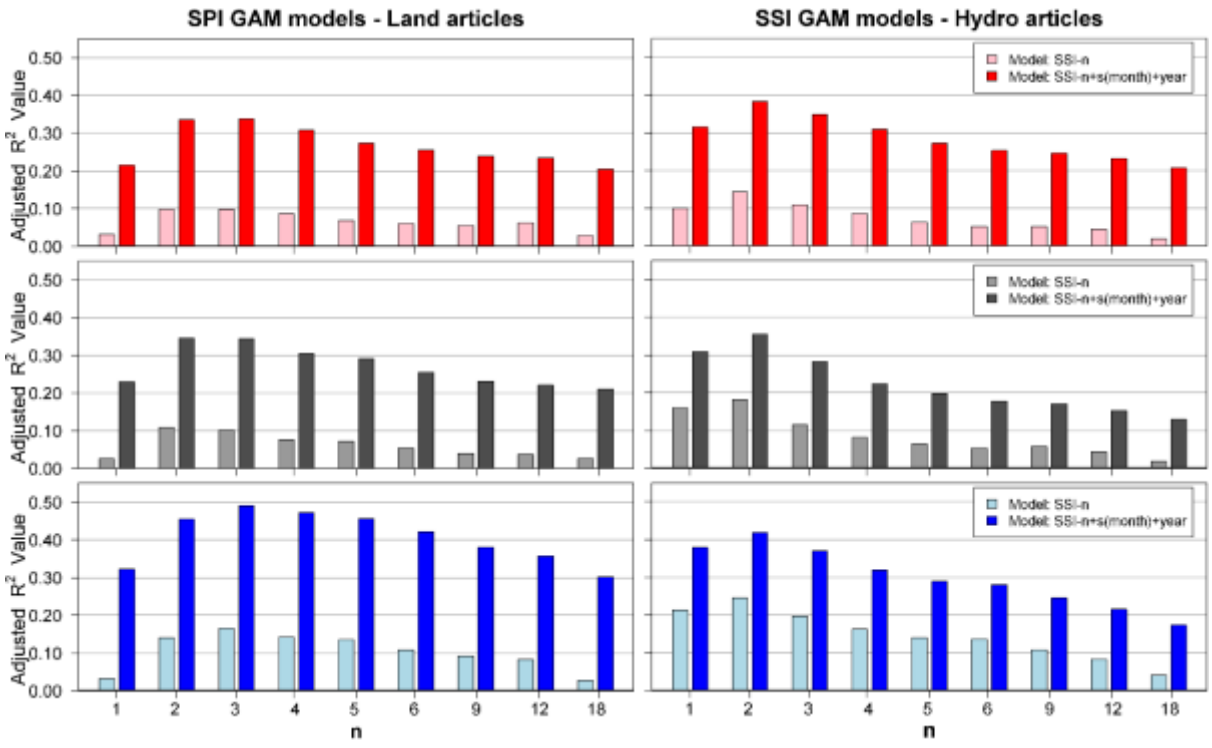

Figure 3. Adjusted R^2 values of the logistic regression models for selected SPI/SSI accumulation periods (n) when simulating monthly land- (left) and hydrological-based (right) impact articles for each cluster during 1900-2016. Results are also shown for models including month and year (darker colours).

Receiver Operator Characteristic (ROC) curves, which demonstrate the ability of models to correctly predict the occurrence or non-occurrence of an event, are shown in Figure 4 (see Stagge *et al*. (2015a) for a similar application). Values are assessed for increasing thresholds across the [0-1] range. For a perfect model the proportion of correctly identified impact articles is equal to 1 across all threshold values and will have an Area Under the Curve (AUC) value of 1. A model with zero skill produces an AUC of 0.5 and will lie on the diagonal (0:1) line. Here, both land- and hydrological-based models show good skill at correctly classifying drought impact reports, with the former performing marginally better overall. For land-based impact reports AUC scores are highest for Cluster 3 (0.90) and lowest for Cluster 2 (0.85). For hydrological-based impact reports AUC scores are highest for Cluster 1 and 3 (0.87) and lowest for Cluster 2 (0.85).

Table 1. Performance indicators for model (SPI-3 + s(month) + year) generated for land-based impact articles and model (SSI-2 + s(month) + year) generated for hydrological-based impact articles (1900-2016).

Model	Cluster No.	Intercept Co-eff.	Indices Co-eff.	Year Co-eff.	Adj R^2	P-value	% Deviance	AUC	AIC	BIC
SPI-3 + s(mont	1	17.30	-1.11	-0.01	0.34	0.001	35.07	0.87	13.61	46.49
	2	25.11	-1.04	-0.01	0.34	0.001	33.55	0.85	13.27	46.24
	3	21.34	-1.43	-0.01	0.49	0.002	45.94	0.90	12.90	46.00
SSI-2 + s(mont	1	2.64	-1.28	0.00	0.38	0.001	37.90	0.87	13.42	46.39
	2	19.30	-1.37	-0.01	0.35	0.001	34.36	0.85	12.71	44.68
	3	20.22	-1.58	-0.01	0.42	0.002	38.21	0.86	12.35	43.83

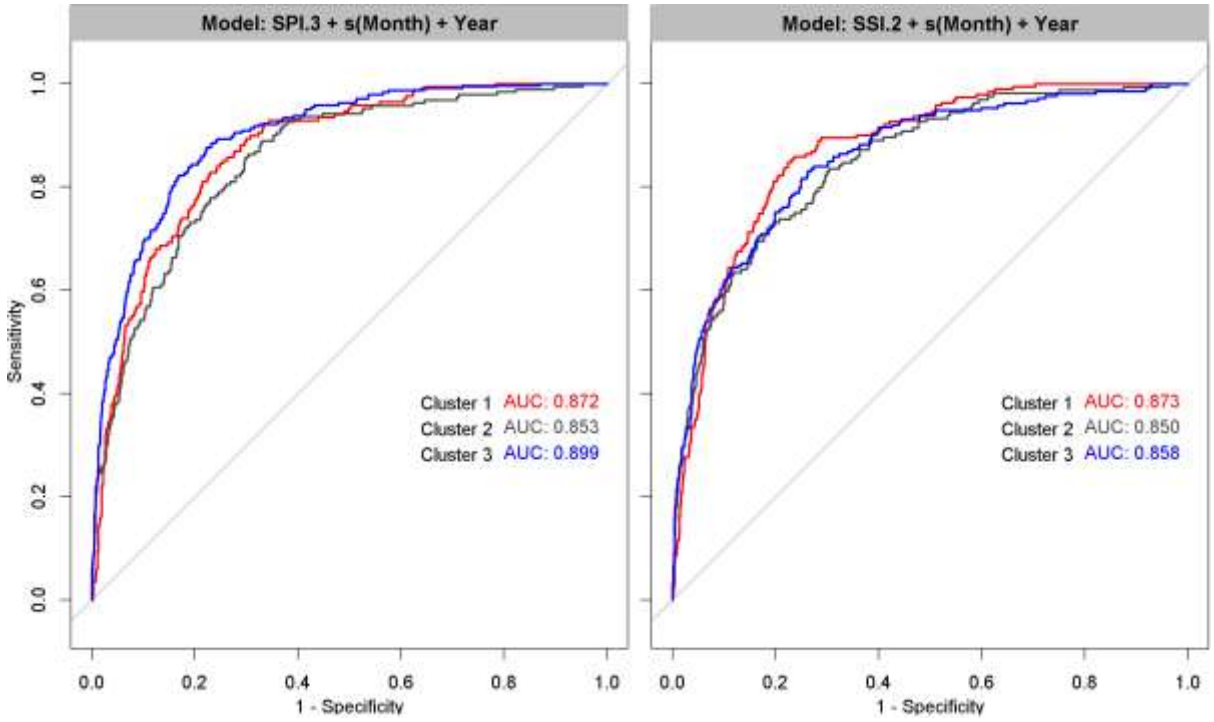

Figure 4. Receiver Operating Characteristic (ROC) curves displaying performance of the logistic regression models generated using land-based newspaper articles and SPI-3 indices (left) and for models generated using hydrological-based newspaper articles and SSI-2 indices (right) for each cluster.

3.3 Linking indices to reported impacts

Derived models were used to determine the likelihood of impact reporting at annual and monthly timescales. Initially, an examination of outputs from models generated using annualised SPI and SSI at 1, 2, 3, 4, 5, 6, 9, 12 and 18 month accumulations was carried out revealing that SPI-3 and SSI-2 generated the highest likelihoods of drought impacts across clusters, specifically at low deficits. Impact likelihood values reduced markedly for accumulations above and below 3 and 2 months respectively. Notably, the patterns of impact likelihoods across clusters remained similar for all accumulations. As SPI-3 and SSI-2 produced the highest impact likelihoods and best model performances for land-based and hydrological-based impact reports they were retained for further analysis. Figure 5 shows reported impact probabilities on an annual basis over the period 1900-2016. Cluster 3 has the highest reported impact probabilities for both SPI and SSI values. Clusters 1 shows the lowest reported impact probabilities for any given SPI value. For SSI-2, Cluster 1 shows a higher likelihood of impact reports than Cluster 2 for modest deficits, while the opposite is the case for more extreme SSI-2 deficits. Figure 5 also identifies SPI/SSI thresholds resulting in at least a high likelihood of impact reports (0.60). For land-based impact reports SPI-3 ≤ -2.68 for Cluster 1, ≤ -2.35 for Cluster 2 and ≤ -1.98 for Cluster 3 are identified as thresholds for high impact probabilities on an annual scale. For hydrological-based impact reports the equivalent values are SSI-2 ≤ -2.48 for Cluster 1, ≤ -2.02 for Cluster 2 and ≤ -1.60 for Cluster 3. Cluster 3 is identified as most likely to experience both land- and hydrological-based

drought impact reports, whereas Cluster 1 the least likely. Indices values required to reach each land- and hydrological-based drought impact report threshold are given in Table 4.

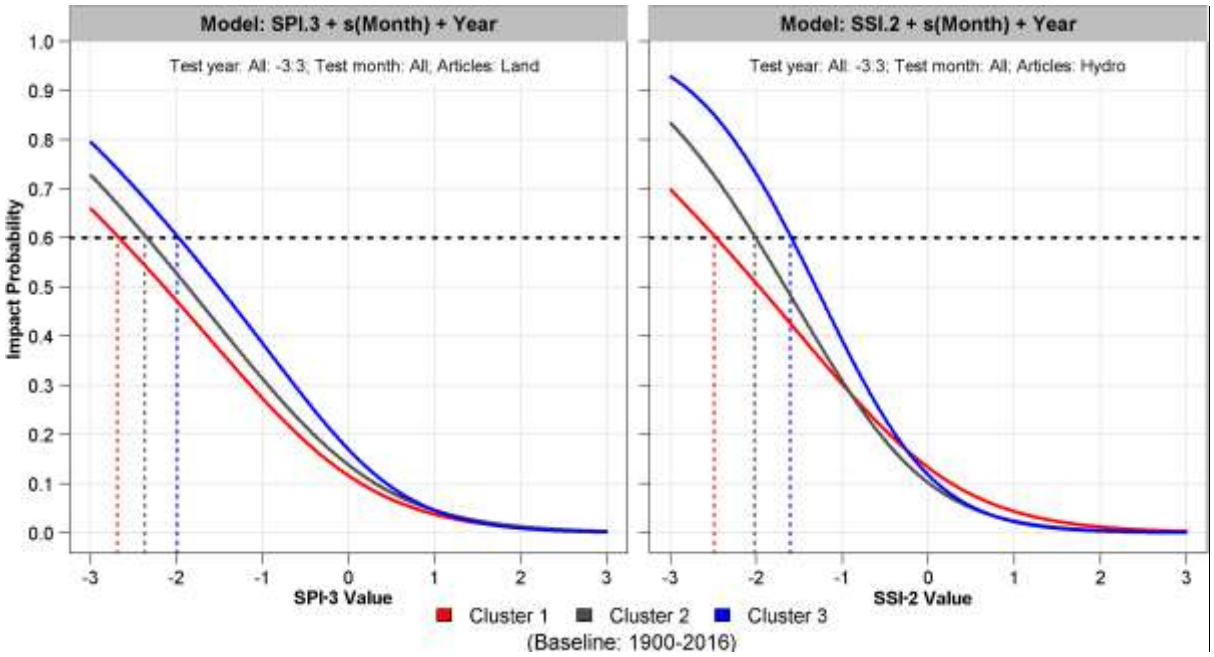

Figure 5. Predicted probability of reported impacts (annual) from models generated using land-based impact articles and SPI-3 indices (left) and from models using hydrological-based impact articles and SSI-2 indices (right). Impact likelihoods for each cluster over the period 1900-2016 are shown for indices values ranging from -3 to 3. Indices values resulting in high reported impact probabilities (0.60) are denoted by the dashed horizontal line.

Figure 6 displays results for likelihoods of monthly land-based drought impact reports. There are large variations in the probability of reported impacts across months and clusters. December and January show very low to low impact report probabilities, even for extreme deficits in SPI-3. February is the winter month with highest land-based impact report probabilities, reaching moderate probabilities for deficits of -3 SPI-3 in Cluster 2 and high probabilities in Cluster 3. Excluding December, Cluster 3 consistently shows the highest probability of impact reports in all months. The 0.6 threshold (dashed black horizontal lines) helps identify SPI-3 deficit values resulting in a high likelihood of impact reports. Notably, in summer (JJA) months only very modest SPI-3 deficits (not less than -1.2 SI) are required to reach this threshold for land-based impact reports in Cluster 3. July (closely followed by June) is the month most prone to reported impacts, with the most modest SPI-3 deficits resulting in high impact report probabilities (-0.90 for Cluster 1, -0.73 for Cluster 2 and -0.28 for Cluster 3). In autumn (SON), the SPI-3 deficits required to reach high reported impact probabilities become more extreme, with Cluster 3 remaining the most vulnerable. Throughout most months (excluding winter) there is little difference in land-based drought impact report probabilities between Clusters 1 and 2.

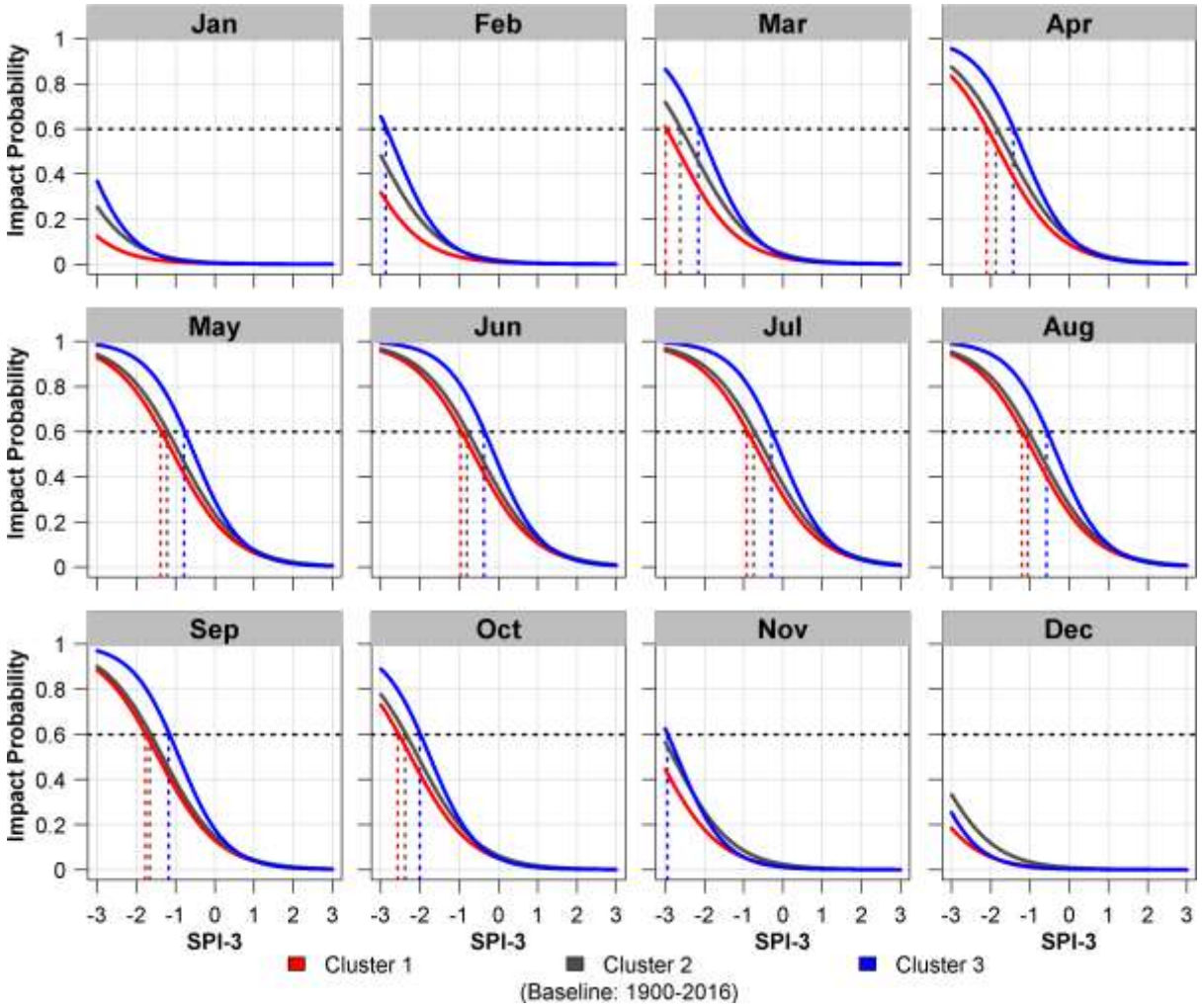

Figure 6. Predicted probability of reported impacts (monthly) from models generated using land-based impact articles and SPI-3 indices. Impact likelihoods for each cluster over the period 1900-2016 are shown for indices values ranging from -3 to 3. Indices values for each cluster resulting in a high reported impact probabilities (0.60) are also identified (dashed horizontal line).

Figure 7 displays monthly impact likelihoods for hydrological-based impact reports. Cluster 3 shows the highest likelihood of reported impacts across all months, particularly in autumn (SON), winter (DJF) and early spring. However, differences with Cluster 1 and 2 during late spring and summer, especially from May to August, are minimal, with Cluster 1 showing higher likelihood of impacts at low deficits during these months. From June through to August Cluster 2 is least sensitive to hydrological-based impact reports. Late autumn and winter months show the greatest differences between clusters with the likelihood of hydrological-based impacts in Cluster 3 markedly greater than that for Cluster 1 and, marginally greater than Cluster 2 from October till March. Cluster 3 consistently reaches the threshold of high probability of reported impacts across the year, but only for extreme SSI-2 deficits in winter months. During summer months, deficits of close to -1 SSI-2 are required to reach the 0.6 high probability of reported impacts threshold in most clusters. July is the month most prone to hydrological-based impact reporting, with the most modest SSI-2 deficits resulting in high impact report probabilities (-0.72 for Cluster 1, -0.98 for Cluster 2

and -0.80 for Cluster 3). The lowest reported impact probabilities are in December for Cluster 1 (very low probabilities) and January for Clusters 2 and 3 (moderate and high probabilities) for SSI-2 values of -3.

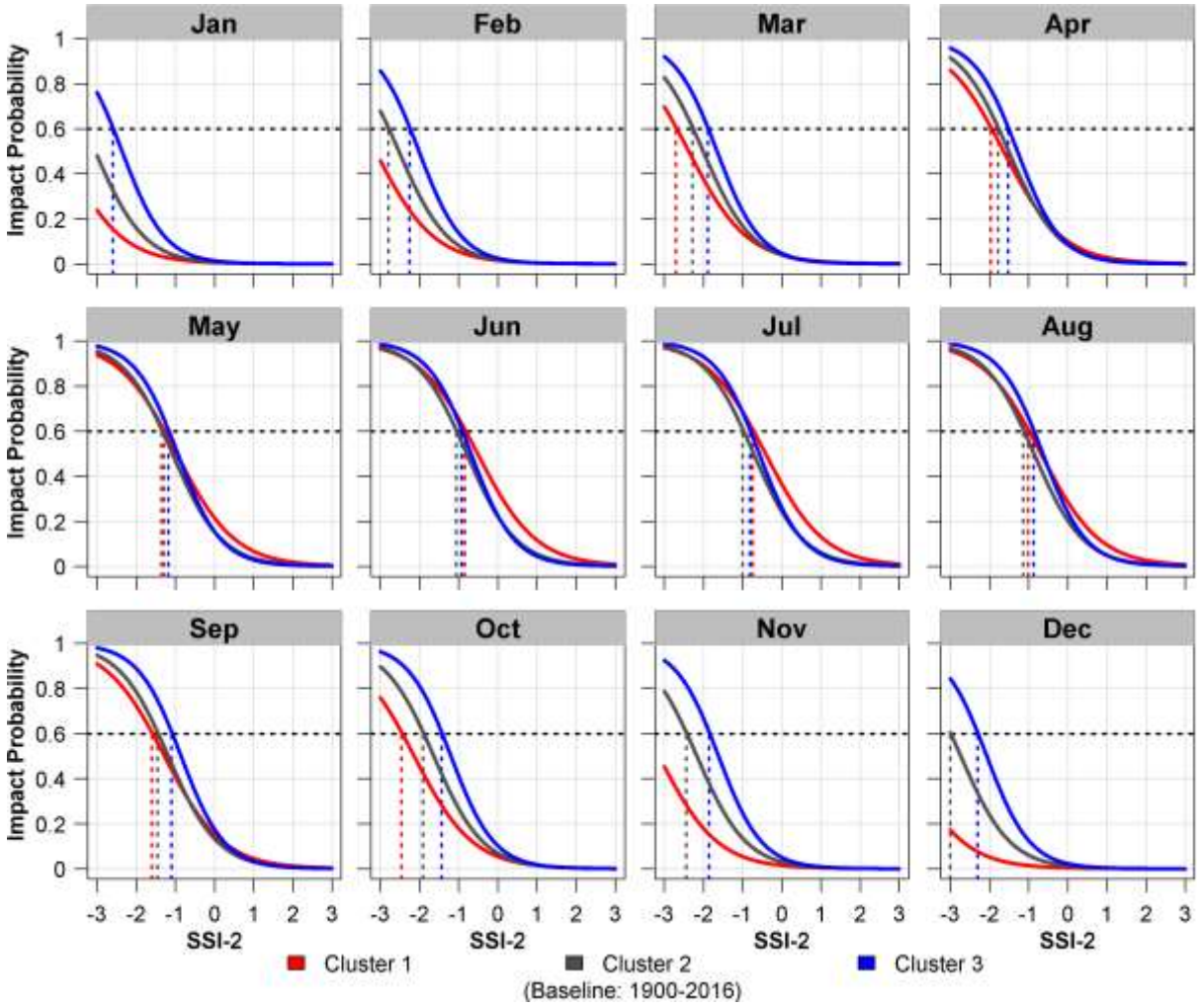

Figure 7. As in Figure 6 but for hydrological-based impact articles and SSI-2 indices.

3.4 Sensitivity of results to impacts baseline

All clusters display a negative year coefficient for land- and hydrological-based impact reports, with the exception of Cluster 1 for hydrological-based reported impacts (Table 1). Significant negative trends across all clusters were confirmed using Theil-Sens slope testing, again with the exception of hydrological-based reported impacts for Cluster 1. This suggests that during the 1900-2016 period there was an overall decline in reported drought impacts. According to the Pettitt test, there are notable step changes in the number of impact articles for each cluster and impact type, with statistically significant changes ($p<0.05$) identifiable in the land-based articles (see Table 2).

Table 2. Step change month and year identified for land and hydrological related articles grouped by each cluster over the 1900-2016 period.

Article Type	Cluster	Month	Year	p-value	Direction
Land -based	1	6	1985	0.03	downward
	2	7	1961	0.01	downward
	3	9	1961	0.02	downward
Hydrological -based	1	8	1977	0.47	downward
	2	6	1961	0.18	downward
	3	9	1959	0.08	downward

In Cluster 1 a significant downward step change in land-based drought impact articles was identified in 1985. In Cluster 2 and 3 significant downward changes were identified in 1961. For reported hydrological-based drought impacts, no significant changes (0.05 level) were found. Given the prominence of 1961 as a step change in drought impacts series, we evaluate the changing likelihood of reported impacts pre and post-1961. Table 3 shows model results and coefficients for the pre/post-1961 periods. Modest reductions in skill between the 1900-1960 and 1961-2016 periods are evident with greatest reductions in R2adj for land-based impact report models occurring in Cluster 2 (from 0.36 to 0.25; both $p<0.05$). The largest reduction in R2adj for hydrological-based impact models occurs for Cluster 3 (from 0.46 to 0.31; both $p<0.05$). The least change in R2adj between periods occurs for Cluster 1, land-based impact models. AUC scores show little change relative to the earlier period. Reductions in model performance post-1961 can be partially attributed to reduced occurrence of drought in the latter period as identified by Noone *et al*. (2017), while article numbers also fall by 59 % (Cluster 1), 69 % (Cluster 2) and 46 % (Cluster 3) for land- and 40 % (Cluster 1), 58 % (Cluster 2) and 63 % (Cluster 3) for hydrological-based impact reports.

Table 3. Performance indicators for model (SPI-3 + s(month) + year) generated for land-based impact articles and model (SSI-2 + s(month) + year) generated for hydrological-based impact articles (1900-1960 & 1961-2016).

Model (Period)	Cluster No.	Intercept Co-	Indices	Year Co-	Adjusted R^2	P-value	% Devian	AUC	AIC	BIC
SPI-3 +	1	-42.10	-1.01	0.02	0.37	0.028	36.46	0.8	13.5	42.0
s(month) +	2	-0.51	-1.01	0.00	0.36	0.007	31.98	0.8	12.8	41.1
(1900-1960)	3	-15.39	-1.48	0.01	0.52	0.007	48.66	0.9	12.5	40.9
SSI-2 +	1	-65.10	-1.34	0.03	0.47	0.025	45.23	0.9	13.2	41.9
s(month) +	2	-2.82	-1.36	0.00	0.37	0.003	34.27	0.8	12.3	39.7
(1900-1960)	3	-25.41	-1.66	0.01	0.46	0.001	41.69	0.8	11.9	38.9

SPI-3 +	1	50.52	-1.37	-0.03	0.36	0.053	38.54	0.8	11.8	38.4
s(month) +	2	6.27	-1.02	-0.01	0.25	0.007	30.63	0.8	11.8	38.6
(1961-2016)	3	-0.91	-1.28	0.00	0.41	0.007	40.85	0.8	11.9	38.8
SSI-2 +	1	11.63	-1.28	-0.01	0.34	0.027	34.58	0.8	11.7	38.2
s(month) +	2	19.80	-1.22	-0.01	0.28	0.000	29.91	0.8	11.6	37.9
(1961-2016)	3	38.78	-1.30	-0.02	0.31	0.001	30.33	0.8	11.1	36.3

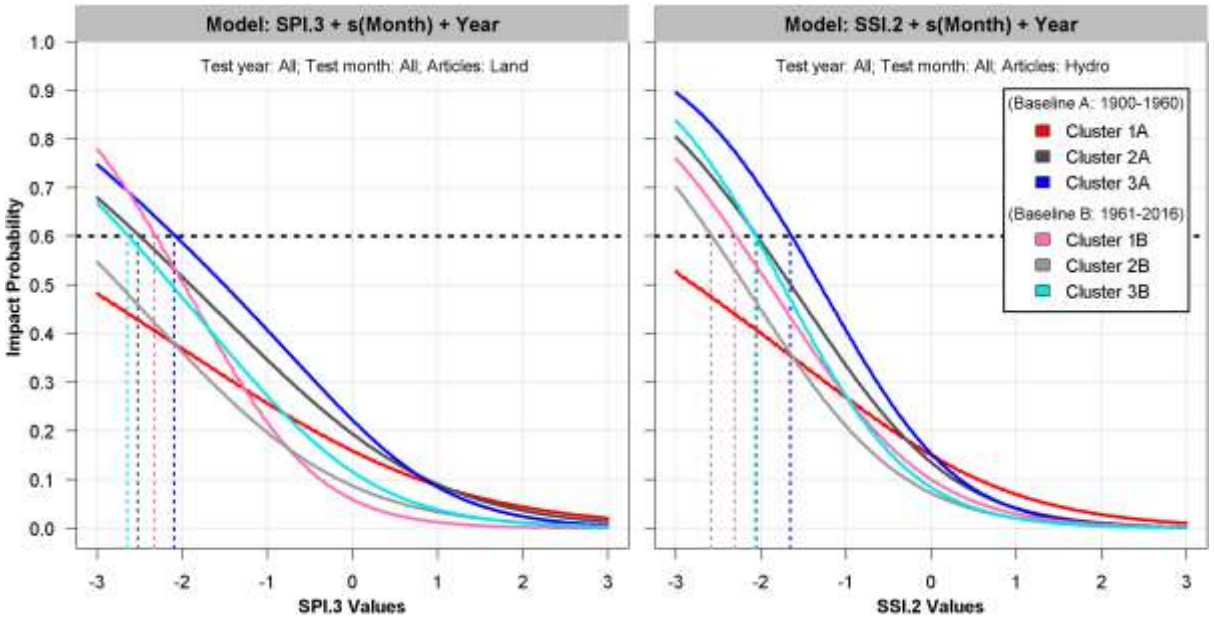

Figure 8. Predicted probability of reported impacts (annual) from models generated using land-based impact articles and SPI-3 indices (left panel) and from hydrological-based impact articles and SSI-2 indices (right panel). Impact likelihoods for each cluster over the baseline period A: 1900-1960 (i.e. Clusters 1A, 2A and 3A) and baseline period B: 1961-2016 (i.e. Clusters 1B, 2B and 3B) are shown in each panel for indices values ranging from -3 to 3. Indices values for each cluster resulting in a high reported impact probabilities (0.60) are also identified (dashed horizontal line).

Table 4. SPI-3 and SSI-2 values producing incremental increasing probabilities of impact reports from very low to very high, for land- and hydrological-based models for the full period 1900-2016 and sub-periods 1900-1960 and 1961-2016.

Index (period)	Cluster Number	Very Low:	Low: (0.20-	Moderate: (0.40-0.59)	High: (0.60-0.79)	Very High:
	1	>3.00	-0.6	-1.65	-2.68	<-3.00
SPI-3 (1900-2016)	2	>3.00	-0.42	-1.41	-2.35	<-3.00
	3	>3.00	-0.17	-1.07	-1.98	<-3.00
	1	>3.00	-0.46	-1.49	-2.48	<-3.00

SSI-2 (1900-2016)	2	>3.00	-0.57	-1.33	-2.02	-2.83
	3	>3.00	-0.39	-1.03	-1.6	-2.27
	1	>3.00	-0.47	-2.27	<-3.00	<-3.00
SPI-3 (1900-1960)	2	>3.00	-0.06	-1.33	-2.51	<-3.00
	3	>3.00	0.12	-0.97	-2.08	<-3.00
	1	>3.00	-0.47	-2	<-3.00	<-3.00
SSI-2 (1900-1960)	2	>3.00	-0.39	-1.26	-2.04	<-2.98
	3	>3.00	-0.23	-0.99	-1.65	<-2.43
	1	>3.00	-0.93	-1.66	-2.32	<-3.00
SPI-3 (1961-2016)	2	>3.00	-1.03	-2.21	<-3.00	<-3.00
	3	>3.00	-0.6	-1.65	-2.63	<-3.00
	1	>3.00	-0.66	-1.52	-2.29	<-3.00
SSI-2 (1961-2016)	2	>3.00	-0.95	-1.82	-2.58	<-3.00
	3	>3.00	-0.71	-1.47	-2.06	<-2.81

Figure 8 shows annual results for reported impact likelihoods for land- and hydrological-based drought, with groupings A and B representing results derived from the 1900-1960 and 1961-2016 baseline periods, respectively for Clusters 1, 2 and 3. Differences between reported impact probability curves are apparent for all three clusters and both impact categories, but are greater for land-based impact reports where agricultural and livestock farming dominate (91% and 79% of land-based reports across all clusters for the 1900-1960 and 1961-2016 periods respectively). For both Clusters 2 and 3 the 1961-2016 period returns lower likelihoods of drought impact reports. For Cluster 1 however larger SPI-3 deficits produce a greater probability of impact reports for the 1961-2016 period, whilst for values closer to zero the risk is higher for the 1900-1960 period, indicating that the likelihood of reported impacts has increased for extreme droughts and decreased for more moderate droughts. For SSI-2 both Cluster 2 and 3 show lower likelihoods of reported hydrological-based drought impacts for the 1961-2016 period, however the reduction is not as large as seen for land-based impacts. Cluster 1 also shows a higher probability of hydrological-based impact reports for the 1961-2016 period but only at larger SSI-2 deficits.

The reduction in impact report probabilities for the 1961-2016 period is reflected in an increase in deficits required to reach the high likelihood of impact threshold (0.6), with differences greatest in Cluster 1 catchments. For Cluster 3 land-based impact reports, the SPI-3 value associated with high impact report probabilities changes from -2.08 SPI-3 for 1900-1960 to -2.63 SPI-3 for 1961-2016. For hydrological-based drought in the same cluster, values change from -1.65 to -2.06 SSI-2. For Cluster 2 catchments the high impact probability for land-based articles occurs at -2.51 SPI-3 for the 1900-1960 period and <-3.00

SPI-3 for the 1961-2016 period. Hydrological-based impact reports change from -2.04 to -2.58 SSI-2. The largest change in deficit thresholds returning high likelihoods of reported impacts is in Cluster 1 for both land- and hydrological-based droughts (<-3.00 to -2.32 SPI-3 and <-3.00 to -2.29 SSI-2). Table 4 provides a cluster specific breakdown of SSI-2 and SPI-3 values required to reach each reported impact probability threshold.

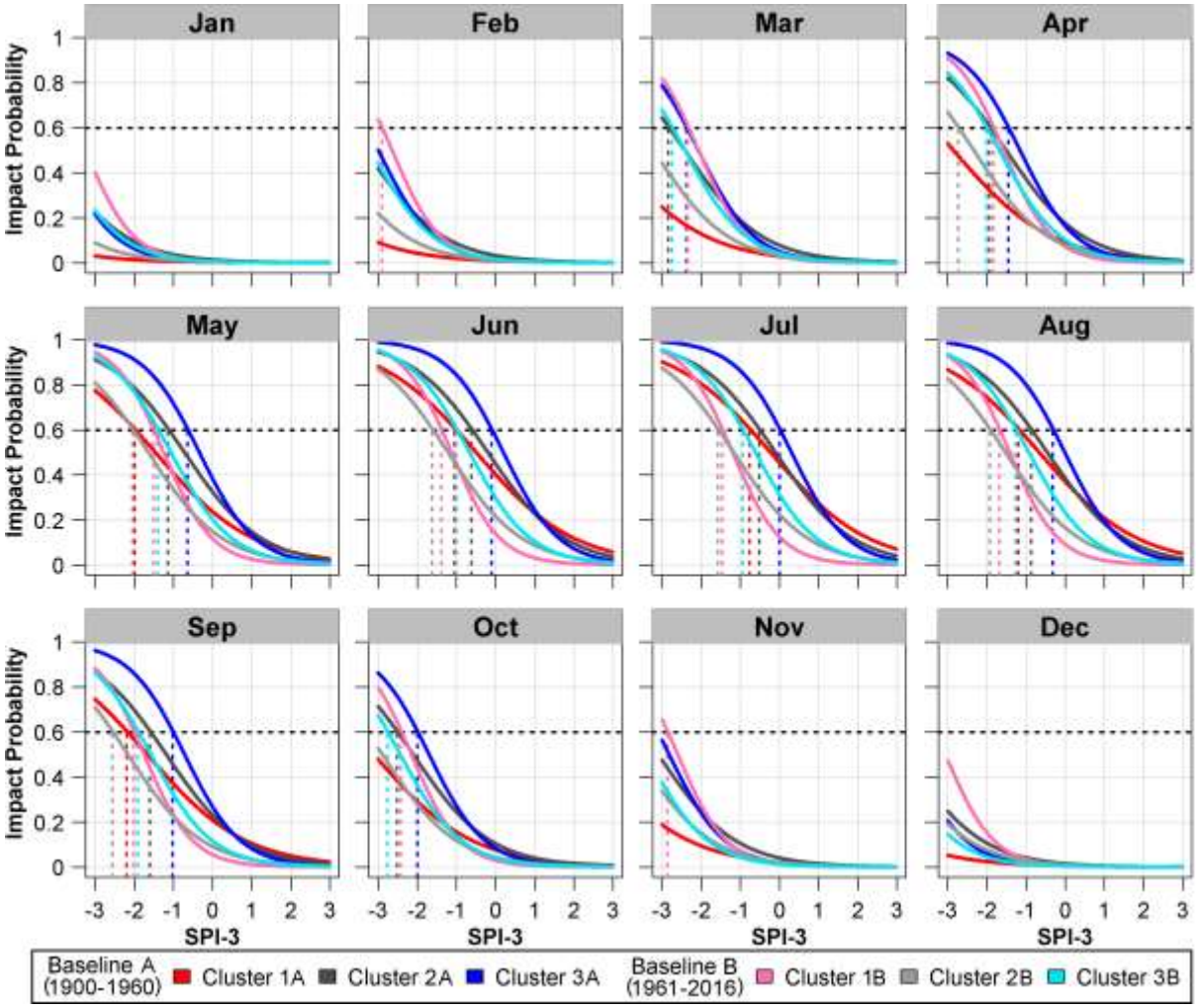

Figure 9. Predicted probability of reported impacts (monthly) from models generated using land-based impact articles and SPI-3 indices. Impact likelihoods for each cluster over the baseline period A: 1900-1960 (i.e. Clusters 1A, 2A and 3A) and baseline period B: 1961-2016 (i.e. Clusters 1B, 2B and 3B) are shown in each panel for indices values ranging from -3 to 3. Indices values for each cluster resulting in a high reported impact probabilities (0.60) are also identified (dashed horizontal line).

Figures 9 and 10 repeat the analysis on a monthly basis for land- and hydrological-based reported impacts, respectively. The likelihood of land-based impacts being reported in Clusters 2 and 3 is consistently lower for all months for the 1961-2016 period, with the exception of January for Cluster 3. The opposite is the case for Cluster 1 where at larger deficits the latter period displays greater likelihoods of reported drought impacts whilst at more modest deficits the earlier period dominates from April to October. For the 1961-2016 period, high impact report probabilities at the 0.6 threshold are most easily attained in June

for Cluster 1 and July for Cluster 2 and 3 with corresponding SPI-3 values of -1.38, -1.56 and -0.93, compared to -0.75, -0.51, 0.01 (all in July) for equivalent values derived from the 1900-1960 period. The lowest likelihood of reported impacts is in January for all Clusters, with the exception for Cluster 3 (1961-2016) which occurs in December. All clusters have low to very low impact report likelihoods at -3 SPI-3. Between baseline periods, impact likelihoods also differ markedly for hydrological-based articles (Figure 10). For the 1961-2016 period, Cluster 3 shows the greatest sensitivity to drought impacts in each month. Also, across the year Cluster 1 consistently produces greater likelihoods of reported impacts at more extreme deficits in the later period compared to 1900-1960. As with land-based impact reports (excluding January in Cluster 3), the likelihood of hydrological-based impact reports in Cluster 2 and Cluster 3 is consistently lower for all months for the 1961-2016 period. The month with the greatest likelihood of reported hydrological-based impacts for 1961-2016 is July with SSI-2 values required to reach the (0.6) threshold having values of -1.23, -1.54 and -1.36 SSI-2 in Clusters 1 to 3 compared to -0.57, -0.92 and -0.76 SSI-2 for the 1900-1960 period.

4. Discussion and Conclusions

Employing drought indices derived from historic river flow and precipitation reconstructions, together with a database of newspaper articles on historical drought impacts, we have shown that it is possible to link historic newspaper articles with drought indicators using GLMs at the regional scale. The process of model development closely followed Parsons *et al*. (2019) and Stagge *et al*. (2015a) who both showed the effectiveness of logistic regression models in linking drought indices and reported impacts. Our model evaluation highlighted the strong relationship between short accumulation SPI/SSI periods and drought impact reports in Ireland. An analysis of model performance scores at accumulations of 1, 2, 3, 4, 5, 6, 9, 12 and 18 months together with an examination of model outputs showed that SPI-3 was best at modelling land-based drought impact reports across each catchment cluster. This is consistent with Bachmair *et al*. (2018), Haro-Monteagudo *et al*. (2018) and Naumann *et al*. (2015), each of whom found SPI-3 correlated well with reported agricultural impacts. For hydrological drought, SSI-2 generated the best model performance scores and the highest impact likelihood values of all accumulations.

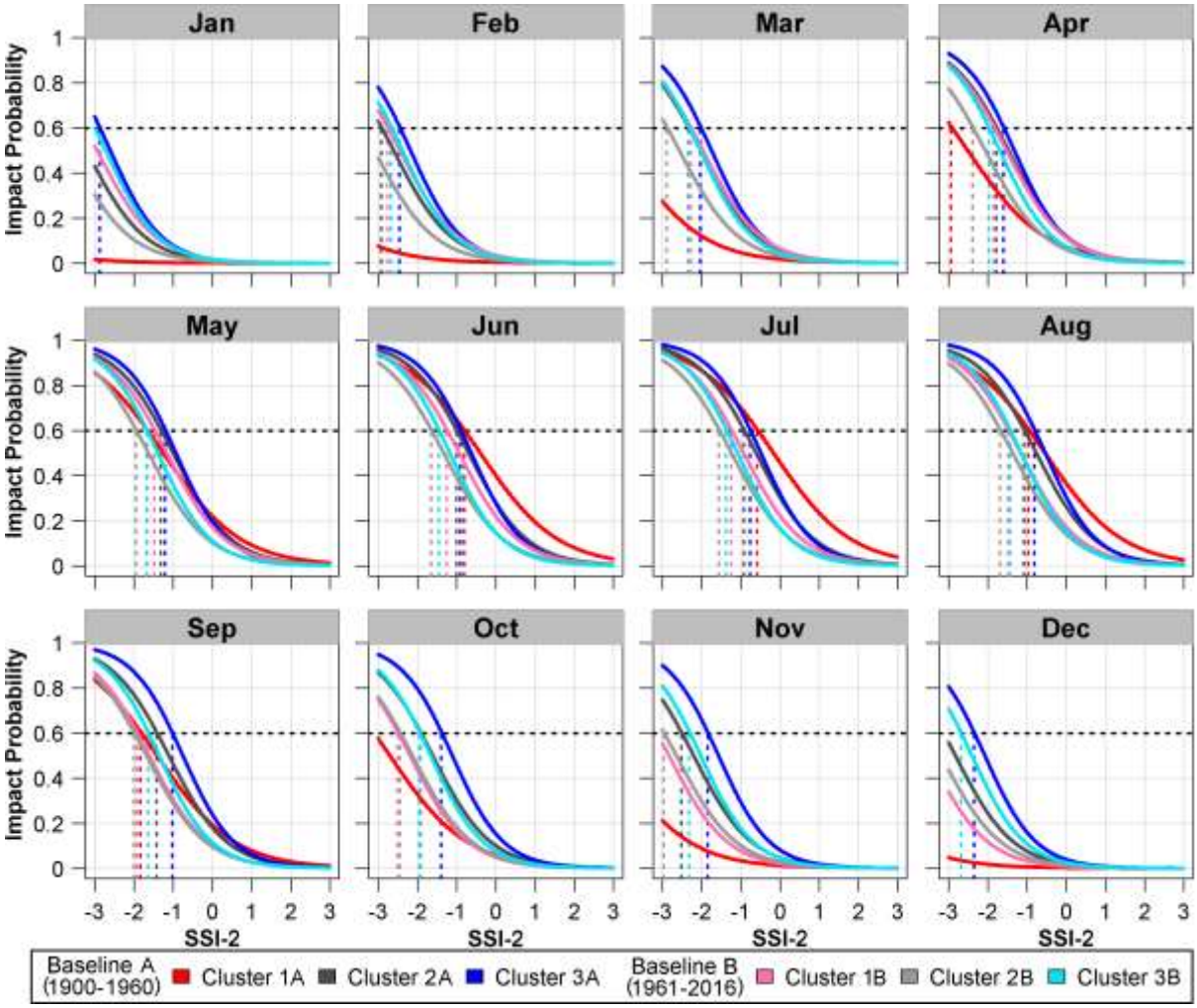

Figure 10 As in Figure 9 but for hydrological-based impact articles and SSI-2 indices.

Model performance varied by region, but overall Cluster 3 in the east/southeast produced the best performing land and hydrological-based models. The weakest land-based model was Cluster 1 in the northwest whilst the weakest hydrological-based model was Cluster 2 in the southwest. Drought impact article numbers have a notable influence on model performance with Cluster 3 catchments, containing the greatest number of land- and hydrological-based articles, producing better results than those for Cluster 1 and 2. Overall, we find that Cluster 1 and 2 models derived from land-based articles and SPI indices perform better than the hydrological-based equivalent, whilst the opposite is the case for Cluster 3 models. Catchment characteristics likely influence model performance with Cluster 3 catchments, which tend to have greater groundwater storage (O'Connor et al., 2022a) and are more influenced by the non-linear propagation of drought through such catchment systems, producing lower model performances than the faster responding catchments in Cluster 1 and 2. The addition of smoothing to monthly values considerably improved model performance (by a factor of 3.1 on average), as was found by Parsons *et al*. (2019). Weighting of predictors by reciprocal rank of drought article occurrence further improved model performance (by a factor of 1.4 on average). Performance scores for our models (R2adj and AUC) compare favourably with similar studies (Parsons *et al*., 2019; Stagge *et al*., 2015a).

Our results show that the likelihood of drought impacts being reported is influenced by location, drought type and time-of-year. On an annual basis Cluster 3 catchments consistently showed the greatest propensity for land- and hydrological-based impact reports, whereas Cluster 1 showed the least likelihood for land- and hydrological-based impact reports at more extreme deficits. At more moderate deficits Cluster 2 showed the least likelihood for hydrological-based impact reports. On a monthly basis, our results indicate large intra-annual variations in the probabilities of reported drought impacts across clusters. In all clusters and for both impact categories, summer shows the highest reported impact likelihoods, which is unsurprising as agricultural activities (crop and livestock production) and water use (consumption) increase markedly in these warmer months. For land-based impacts, all clusters display a high probability of impact reports in July, brought about by only very modest SPI-3 deficits (not less than -1), indicating a very high vulnerability to drought in that month. Conversely, winter months show lower probabilities of drought impacts being reported, with deficits as extreme as <-3 SPI-3 in January resulting in low likelihoods across clusters. Previous studies on drought characterisation in Ireland (e.g. Noone *et al*., 2017, O'Connor *et al*., 2022a) have employed a common year-round threshold of -1 SPI to identify the onset of drought events. These finding suggest that the use of such fixed thresholds for drought analysis in Ireland, which has a strong seasonal cycle in both the mean and variability of precipitation and flows, inaccurately captures drought conditions. Our work suggests that non-stationary, location dependent threshold values would more accurately capture the changing impacts of drought across seasons on the island.

We find a close relationship between hydrological drought impact reporting and catchment characteristics. Despite revealing the lowest likelihood of reported land-based impacts, for hydrological-based impact reports Cluster 1 catchments show the highest likelihood of recorded impacts at low deficits in summer months. These findings are consistent with O'Connor *et al*. (2022a) who identify Cluster 1 catchments as being the most susceptible to hydrological drought in summer due to the lack of groundwater storage. Cluster 3 catchments show the highest probabilities of impact reporting from September through April where even in December at more extreme deficits there exists a very high likelihood of drought related impact reports. These catchments tend to have higher groundwater storage and more delayed hydrological drought onset, consistent with higher impact report probabilities from September through April. As per many aspects of the analysis, Cluster 2 catchments show likelihood patterns intermediate between Cluster 1 and 3.

Inclusion of the 'year' predictor variable in our model revealed a decreasing trend in reported drought impacts across all three clusters for both land- and hydrological-based models during the 1900-2016 period, a result confirmed by Theil-Sens slope testing. We also identify step changes towards fewer drought impact reports for recent decades in each cluster, especially for land-based impact reports. As drought reports in this category are dominated by impacts on agricultural and livestock farming this may be indicative of autonomous adaptation in that sector. These results differ to the UK where Parsons *et al*. (2019) found a marked increase in the probability of reported drought impacts in the agricultural sector. Similarly, Stagge *et al*. (2015a) found notable differences in trends in agricultural drought impacts between five

European countries. Both studies linked possible biases in reporting of impacts, resulting from a change in the actual or perceived drought vulnerability of farms and/or changes in reporting practices, as a cause of such deviations, something that may well affect results obtained here. Furthermore, it should be noted that the period since the 1980s in Ireland has been relatively drought poor (Wilby *et al*., 2015; Noone *et al*., 2017), as reflected by the relative lack of articles on the subject. For the 1961-2016 period the risk of reported land-based impacts is lower for Clusters 2 and 3. Changes in the reporting of hydrological drought impacts are less extreme but nevertheless notable and coincide with findings by O'Connor *et al*. (2022a) showing reduced hydrological drought occurrence in recent years. However, Cluster 1 catchments contradict this trend, whereby an increased probability of drought impact reports for extreme deficits in the 1961-2016 period was found. One plausible explanation for the difference is that the economic growth and industrial development that occurred in Ireland from the 1960s (Daly, 2016), which likely resulted in reduced vulnerability to drought impacts, was not universally felt across the island with the northwest the latest to benefit from these changes, as suggested by Martin and Townroe (2013). However drought impacts are not a direct measure of, but a symptom of drought vulnerability (Wang *et al*., 2020b). Furthermore, drought vulnerability is also a function of exposure, sensitivity and adaptive capacity (Smit and Wandel, 2006) so accurately apportioning attribution for such changes is not possible without a more in-depth analysis.

Linking drought metrics and reported impacts at the regional scale opens the possibility for better informing drought monitoring and warning systems (Bachmair *et al*., 2016). This work identifies the accumulation periods for SSI and SPI that are most closely associated with drought impact reporting and identifies thresholds for impact probabilities associated with different values of each drought metric for various catchment types. Although we detect a decrease in the probability of drought impact reports for some catchment clusters in recent decades, this may be an artefact of reduced drought occurrence in that period given the widespread and significant impacts of the 2018 drought in Ireland (Dillon *et al*., 2018; Falzoi *et al*., 2019; Government of Ireland, 2020). Moreover, we show the value of newspaper archives as a source of information on drought impacts. The IDID (Jobbová *et al*., 2022a) provides an unprecedented resource for investigating drought impacts in Ireland, as well as new opportunities for evaluating societal effects and responses to drought events.

There are a number of limitations to note. Historic precipitation reconstructions from which SPI indices have been generated are subject to varying uncertainties across seasons (Casty *et al*., 2007). Flow values from which SSI values have been derived also have uncertainties, relating to the underlying precipitation data and rainfall runoff models used in their generation. Considerable efforts were made to address these concerns using different model structures and datasets to evaluate the quality of the reconstructions (see O'Connor *et al*., 2020). Whilst drought impact reports have been meticulously assessed and grouped, uncertainty arises from differences in the duration, frequency, spatial extent and regional density of the newspaper publications (see Jobbová *et al*., 2022b). For example, some publications were only in print in the early half of the 20th century whilst others commenced in the latter half of the century. The frequency of publication also differed between some

newspapers whilst smaller regional publications had a greater local emphasis in reports. Furthermore, drought reporting is dependent on local/national events with more pressing news content impacting the number of and space provided for drought articles. The count of drought impact articles is therefore an imperfect proxy for the significance of reported impacts. As the models applied weights based on reciprocal ranking of total monthly articles numbers, the aforementioned sources of bias would all impact model performance. Whilst aggregation of data by catchment clusters helps limit the impacts of some of these biases, a much more substantive assessment of the text of the articles together with a sectoral based approach of model generation would help reduce this source of uncertainty further.

Possibilities for future work include the application of other drought metrics such as SPEI and/or low flow indicators. Alternative modelling approaches may also be considered. For instance, Bachmair *et al*. (2017) demonstrate the utility of machine learning for linking drought impacts and metrics which could potentially better handle the complex, multi-threshold relationships found here, including accounting for non-binary impact series. Other impact datasets could be explored to supplement use of newspaper articles including historical inventories, such as harvest volumes, and/or records of impacts on online social media platforms such as Twitter, as has been demonstrated for flood impacts (Basnyat *et al*., 2017; Thompson *et al*., 2021). Our analysis has shown that drought indices and article numbers do not always coincide (e.g. the 1945 and 1921 drought events). Examining the relationships between the frequencies of drought impact reporting and evolving drought indices for such events would be beneficial. Finally, drought monitoring is an essential component of drought risk management (Senay *et al*., 2015), with the success of drought mitigation measures largely dependent upon the gathering of information on drought onset, progress and areal extent (Morid *et al*., 2006). The identification of regional vulnerability to drought impacts here is an additional element to drought monitoring that could potentially produce societal benefits. The development of such a system for Ireland, using these research findings, should be explored further.

This paper applied logistic regression and GAMs to link reconstructed SPI and SSI metrics to reported land- and hydrological-based drought impacts as inferred from newspaper reports covering the period 1900-2016 in 51 catchments in Ireland. We find that, based on model performance metrics and impact likelihood scores, SPI-3 and SSI-2 are most closely related to reported land- and hydrological-based impacts, respectively. Catchments in the east/southeast show the highest probabilities of land- and hydrological-based impact reports on an annual timescale, displaying notably higher impact reporting probabilities during winter months which can possibly be attributed to the high ground water content in these catchments. During summer months catchments in the northwest display the highest hydrological-based impact reporting probabilities at low SSI-2 deficits, despite having the lowest equivalent land-based impact reporting likelihoods. Our findings show that maximum drought impact likelihoods across the 1900-2016 period occur in July for SPI-3 and SSI-2 with even modest deficits resulting in a high likelihood of impact reports. Overall, the lowest impact likelihoods occur in January for SPI-3 and SSI-2 were indices values of <-3 for the former only generate very low to low likelihoods of impact reports, whilst for the latter they

generate differences from low impacts (Cluster 1) to high impacts (Cluster 3). These findings suggest that the use of fixed thresholds for identifying drought impacts is not suitable. Changes in impact likelihoods over the last 116 years reveal a falling likelihood of drought impact reports for catchments in the east/southeast and southwest. Northwestern catchments show heightened likelihood of reported impacts for more extreme drought deficits in recent decades, particularly in respect of agricultural and livestock farming. The results reported here have the potential to inform the development of a drought monitoring and warning system both regionally and at the catchment scale in Ireland.

References

Ashcroft, L., Coll, J.R., Gilabert, A., Domonkos, P., Brunet, M., Aguilar, E., Castella, M., Sigro, J., Harris, I., Unden, P. and Jones, P., 2018. A rescued dataset of sub-daily meteorological observations for Europe and the southern Mediterranean region, 1877–2012. *Earth System Science Data*, 10(3), pp.1613-1635. https://doi.org/10.5194/essd-10-1613-2018

Bachmair, S., Kohn, I. and Stahl, K., 2015. Exploring the link between drought indicators and impacts. *Natural Hazards and Earth System Sciences*, 15(6), pp.1381-1397. https://doi.org/10.5194/nhess-15-1381-2015

Bachmair, S., Stahl, K., Collins, K., Hannaford, J., Acreman, M., Svoboda, M., Knutson, C., Smith, K.H., Wall, N., Fuchs, B. and Crossman, N.D., 2016. Drought indicators revisited: the need for a wider consideration of environment and society. *Wiley Interdisciplinary Reviews: Water*, 3(4), pp.516-536. https://doi.org/10.1002/wat2.1154

Bachmair, S., Svensson, C., Prosdocimi, I., Hannaford, J. and Stahl, K., 2017. Developing drought impact functions for drought risk management. *Natural Hazards and Earth System Sciences*, 17(11), pp.1947-1960. https://doi.org/10.5194/nhess-17-1947-2017

Bachmair, S., Tanguy, M., Hannaford, J. and Stahl, K., 2018. How well do meteorological indicators represent agricultural and forest drought across Europe? *Environmental Research Letters*, 13(3), p.034042. https://doi.org/10.1088/1748-9326/aaafda

Bakke, S.J., Ionita, M. and Tallaksen, L.M., 2020. The 2018 northern European hydrological drought and its drivers in a historical perspective. *Hydrology and Earth System Sciences Discussions*, pp.1-44. https://doi.org/10.5194/hess-24-5621-2020

Barker, L.J., Hannaford, J., Chiverton, A. and Svensson, C., 2016. From meteorological to hydrological drought using standardised indicators. *Hydrology and Earth System Sciences*, 20(6), pp.2483-2505. https://doi.org/10.5194/hess-20-2483-2016

Basnyat, B., Anam, A., Singh, N., Gangopadhyay, A. and Roy, N., 2017, May. Analyzing social media texts and images to assess the impact of flash floods in cities. In *2017 IEEE International Conference on Smart Computing (SMARTCOMP)* (pp. 1-6). IEEE. https://doi.org/10.1109/SMARTCOMP.2017.7946987

Blauhut, V., Gudmundsson, L. and Stahl, K., 2015. Towards pan-European drought risk maps: quantifying the link between drought indices and reported drought impacts. *Environmental Research Letters*, 10(1), p.014008. https://doi.org/10.1088/1748-9326/10/1/014008

Brázdil, R., Demarée, G.R., Kiss, A., Dobrovolný, P., Chromá, K., Trnka, M., Dolák, L., Řezníčková, L., Zahradníček, P., Limanowka, D. and Jourdain, S., 2019. The extreme drought of 1842 in Europe as described by both documentary data and instrumental measurements. *Climate of the Past*, 15(5), pp.1861-1884. https://doi.org/10.5194/cp-15-1861-2019

Brigode, P., Brissette, F., Nicault, A., Perreault, L., Kuentz, A., Mathevet, T. and Gailhard, J., 2016. Streamflow variability over the 1881–2011 period in northern Québec: comparison of hydrological reconstructions based on tree rings and geopotential height field reanalysis. *Climate of the Past*, 12(9), pp.1785-1804. https://doi.org/10.5194/cp-12-1785-2016

Brunet, M. and Jones, P., 2011. Data rescue initiatives: bringing historical climate data into the 21st century. *Climate Research*, 47(1-2), pp.29-40. https://doi.org/10.3354/cr00960

Caillouet, L., Vidal, J.P., Sauquet, E., Devers, A. and Graff, B., 2017. Ensemble reconstruction of spatio-temporal extreme low-flow events in France since 1871. *Hydrology and Earth System Sciences*, 21(6), pp.2923-2951. https://doi.org/10.5194/hess-21-2923-2017

Crooks, S.M. and Kay, A.L., 2015. Simulation of river flow in the Thames over 120 years: evidence of change in rainfall-runoff response? *Journal of Hydrology: Regional Studies*, 4, pp.172-195. https://doi.org/10.1016/j.ejrh.2015.05.014

Daly, M.E., 2016. *Sixties Ireland: reshaping the economy, state and society, 1957–1973*. Cambridge University Press. https://doi.org/10.1016/j.ejrh.2015.05.014

Dayrell, C., Svensson, C., Hannaford, J., McEnery, T., Barker, L.J., Baker, H. and Tanguy, M., 2022. Representation of Drought Events in the United Kingdom: Contrasting 200 years of News Texts and Rainfall Records. *Frontiers in Environmental Science*, p.146. https://doi.org/10.3389/fenvs.2022.760147

Deo, R.C., Byun, H.R., Adamowski, J.F. and Begum, K., 2017. Application of effective drought index for quantification of meteorological drought events: a case study in Australia. *Theoretical and Applied Climatology*, 128(1), pp.359-379. https://doi.org/10.1007/s00704-015-1706-5

Dillon, E., Donnellan, T., Hanrahan, K., Houlihan, T., Kinsella, A., Loughrey, J., McKeon, M., Moran, B. and Thorne, F., 2018. *Outlook 2019–Economic Prospects for Agriculture*. Agricultural Economics and Farm Surveys Department, Teagasc, Carlow. Available from: https://www.teagasc.ie/media/website/publications/2018/Outlook2019.pdf [Accessed 13 January 2022].

Ekström, M., Gutmann, E.D., Wilby, R.L., Tye, M.R. and Kirono, D.G., 2018. Robustness of hydroclimate metrics for climate change impact research. *Wiley Interdisciplinary Reviews: Water*, 5(4), p.e1288. https://wires.onlinelibrary.wiley.com/doi/full/10.1002/wat2.1288

Erfurt, M., Glaser, R. and Blauhut, V., 2019. Changing impacts and societal responses to drought in southwestern Germany since 1800. *Regional Environmental Change*, 19(8), pp.2311-2323. https://doi.org/10.1007/s10113-019-01522-7

Erfurt, M., Skiadaresis, G., Tijdeman, E., Blauhut, V., Bauhus, J., Glaser, R., Schwarz, J., Tegel, W. and Stahl, K., 2020. A multidisciplinary drought catalogue for southwestern Germany dating back to 1801. *Natural Hazards and Earth System Sciences*, 20(11), pp.2979-2995. https://doi.org/10.5194/nhess-20-2979-2020

Falzoi, S., Gleeson, E., Lambkin, K., Zimmermann, J., Marwaha, R., O'Hara, R., Green, S. and Fratianni, S., 2019. Analysis of the severe drought in Ireland in 2018. *Weather*, 74(11), pp.368-373. https://doi.org/10.1002/wea.3587

García-León, D., Standardi, G. and Staccione, A., 2021. An integrated approach for the estimation of agricultural drought costs. *Land Use Policy*, 100, p.104923. https://doi.org/10.1016/j.landusepol.2020.104923

Gil, M., Garrido, A. and Hernández-Mora, N., 2013. Direct and indirect economic impacts of drought in the agri-food sector in the Ebro River basin (Spain). *Natural Hazards & Earth System Sciences*, 13(10). https://doi.org/10.5194/nhess-13-2679-2013

Gudmundsson, L., Rego, F.C., Rocha, M. and Seneviratne, S.I., 2014. Predicting above normal wildfire activity in southern Europe as a function of meteorological drought. *Environmental Research Letters*, 9(8), p.084008. https://doi.org/10.1088/1748-9326/9/8/084008

Gudmundsson, L. and Stagge, J. H., 2016. SCI: Standardized Climate Indices such as SPI, SRI or SPEI. R package version 1.0-2. Retrieved from https://cran.r-project.org/web/packages/SCI/SCI.pdf

Hanel, M., Rakovec, O., Markonis, Y., Máca, P., Samaniego, L., Kyselý, J. and Kumar, R., 2018. Revisiting the recent European droughts from a long-term perspective. *Scientific Reports*, 8(1), pp.1-11. https://doi.org/10.1038/s41598-018-27464-4

Haro-Monteagudo, D., Daccache, A. and Knox, J., 2018. Exploring the utility of drought indicators to assess climate risks to agricultural productivity in a humid climate. *Hydrology Research*, 49(2), pp.539-551. https://doi.org/10.2166/nh.2017.010

Hawkins, E., Burt, S., Brohan, P., Lockwood, M., Richardson, H., Roy, M. and Thomas, S., 2019. Hourly weather observations from the Scottish Highlands (1883–1904) rescued by volunteer citizen scientists. *Geoscience Data Journal*, 6(2), pp.160-173. https://doi.org/10.1002/gdj3.79

Hickey, K., 2011. The historic record of cold spells in Ireland. *Irish Geography*, 44(2-3), pp.303-321. https://doi.org/10.1080/00750778.2011.669348

Jobbová, E., Crampsie, A., Seifert, N., Myslinski, T., Sente, L., Murphy, C., McLeman, R.A., Ludlow, F., Horvath, C. 2022a. Irish Drought Impacts Database v.1.0. *Zenodo*. https://doi.org/10.5281/zenodo.7216126

Jobbová, E., Crampsie, A., Murphy, C., Ludlow, F., McLeman, R.A., Horvath, C., 2022b. Irish Drought Impacts Database (IDID): A 287-year database of drought impacts from newspaper archives. *Geoscience Data Journal*. Manuscript in preparation for Submission.

Jones, P.D., 1984. Riverflow reconstruction from precipitation data. *Journal of Climatology*, 4(2), pp.171-186. https://doi.org/10.1002/joc.3370040206

Karl, T.R., 1986. The sensitivity of the Palmer Drought Severity Index and Palmer's Z-index to their calibration coefficients including potential evapotranspiration. *Journal of Climate and Applied Meteorology*, pp.77-86. https://www.jstor.org/stable/26182460

Kchouk, S., Melsen, L.A., Walker, D.W. and van Oel, P.R., 2021. A review of drought indices: predominance of drivers over impacts and the importance of local context. *Natural Hazards and Earth System Sciences Discussions*, pp.1-28. https://doi.org/10.5194/nhess-22-323-2022

Kreibich, H., Blauhut, V., Aerts, J.C., Bouwer, L.M., Van Lanen, H.A., Mejia, A., Mens, M. and Van Loon, A.F., 2019. How to improve attribution of changes in drought and flood impacts. *Hydrological sciences journal*, 64(1), pp.1-18. https://doi.org/10.1080/02626667.2018.1558367

Lloyd-Hughes, B. and Saunders, M.A., 2002. A drought climatology for Europe. *International Journal of Climatology: A Journal of the Royal Meteorological Society*, 22(13), pp.1571-1592. https://doi.org/10.1002/joc.846

Llasat, M.C., Llasat-Botija, M., Barnolas, M., López, L. and Altava-Ortiz, V., 2009. An analysis of the evolution of hydrometeorological extremes in newspapers: the case of Catalonia, 1982–2006. *Natural Hazards and Earth System Sciences*, 9(4), pp.1201-1212. https://doi.org/10.5194/nhess-9-1201-2009

Ludlow F. 2006. Three hundred years of weather extremes from the Annals of Connacht. *Journal of Postgraduate Research*, 5: 46-65.

McKee, T.B., Doesken, N.J. and Kleist, J., 1993, January. The relationship of drought frequency and duration to time scales. *Proceedings of the 8th Conference on Applied Climatology*, 17(22), pp. 179-183).

Mechler, R. and Bouwer, L.M., 2015. Understanding trends and projections of disaster losses and climate change: is vulnerability the missing link? *Climatic Change*, 133(1), pp.23-35. https://doi.org/10.1007/s10584-014-1141-0

Mediero, L., Kjeldsen, T.R., Macdonald, N., Kohnova, S., Merz, B., Vorogushyn, S., Wilson, D., Alburquerque, T., Blöschl, G., Bogdanowicz, E. and Castellarin, A., 2015. Identification of coherent flood regions across Europe by using the longest streamflow records. *Journal of Hydrology*, 528, pp.341-360. https://doi.org/10.1016/j.jhydrol.2015.06.016

Government of Ireland, 2020. *Summer 2018: An analysis of the heatwaves and droughts that affected Ireland and Europe in the summer of 2018*, Issued by the Climatology and Observations Division of Met Éireann. https://www.met.ie/cms/assets/uploads/2020/06/Summer2018.pdf [Accessed 13 January 2022].

Mishra, A.K. and Singh, V.P., 2010. A review of drought concepts. *Journal of hydrology*, 391(1-2), pp.202-216. https://doi.org/10.1016/j.jhydrol.2010.07.012

Moravec, V., Markonis, Y., Rakovec, O., Kumar, R. and Hanel, M., 2019. A 250-year European drought inventory derived from ensemble hydrologic modeling. *Geophysical Research Letters*, 46(11), pp.5909-5917. https://doi.org/10.1029/2019GL082783

Morgan, S.P. and Teachman, J.D., 1988. Logistic regression: Description, examples, and comparisons. *Journal of Marriage and Family*, 50(4), pp.929-936. https://doi.org/10.2307/352104

Morid, S., Smakhtin, V. and Moghaddasi, M., 2006. Comparison of seven meteorological indices for drought monitoring in Iran. *International Journal of Climatology: A Journal of the Royal Meteorological Society*, 26(7), pp.971-985. https://doi.org/10.1002/joc.1264

Murphy, C., Noone, S., Duffy, C., Broderick, C., Matthews, T. and Wilby, R.L., 2017. Irish droughts in newspaper archives: rediscovering forgotten hazards? *Weather*, 72(6), pp.151-155. https://doi.org/10.1002/wea.2904

Naumann, G., Spinoni, J., Vogt, J.V. and Barbosa, P., 2015. Assessment of drought damages and their uncertainties in Europe. *Environmental Research Letters*, 10(12), p.124013. https://doi.org/10.1088/1748-9326/10/12/124013

Nie, N., Zhang, W., Chen, H. and Guo, H., 2018. A global hydrological drought index dataset based on gravity recovery and climate experiment (GRACE) data. *Water Resources Management*, 32(4), pp.1275-1290. https://doi.org/10.1007/s11269-017-1869-1

Noone, S. and Murphy, C., 2020. Reconstruction of hydrological drought in Irish catchments (1850–2015). *Proceedings of the Royal Irish Academy: Archaeology, Culture, History, Literature*, 120, pp.365-390. https://doi.org/10.3318/priac.2020.120.11

Noone, S., Broderick, C., Duffy, C., Matthews, T., Wilby, R.L. and Murphy, C., 2017. A 250-year drought catalogue for the island of Ireland (1765–2015). International Journal of Climatology, 37, pp.239-254. https://doi.org/10.1002/joc.4999

O'Connor, P., Murphy, C., Matthews, T. and Wilby, R.L., 2021a. Reconstructed monthly river flows for Irish catchments 1766–2016. *Geoscience Data Journal*, 8(1), pp.34-54. https://doi.org/10.1002/gdj3.107

O'Connor, P., Murphy, C., Matthews, T. and Wilby, R.L., 2021b. Historical droughts in Irish catchments 1767-2016. *International Journal of Climatology*, Early View. https://doi.org/10.1002/joc.7542

Parsons, D.J., Rey, D., Tanguy, M. and Holman, I.P., 2019. Regional variations in the link between drought indices and reported agricultural impacts of drought. *Agricultural Systems*, 173, pp.119-129. https://doi.org/10.1016/j.agsy.2019.02.015

Pettitt, A.N., 1979. A non-parametric approach to the change-point problem. *Journal of the Royal Statistical Society: Series C (Applied Statistics)*, 28(2), pp.126-135. https://doi.org/10.2307/2346729

Rudd, A.C., Bell, V.A. and Kay, A.L., 2017. National-scale analysis of simulated hydrological droughts (1891–2015). *Journal of Hydrology*, 550, pp.368-385. https://doi.org/10.1016/j.jhydrol.2017.05.018

Rust, W., Cuthbert, M., Bloomfield, J., Corstanje, R., Howden, N. and Holman, I., 2021. Exploring the role of hydrological pathways in modulating multi-annual climate teleconnection periodicities from UK rainfall to streamflow. *Hydrology and Earth System Sciences*, 25(4), pp.2223-2237. https://doi.org/10.5194/hess-25-2223-2021

Ryan, C., Murphy, C., McGovern, R., Curley, M., Walsh, S. and 476 students, 2020. Ireland's pre-1940 daily rainfall records. *Geoscience Data Journal*, Early View. https://doi.org/10.1002/gdj3.103

Salmoral, G., Ababio, B. and Holman, I.P., 2020. Drought impacts, coping responses and adaptation in the UK outdoor livestock sector: insights to increase drought resilience. *Land*, 9(6), p.202. https://doi.org/10.3390/land9060202

Sen, P.K., 1968. Estimates of the regression coefficient based on Kendall's tau. *Journal of the American statistical association*, 63(324), pp.1379-1389. https://doi.org/10.1080/01621459.1968.10480934

Senay, G.B., Velpuri, N.M., Bohms, S., Budde, M., Young, C., Rowland, J. and Verdin, J.P., 2015. Drought monitoring and assessment: remote sensing and modeling approaches for the famine early warning systems network. *In Hydro-meteorological hazards, risks and disasters* (pp. 233-262). Elsevier. https://doi.org/10.1016/B978-0-12-394846-5.00009-6

Smit, B. and Wandel, J., 2006. Adaptation, adaptive capacity and vulnerability. *Global environmental change*, 16(3), pp.282-292. https://doi.org/10.1016/j.gloenvcha.2006.03.008

Smith, K.A., Barker, L.J., Tanguy, M., Parry, S., Harrigan, S., Legg, T.P., Prudhomme, C. and Hannaford, J., 2019. A multi-objective ensemble approach to hydrological modelling in

the UK: an application to historic drought reconstruction. *Hydrology and Earth System Sciences*, 23(8), pp.3247-3268. https://doi.org/10.5194/hess-23-3247-2019

Spraggs, G., Peaver, L., Jones, P. and Ede, P., 2015. Re-construction of historic drought in the Anglian Region (UK) over the period 1798–2010 and the implications for water resources and drought management. *Journal of Hydrology*, 526, pp.231-252. https://doi.org/10.1016/j.jhydrol.2015.01.015

Stahl, K, Blauhut, V, Kohn, I, Acácio, V, Assimacopoulos, D, Bifulco, C, De Stefano, L, Dias, S, Eilertz, D, Freilingsdorf, B, Hegdahl, TJ, Kampragou, E, Kourentzis, E, Melsen, L, van Lanen, HAJ, van Loon, AF, Massarutto, A, Musolino, D, De Paoli, L, Senn, L, Stagge, JH, Tallaksen, LM & Urquijo, J 2012, *A European drought impact report inventory (EDII): Design and test for selected recent droughts in Europe*. DROUGHT-R&SPI technical report, no. 3, Wageningen Universiteit, Wageningen.

Stagge, J.H., Tallaksen, L.M., Gudmundsson, L., van Loon, A., Stahl, K., 2015. Candidate distributions for climatological drought indices (SPI and SPEI). *International Journal of Climatology*, 35, pp. 4027-4040, https://doi.org/10.1002/joc.4267

Steinemann, A., Iacobellis, S.F. and Cayan, D.R., 2015. Developing and evaluating drought indicators for decision-making. *Journal of Hydrometeorology*, 16(4), pp.1793-1803. https://doi.org/10.1175/JHM-D-14-0234.1

Sutanto, S.J. and Van Lanen, H.A., 2020. Hydrological Drought Characteristics Based on Groundwater and Runoff Across Europe. *Proceedings of the International Association of Hydrological Sciences*, 383, pp.281-290. https://doi.org/10.5194/piahs-383-281-2020

Sutanto, S.J., van der Weert, M., Wanders, N., Blauhut, V. and Van Lanen, H.A., 2019. Moving from drought hazard to impact forecasts. *Nature communications*, 10(1), pp.1-7. https://doi.org/10.1038/s41467-019-12840-z

Thompson, J.J., Wilby, R.L., Matthews, T. and Murphy, C., 2021. The utility of Google Trends as a tool for evaluating flooding in data-scarce places. *Area*. https://doi.org/10.1111/area.12719

Tsakiris, G., Pangalou, D. and Vangelis, H., 2007. Regional drought assessment based on the Reconnaissance Drought Index (RDI). *Water Resources Management*, 21(5), pp.821-833. https://doi.org/10.1007/s11269-006-9105-4

UKCEH, 2021. *Historic Drought Inventory*. Available at: https://historicdroughts.ceh.ac.uk/content/drought-inventory [Accessed: 10 September 2021].

Van Loon, A.F. and Laaha, G., 2015. Hydrological drought severity explained by climate and catchment characteristics. *Journal of hydrology*, 526, pp.3-14. https://doi.org/10.1016/j.jhydrol.2014.10.059

Van Loon, A.F., Van Lanen, H.A., Hisdal, H.E.G.E., Tallaksen, L.M., Fendeková, M., Oosterwijk, J., Horvát, O. and Machlica, A., 2010. Understanding hydrological winter

drought in Europe. Global Change: Facing Risks and Threats to Water Resources, IAHS Publ, 340, pp.189-197.

Van Vliet, M.T., Sheffield, J., Wiberg, D. and Wood, E.F., 2016. Impacts of recent drought and warm years on water resources and electricity supply worldwide. *Environmental Research Letters*, 11(12), p.124021. https://doi.org/10.1088/1748-9326/11/12/124021

Vicente-Serrano, S.M., Beguería, S. and López-Moreno, J.I., 2011. Comment on "Characteristics and trends in various forms of the Palmer Drought Severity Index (PDSI) during 1900–2008" by Aiguo Dai. *Journal of Geophysical Research: Atmospheres*, 116(D19). https://doi.org/10.1029/2011JD016410

Vicente-Serrano, S.M., Beguería, S., Lorenzo-Lacruz, J., Camarero, J.J., López-Moreno, J.I., Azorin-Molina, C., Revuelto, J., Morán-Tejeda, E. and Sanchez-Lorenzo, A., 2012. Performance of drought indices for ecological, agricultural, and hydrological applications. *Earth Interactions*, 16(10), pp.1-27. https://doi.org/10.1175/2012EI000434.1

Vicente-Serrano, S.M., Peña-Angulo, D., Murphy, C., López-Moreno, J.I., Tomas-Burguera, M., Dominguez-Castro, F., Tian, F., Eklundh, L., Cai, Z., Alvarez-Farizo, B. and Noguera, I., 2021. The complex multi-sectoral impacts of drought: Evidence from a mountainous basin in the Central Spanish Pyrenees. *Science of the Total Environment*, 769, p.144702. https://doi.org/10.1016/j.scitotenv.2020.144702

Martin, R. and Townroe, P., 2013. *Regional development in the 1990s: the British Isles in transition*. Routledge, p.127. https://doi.org/10.4324/9781315000213

Wang, Y., Lv, J., Hannaford, J., Wang, Y., Sun, H., Barker, L.J., Ma, M., Su, Z. and Eastman, M., 2020. Linking drought indices to impacts to support drought risk assessment in Liaoning province, China. *Natural Hazards and Earth System Sciences*, 20(3), pp.889-906. https://doi.org/10.5194/nhess-20-889-2020

Wilby, R.L., Prudhomme, C., Parry, S. and Muchan, K.G.L., 2015. Persistence of hydrometeorological droughts in the United Kingdom: a regional analysis of multi-season rainfall and river flow anomalies. *Journal of Extreme Events*, 2(02), p.1550006. https://doi.org/10.1142/S2345737615500062

Wilhite, D.A., Svoboda, M.D. and Hayes, M.J., 2007. Understanding the complex impacts of drought: A key to enhancing drought mitigation and preparedness. *Water Resources Management*, 21(5), pp.763-774. https://doi.org/10.1007/s11269-006-9076-5

Wilhite, D.A., Sivakumar, M.V. and Pulwarty, R., 2014. Managing drought risk in a changing climate: The role of national drought policy. *Weather and Climate Extremes*, 3, pp.4-13. https://doi.org/10.1016/j.wace.2014.01.002

Wood, S. N., 2012. Package 'mgcv'. R package version 1.0-2. Retrieved from https://cran.r-project.org/web/packages/mgcv/index.html.

Wu, H., Hayes, M.J., Wilhite, D.A. and Svoboda, M.D., 2005. The effect of the length of record on the standardized precipitation index calculation. *International Journal of Climatology: A Journal of the Royal Meteorological Society*, 25(4), pp.505-520. https://doi.org/10.1002/joc.1142

Supplementary Information

Table S1. Breakdown of article numbers based on county, cluster and related article type/grouping.

		Hydrological-Based Impact Articles								Land-Based Impact Articles							
County Name	**Cluster No.**	**Aquaculture and Fisheries**	**Waterborne Transport**	**Energy and Industry**	**Tourism and Recreation**	**Public Water Supply**	**Water Quality**	**Freshwater Ecosystem**	**Sub-Total**	**Agriculture & Livestock farming**	**Terrestrial Ecosystems**	**Soil Systems**	**Wildfires**	**Air Quality**	**Forestry**	**Sub-Total**	**Total**
Carlow	3	4	2	3	1	26	1	12	49	55	2	11	0	0	0	68	117
Cavan	3	8	1	3	2	36	2	22	74	85	4	1	5	0	0	95	169
Clare	2	1	1	4	3	20	1	7	37	22	0	2	3	0	0	27	64
Cork	2	20	0	6	17	121	8	49	221	221	9	12	4	2	0	248	469
Donegal	1	30	0	5	3	79	4	42	163	79	1	2	9	0	0	91	254
Fermanagh	1	5	1	0	1	14	0	9	30	20	2	1	5	0	0	28	58
Galway	1	15	1	0	6	83	6	38	149	116	3	4	7	0	1	131	280
Kerry	2	22	2	0	5	53	3	26	111	112	6	1	0	0	0	119	230
Kildare	3	6	1	0	6	14	0	7	34	39	2	4	3	0	0	48	82
Kilkenny	3	2	0	2	2	32	0	10	48	81	0	4	2	0	0	87	135
Laois	3	1	0	2	2	30	2	12	49	63	3	0	7	0	0	73	122
Leitrim	1	6	2	1	0	21	1	13	44	45	2	2	1	0	0	50	94
Limerick	2	7	0	2	5	72	3	20	109	121	13	3	6	0	1	144	253
Longford	3	1	2	3	3	24	0	8	41	46	2	1	0	0	0	49	90
Louth	3	8	0	1	4	40	0	7	60	46	1	2	4	0	0	53	113
Mayo	1	11	1	2	3	48	6	30	101	46	5	6	0	1	3	61	162
Meath	3	10	0	0	8	38	0	14	70	57	3	3	2	0	0	65	135
Monaghan	3	5	1	4	0	53	2	12	77	60	4	1	4	0	0	69	146
Offaly	3	1	1	1	0	16	0	9	28	40	2	2	1	0	2	47	75
Roscommon	1	1	2	2	3	27	0	18	53	42	2	0	3	1	0	48	101
Sligo	1	5	0	1	3	32	1	8	50	20	1	0	0	0	0	21	71
Tipperary	3	9	0	3	7	75	0	16	110	158	6	4	7	0	0	175	285
Tyrone	1	22	0	0	1	67	5	26	121	51	4	1	4	0	0	60	181
Waterford	3	8	0	0	6	48	0	15	77	81	6	3	4	0	2	96	173
Westmeath	3	5	5	1	5	29	4	23	72	57	5	1	2	0	0	65	137
Wexford	3	0	1	6	1	29	1	9	47	81	4	9	1	0	0	95	142
Wicklow	3	1	0	0	0	20	0	4	25	23	0	3	3	0	0	29	54
Total	-	214	24	52	97	1147	50	466	2050	1867	92	83	87	4	9	2142	4192

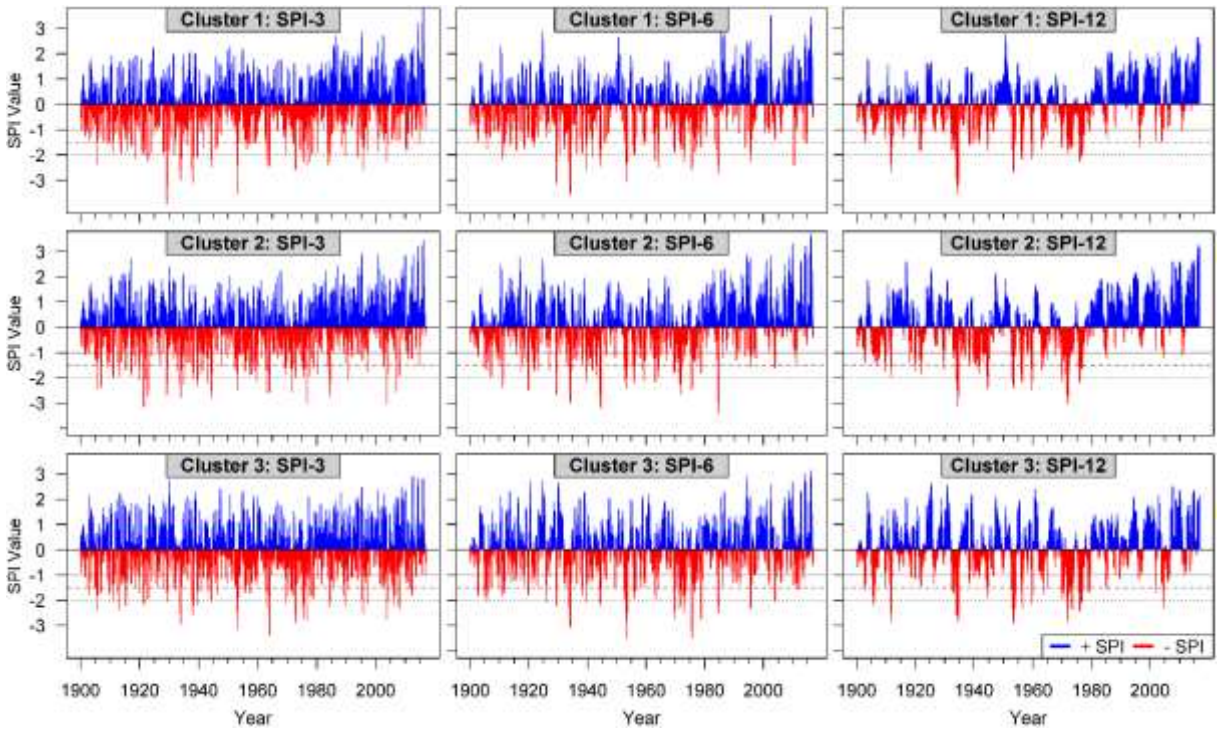

Figure S1. Time-series of SPI 3, 6 and 12, derived from median flows for each cluster (1900-2016), using the Tweedie distribution and 1930-1999 reference period. Horizontal lines represent moderate, severe and extreme drought thresholds in all plots.

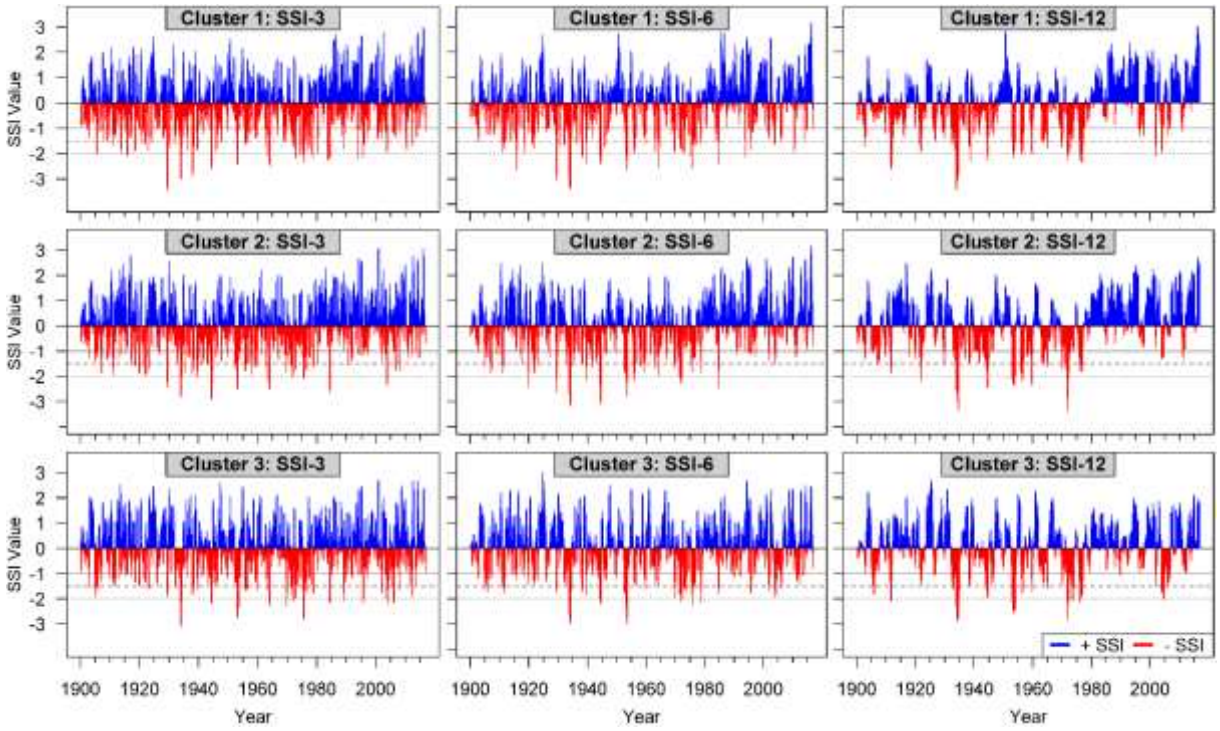

Figure S2. As Figure S1 but for SSI 3, 6 and 12.